On Quantum Optics of Random Media

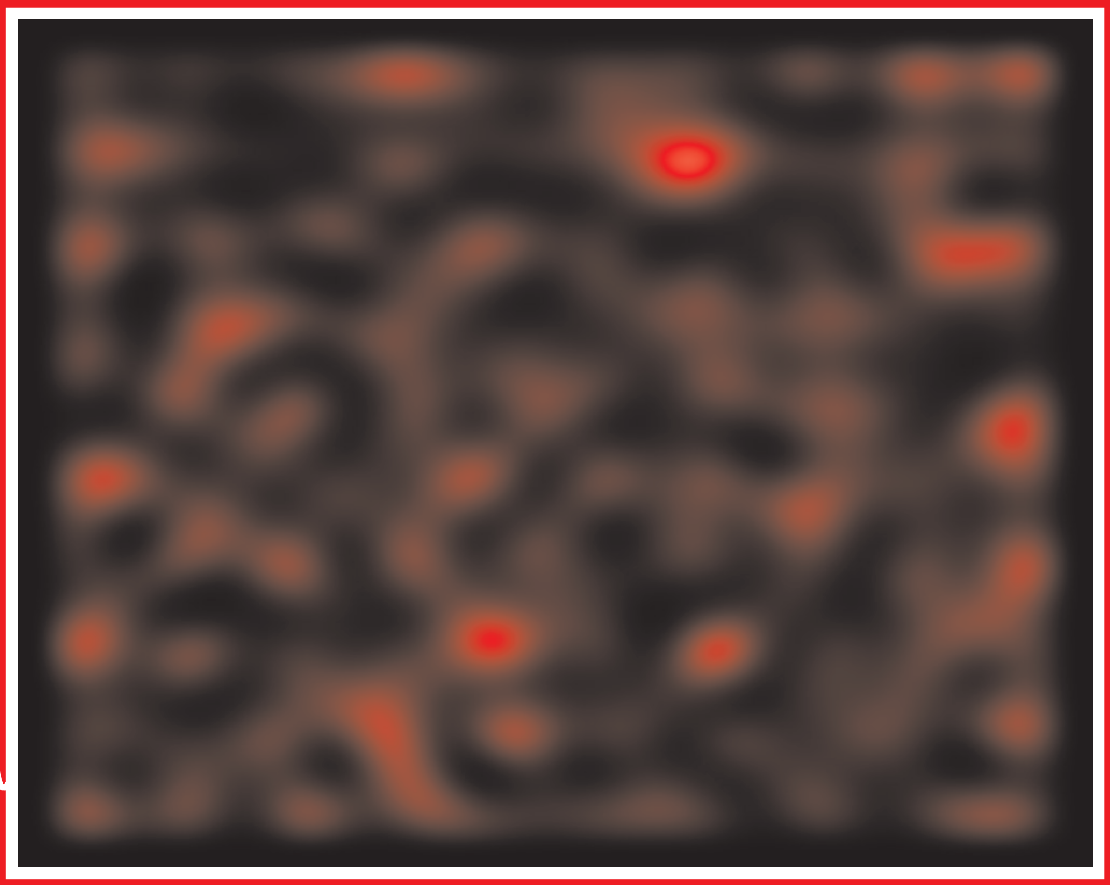

Michael Patra

On Quantum Optics of Random Media

Michael Patra

The cover depicts the radiation emitted through a small rectangular opening by a cavity filled with an amplifying random medium. The front shows the intensity at one fixed frequency, looking into the opening. The back shows the total intensity (integrated over the opening) as a function of frequency.

On Quantum Optics of Random Media

PROEFSCHRIFT

TER VERKRIJGING VAN
DE GRAAD VAN DOCTOR AAN DE UNIVERSITEIT LEIDEN,
OP GEZAG VAN DE RECTOR MAGNIFICUS DR. W. A. WAGENAAR,
HOOGLERAAR IN DE FACULTEIT DER SOCIALE WETENSCHAPPEN,
VOLGENS BESLUIT VAN HET COLLEGE VOOR PROMOTIES
TE VERDEDIGEN OP WOENSDAG 6 SEPTEMBER 2000
TE KLOKKE 16.15 UUR

DOOR

Michael Patra

GEBOREN TE BERLIJN IN 1971

Promotiecommissie:

Promotor:	Prof. dr. C.W. J. Beenakker
Referent:	Prof. dr. G. Nienhuis
Overige leden:	Prof. dr. P. H. Kes
	Prof. dr. J. M. J. van Leeuwen
	Prof. dr. D. Lenstra (Vrije Universiteit Amsterdam)
	Prof. dr. ir. W. van Saarloos
	Prof. dr. J. P. Woerdman

Contents

Chapter 1

Introduction

A random medium in optics is a medium in which the dielectric function varies randomly with position. Frosted glass is a familiar example. In a laboratory setting, one can suspend particles in a fluid to achieve strong multiple scattering with little absorption. On a much larger scale, interstellar clouds and stellar atmospheres provide a random medium for the radiation propagating through them.

For many applications, a classical description of the electromagnetic field is sufficient. The theory of propagation of classical waves through random media has been developped extensively in the last two decades [Ish78, She90]. Quantum effects such as vacuum fluctuations and spontaneous emission of radiation are not taken into account in these studies. These are the subject of quantum optics, which however rarely goes beyond one-dimensional scattering.

The essentially three-dimensional, chaotic scattering present in random media has so far received little attention in the context of quantum optics. This deficiency is felt particularly strongly for amplifying media (so called "random lasers"), where the interplay of spontaneous and stimulated emission with chaotic scattering plays a central role. It is the purpose of this thesis to make a first step towards a bridging of the gap between random media and quantum optics. In this introduction we present an overview of some of the concepts that will appear in more detail in the following chapters.

1.1 Classical electrodynamics

1.1.1 Classical waves

Classical waves allow a simultaneous measurement of amplitude and phase. Classical electromagnetic waves are described by the Maxwell equations. In a dielectric medium the Fourier component $\vec{E}(\vec{r},\omega)$ of the electric field satisfies the wave equation

$$\Delta\vec{E}(\vec{r},\omega) - \operatorname{grad}\operatorname{div}\vec{E}(\vec{r},\omega) + \frac{\omega^2}{c^2}\varepsilon(\vec{r},\omega)\vec{E}(\vec{r},\omega) = 0\,, \tag{1.1}$$

together with the transversality condition

$$\operatorname{div}\operatorname{grad}\varepsilon(\vec{r},\omega)\vec{E}(\vec{r},\omega) = 0\,. \tag{1.2}$$

Here c is the speed of light in vacuum and $\varepsilon(\vec{r},\omega)$ is the position and frequency dependent dielectric constant (relative to vacuum).

In a random medium $\varepsilon(\vec{r},\omega)$ fluctuates randomly from point to point. The polarisation of the electric field is randomised and effectively we may work with a scalar field $E(\vec{r},\omega)$. The scalar wave equation

$$\Delta E(\vec{r},\omega) + \frac{\omega^2}{c^2}\varepsilon(\vec{r},\omega)E(\vec{r},\omega) = 0 \tag{1.3}$$

is known as the Helmholtz equation.

The dielectric constant is real in the absence of absorption. Absorption adds a positive imaginary part. If $\varepsilon = 1 + \mathrm{i}\varepsilon''$ with $\varepsilon'' \ll 1$, then the imaginary part is related to the absorption rate $1/\tau_{\mathrm{a}}$ at frequency ω by $\omega\varepsilon'' = 1/\tau_{\mathrm{a}}$. A negative imaginary part corresponds to amplification by stimulated emission. Spontaneous emission of radiation cannot be described by a classical wave equation, it requires a quantisation of the electromagnetic field. That is the topic of the next section, but first we describe the scattering theory that we will use.

1.1.2 Scattering theory

To formulate a scattering theory, we embed the dielectric medium in a waveguide (see Fig. 1.1). We assume that $\varepsilon = 1$ outside of the region of length L that contains the dielectric medium. Far from the medium the solutions of the Helmholtz equation (1.3) have the form

$$E_{n,\pm}(\vec{r},\omega) = \mathrm{e}^{\pm\mathrm{i}kz}\phi_n(x,y)\,, \tag{1.4}$$

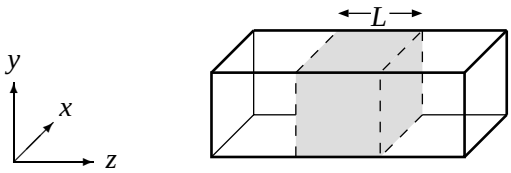

Figure 1.1: A long waveguide that is open at both ends and contains the disordered dielectric medium over a length L (dotted region).

with wave number $k = \omega/c$. The integer $n = 1, 2, \ldots, N$ is the mode index, and $\phi_n(x, y)$ is the corresponding transverse mode profile. The total number N of propagating modes is given by $N \simeq \pi A/\lambda^2$ for cross-sectional area A and wavelength $\lambda = 2\pi/k$. (If we would count the polarisations of the electromagnetic field, the number N would be twice as large.) Evanescent waves (solutions with imaginary k) do not play a role far from the dielectric medium.

A wave at frequency ω incident on the medium from the left can be represented by

$$E(\vec{r}, \omega) = \sum_{n=1}^{N} c_n^{\mathrm{in,L}} E_{n,+}(\vec{r}, \omega)\,, \tag{1.5}$$

with complex coefficients $c_n^{\mathrm{in,L}}$. Similarly, a wave reflected from the medium at the left has the form

$$E(\vec{r}, \omega) = \sum_{n=1}^{N} c_n^{\mathrm{out,L}} E_{n,-}(\vec{r}, \omega)\,. \tag{1.6}$$

In the same way we can introduce coefficients $c_n^{\mathrm{in,R}}$ and $c_n^{\mathrm{out,R}}$ for incoming and outgoing waves at the right of the medium (see Fig. 1.2).

The coefficients for incoming and outgoing waves are related by a linear trans-

Figure 1.2: Incoming and outgoing waves are described by four sets of complex coefficients c_n. The coefficients for incoming and outgoing waves are related by the scattering matrix.

Figure 1.3: The scattering matrix S can be decomposed into transmission matrices (t and t') and reflection matrices (r and r').

formation,

$$\left(c_1^{\text{out,L}},\ldots,c_N^{\text{out,L}},c_1^{\text{out,R}},\ldots,c_N^{\text{out,R}}\right)^T = S\cdot\left(c_1^{\text{in,L}},\ldots,c_N^{\text{in,L}},c_1^{\text{in,R}},\ldots,c_N^{\text{in,R}}\right)^T . \quad (1.7)$$

The $2N\times 2N$-matrix S is called the *scattering matrix*. Frequently we will adopt the convention that modes $1,\ldots,N$ are to the left of the sample and modes $N+1,\ldots,2N$ to the right. We can write Eq. (1.7) in a short-hand form,

$$c^{\text{out}} = Sc^{\text{in}} . \quad (1.8)$$

This is the input-output relation for classical waves.

The scattering matrix S can be decomposed into $N\times N$ submatrices (see Fig. 1.3), the reflection matrices r and r', and the transmission matrices t and t',

$$S = \begin{pmatrix} r & t' \\ t & r' \end{pmatrix} . \quad (1.9)$$

For a time-reversal invariant system, S equals its transpose S^T, thus $r = r^T$, $r' = r'^T$, and $t = t'^T$. In contrast to electronic systems, where time-reversal symmetry is easily broken by a magnetic field, time-reversal symmetry is very difficult to break for optical systems. In the absence of absorption or amplification, hence for a real dielectric constant, current conservation dictates that S is a unitary matrix ($SS^\dagger$ equals the unit matrix $\mathbb{1}$). This implies additional relations between reflection and transmission matrices.

1.2 Quantisation of the electromagnetic field

1.2.1 Wave equation

In a quantum mechanical description the electric field $\hat{E}(\vec{r},t)$ is an operator in Heisenberg representation, canonically conjugate to the vector potential $\hat{A}(\vec{r},t)$.

(We assume the Coulomb gauge, in which $\hat{E} = -\partial\hat{A}/\partial t$, and as before treat the case of a scalar wave.) The canonical commutation relation is

$$[\hat{E}(\vec{r},t), \hat{A}(\vec{r}',t)] = \frac{\mathrm{i}\hbar}{\varepsilon_0}\delta(\vec{r}-\vec{r}')\,. \tag{1.10}$$

In Fourier representation,

$$\hat{E}(\vec{r},t) = \frac{1}{\sqrt{2\pi}}\int_0^\infty \mathrm{d}\omega\, \hat{E}(\vec{r},\omega)\mathrm{e}^{-\mathrm{i}\omega t} + \mathrm{H.\,c.}\,, \tag{1.11}$$

where H. c. stands for Hermitian conjugate. The frequency dependent operators $\hat{E}(\vec{r},\omega)$ do not have any simple commutation relation.

The Helmholtz equation (1.3) for the classical fields carries over to the operators,

$$\Delta\hat{E}(\vec{r},\omega) + \frac{\omega^2}{c^2}\varepsilon(\vec{r},\omega)\hat{E}(\vec{r},\omega) = \hat{f}(\vec{r},\omega)\frac{\omega}{c^2}\sqrt{\frac{\hbar\varepsilon''(\vec{r},\omega)}{\pi}}\,, \tag{1.12}$$

but with an additional fluctuating source on the right-hand side [Gru96a, Mat95, Mat97]. It describes the effects of spontaneous emission, that are not included in the classical wave equation. The operators $\hat{f}$ satisfy the bosonic commutation relations

$$[\,\hat{f}(\vec{r},\omega),\, \hat{f}^\dagger(\vec{r}',\omega')] = \delta(\vec{r}-\vec{r}')\delta(\omega-\omega')\,, \tag{1.13}$$

$$[\,\hat{f}(\vec{r},\omega),\, \hat{f}(\vec{r}',\omega')] = 0\,. \tag{1.14}$$

These commutation relations ensure that the solution of the wave equation (1.12), Fourier transformed into the time domain, satisfies the original commutation relations (1.10).

1.2.2 Input-output relations

The representation (1.5) of an incoming (or outgoing) classical wave in terms of a sum over modes carries over to the operators,

$$\hat{E}(\vec{r},\omega) = \sum_{n=1}^{N} \hat{a}_n^{\mathrm{in,L}} E_{n,+}(\vec{r},\omega)\,, \tag{1.15}$$

but now instead of complex coefficients c_n we have operators $\hat{a}_n$. These are annihilation operators, their Hermitian conjugates $\hat{a}_n^\dagger$ being creation operators. They

satisfy the bosonic commutation relations

$$[\hat{a}_n^x(\omega), \hat{a}_m^{x\,\dagger}(\omega')] = \delta_{nm}\delta(\omega-\omega')\,, \tag{1.16}$$

$$[\hat{a}_n^x(\omega), \hat{a}_m^x(\omega')] = 0\,, \tag{1.17}$$

where x stands for "in" or "out", and the mode indices range from 1 to $2N$. Creation (or annihilation) operators for incoming states commute among themselves, as do the operators for outgoing states, but creation operators for incoming states do not commute with creation operators for outgoing states.

The same scattering matrix S that related the incoming and outgoing classical waves now relates the incoming and outgoing creation or annihilation operators,

$$\hat{a}^{\text{out}} = S\cdot\hat{a}^{\text{in}} + U\cdot\hat{b} + V\cdot\hat{c}^\dagger\,, \tag{1.18}$$

but there are two additional fluctuating source terms. These sources represent the effects of the fluctuating source term $\hat{f}$ in the wave equation (1.12). The operators $\hat{b}$ and $\hat{c}$ satisfy bosonic commutation relations, just like the operators $\hat{a}^{\text{in}}$ and $\hat{a}^{\text{out}}$. This implies a relationship between the matrices U, V and the scattering matrix S,

$$UU^\dagger - VV^\dagger = \mathbb{1} - SS^\dagger\,. \tag{1.19}$$

Eq. (1.19) represents the fluctuation-dissipation theorem for this problem. In an absorbing system, the matrix product $SS^\dagger$ is sub-unitary, hence V can be set equal to 0 and $UU^\dagger = \mathbb{1} - SS^\dagger$. In an amplifying system, $SS^\dagger$ is super-unitary, hence U can be set equal to 0 and $VV^\dagger = SS^\dagger - \mathbb{1}$.

1.3 Photodetection

A photodetection experiment provides information on the quantum mechanical state of the electromagnetic radiation. It plays a central role in this thesis.

1.3.1 Statistical description

A photodetector absorbs n photons within a time interval t. If this experiment is repeated many times with the same incident light field, a sequence of fluctuating values of the photocount n will be generated. The photocount distribution $p(n)$ gives the probability that n photons are detected. It has the moments

$$\overline{n^k} = \sum_{n=0}^{\infty} n^k\, p(n)\,. \tag{1.20}$$

We also introduce the factorial moments

$$n^{(k)} = \overline{n \cdot (n-1) \cdot (n-2) \cdots (n-k+1)} \,. \tag{1.21}$$

In particular, $n^{(1)} = \overline{n}$ and $n^{(2)} = \overline{n^2} - \overline{n}$.

Cumulants are constructed from the moments and the factorial moments in the usual way. For example, the second cumulant (or variance) is $\overline{n^2} - \overline{n}^2$ and the second factorial cumulant is $n^{(2)} - [n^{(1)}]^2$. (The first cumulant equals the first factorial cumulant equals the mean $\overline{n}$.) Cumulants are convenient to characterise a Gaussian distribution, because only the first two are non-zero. Factorial cumulants are convenient to characterise a Poisson distribution, because only the first is non-zero.

It is useful to work with generating functions. The moment generating function $F_{\rm m}$ is defined by

$$F_{\rm m}(\xi) = \overline{{\rm e}^{\xi n}} = \sum_{n=0}^{\infty} {\rm e}^{\xi n} p(n) = \sum_{p=0}^{\infty} \frac{\xi^p}{p!} \overline{n^p} \,. \tag{1.22}$$

In a similar manner the factorial moments can be generated from the factorial moment generating function $F_{\rm f}$, defined by

$$F_{\rm f}(\xi) = \sum_{n=0}^{\infty} (1+\xi)^n p(n) = \sum_{p=0}^{\infty} \frac{\xi^p}{p!} n^{(p)} \,. \tag{1.23}$$

Note the relation $F_{\rm m}(\xi) = F_{\rm f}({\rm e}^{\xi} - 1)$.

The logarithm of the moment generating function generates the cumulants, and the same applies to the factorial moments and factorial cumulants. If we denote by κ_p the pth factorial cumulant, then

$$\ln F_{\rm f}(\xi) = \sum_{p=1}^{\infty} \frac{\kappa_p \xi^p}{p!} \,. \tag{1.24}$$

1.3.2 Photocount distribution

In the limit $t \to \infty$ of a long counting time, we may assume a frequency resolved measurement within an interval $\Delta = 2\pi/t$ around some frequency $\omega_p = p\Delta$. We assume that all outgoing modes at one end of the waveguide are detected with unit efficiency by the photodetector (see Fig. 1.4). For simplicity we assume in this introduction that there is no outgoing radiation at the other end of the waveguide,

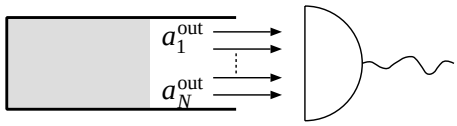

Figure 1.4: A photodetector absorbs the photons in modes $k = 1, \ldots, N$ within a time t.

so that the scattering matrix has dimension $N \times N$ instead of $2N \times 2N$. The operator of the photocount is

$$\hat{n} = \sum_{n=1}^{N} \hat{a}_n^{\text{out}\dagger}(\omega_p)\hat{a}_n^{\text{out}}(\omega_p)\,. \tag{1.25}$$

[Because we have discretised the frequency, the commutation relation $[\hat{a}_n^\dagger(\omega_p), \hat{a}_m(\omega_q)] = \delta_{nm}\delta_{pq}$ now contains a Kronecker delta δ_{pq} instead of a delta function $\delta(\omega_p - \omega_q)$.]

The moments are $\overline{n^p} = \langle \hat{n}^p \rangle$, where $\langle \cdots \rangle$ indicates a quantum mechanical average over the state of the electromagnetic field. The moment generating function is

$$F_{\text{m}}(\xi) = \langle \mathrm{e}^{\xi \hat{n}} \rangle\,. \tag{1.26}$$

We can write this as a normally ordered expectation value $\langle : \cdots : \rangle$, where normal ordering means that all creation operators are moved to the left of the annihilation operators. We use the identity

$$\langle \mathrm{e}^{\xi \hat{a}^\dagger \hat{a}} \rangle = \langle : \exp\big[(\mathrm{e}^{\xi} - 1)\hat{a}^\dagger \hat{a}\big] : \rangle\,, \tag{1.27}$$

valid for any bosonic operator $\hat{a}$. Hence

$$F_{\text{m}}(\xi) = \langle : \exp\big[(\mathrm{e}^{\xi} - 1)\hat{n}\big] : \rangle\,. \tag{1.28}$$

The factorial moment generating function is thus given by

$$F_{\text{f}}(\xi) = \langle : \mathrm{e}^{\xi \hat{n}} : \rangle\,. \tag{1.29}$$

This is for a single frequency $\omega_p = p\Delta$. Since different frequencies are independent, the generating function factorises,

$$F_{\text{f}}(\xi) = \prod_p \langle : \exp\big[\xi \sum_{n=1}^{N} \hat{a}_n^{\text{out}\dagger}(\omega_p)\hat{a}_n^{\text{out}}(\omega_p)\big] : \rangle\,. \tag{1.30}$$

By taking the logarithm, and converting $\sum_p \to \int \mathrm{d}\omega/\Delta = (t/2\pi)\int \mathrm{d}\omega$, we find the factorial cumulant generating function in the long-time limit,

$$\ln F_{\mathrm{f}}(\xi) = \frac{t}{2\pi}\int_0^\infty \mathrm{d}\omega \ln\langle : \exp\Big[\xi \sum_{n=1}^{N} \hat{a}_n^{\mathrm{out}\dagger}(\omega)\hat{a}_n^{\mathrm{out}}(\omega)\Big] : \rangle \,. \tag{1.31}$$

There exists a more general formula due to Glauber, Kelley, and Kleiner [Gla63, Kel64], that is valid for arbitrary counting times t, and for detection efficiencies α_n different from unity. The photocount operator becomes

$$\hat{n} = \frac{1}{2\pi}\int_0^t \mathrm{d}t' \int_0^\infty \mathrm{d}\omega \int_0^\infty \mathrm{d}\omega' \sum_{n=1}^{N} \alpha_n \mathrm{e}^{\mathrm{i}t'(\omega-\omega')} \hat{a}_n^{\mathrm{out}\dagger}(\omega)\hat{a}_n^{\mathrm{out}}(\omega') \,, \tag{1.32}$$

and the factorial moment generating function $F_{\mathrm{f}}(\xi) = \langle : \mathrm{e}^{\xi\hat{n}} : \rangle$, just as in Eq. (1.29). The corresponding probability to count m photons within time t is given by

$$p(m) = \frac{1}{m!}\langle : \hat{n}^m \mathrm{e}^{-\hat{n}} : \rangle \,. \tag{1.33}$$

It looks like a Poisson distribution, but it is not because $\hat{n}$ is an operator and not a c-number.

1.4 Applications

1.4.1 Black-body radiation

As a first simple application we consider the case of black-body radiation. A black body is characterised by complete absorption, so $S = 0$ and $U = \mathbb{1}$, $V = 0$. The operator $\hat{a}_n^{\mathrm{out}}$ can therefore be identified with the operator $\hat{b}_n$. The black body is in thermal equilibrium at temperature T. The average of the operators $\hat{b}$ is

$$\langle \hat{b}_k^\dagger(\omega)\hat{b}_l(\omega')\rangle = \delta_{kl}\delta(\omega-\omega')\, f(\omega,T) \,, \tag{1.34}$$

with $f(\omega,T)$ the Bose-Einstein function,

$$f(\omega,T) = \left[\exp\left(\frac{\hbar\omega}{k_{\mathrm{B}}T}\right) - 1\right]^{-1} \,, \tag{1.35}$$

also referred to as the Planck function in this context. Higher moments follow from the factorisation rule of Gaussian averages,

$$\langle \hat{b}_{i_1}^\dagger \cdots \hat{b}_{i_M}^\dagger \hat{b}_{j_1} \cdots \hat{b}_{j_M}\rangle = \sum_\sigma \prod_{k=1}^{M} \langle \hat{b}_{i_k}^\dagger \hat{b}_{i_{\sigma(k)}}\rangle \,, \tag{1.36}$$

where σ is a permutation of the integers $1, 2, \ldots, M$.

Substituting $\hat{a}^{\text{out}} \to \hat{b}$ in Eq. (1.31) and carrying out the Gaussian averages, we find

$$\ln F_{\text{f}}(\xi) = -tN\frac{\delta\omega}{2\pi}\ln\bigl[1-\xi f(\omega,T)\bigr]\,, \tag{1.37}$$

where we have assumed a frequency resolved measurement in an interval $\delta\omega$ around ω. The corresponding probability distribution can be reconstructed from the inversion formula

$$p(n) = \lim_{\xi\to -1}\frac{1}{n!}\frac{\mathrm{d}^n}{\mathrm{d}\xi^n}F_{\text{f}}(\xi)\,. \tag{1.38}$$

The result is known as a negative binomial distribution,

$$p(n) = \binom{n+\nu-1}{n} f^n(\omega,T)\bigl[1+f(\omega,T)\bigr]^{-n-\nu}\,. \tag{1.39}$$

The quantity $\nu = Nt\delta\omega/2\pi$ is the number of degrees of freedom of the distribution.

The mean and variance of the photocount are given by

$$\overline{n} = \nu f(\omega,T)\,, \tag{1.40}$$

$$\mathrm{var}\, n = \nu f(\omega,T)\bigl[1+f(\omega,T)\bigr] = \overline{n}\bigl(1+\frac{\overline{n}}{\nu}\bigr)\,. \tag{1.41}$$

This is Einstein's formula of black-body radiation [Ein09]. For a Poisson process the variance would be equal to the mean. That would apply to uncorrelated classical particles. Because of Bose statistics the variance is bigger by a factor $1+\overline{n}/\nu$. This is called photon bunching. The source of correlations is the indistinguishability of the particles. It has no classical analogue. In a typical black body the factor $1+\overline{n}/\nu$ is close to 1, because $\overline{n}/\nu = f \ll 1$. For example, $f \approx 10^{-3}$ at optical frequencies and $T = 3000\,\text{K}$, and $f \approx 10^{-2}$ at infrared frequencies and room temperatures. Much larger effects of photon bunching can be achieved in an amplifying medium, as we will discuss shortly.

1.4.2 Grey-body radiation

This thesis is about media that are not a black body, hence for which the scattering matrix $S \neq 0$. If the medium is still in thermal equilibrium it is sometimes called a "grey body". The generalisation of Eq. (1.37) to grey-body radiation is [Bee98]

$$\ln F_{\text{f}}(\xi) = -t\frac{\delta\omega}{2\pi}\ln\det\bigl[\mathbb{1}-(\mathbb{1}-SS^\dagger)\xi f(\omega,T)\bigr]\,. \tag{1.42}$$

The mean photocount is given by

$$\overline{n} = \frac{t\delta\omega}{2\pi} f(\omega, T)\,\mathrm{tr}(\mathbb{1} - SS^\dagger)\,. \tag{1.43}$$

This is Kirchhoff's law of thermal radiation [Kir60]. The variance can be written in the form

$$\mathrm{var}\, n = \overline{n}\big(1 + \frac{\overline{n}}{\nu_{\mathrm{eff}}}\big)\,, \tag{1.44}$$

with ν_{eff} the effective number of degrees of freedom,

$$\frac{\nu_{\mathrm{eff}}}{\nu} = \frac{\big[\mathrm{tr}(\mathbb{1} - SS^\dagger)\big]^2}{N\,\mathrm{tr}(\mathbb{1} - SS^\dagger)^2} \leqslant 1\,. \tag{1.45}$$

A grey body has a smaller number of degrees of freedom (at a given value of N, t, and $\delta\omega$) than a black body. Intermode scattering is essential for this: There is no reduction if $N = 1$ or if S is diagonal. This will be a recurrent theme throughout this thesis. The interplay between absorption (or amplification) and intermode scattering causes a qualitative change in the state of the radiation and hence in the photodetection statistics.

1.4.3 Linear amplifier

A linear amplifier can be described as a system in thermal equilibrium at a negative temperature [Jef93, Mat97]. The effective temperature $T_{\mathrm{eff}} < 0$ is fixed by the degree of population inversion of the pair of atomic levels (with separation $\hbar\omega_0$) responsible for the amplification by stimulated emission at frequency ω_0. If the mean number of atoms in the upper (lower) state is N_{upper} (N_{lower}), then

$$f \equiv \left[\exp\left(\frac{\hbar\omega_0}{k_{\mathrm{B}}T_{\mathrm{eff}}}\right) - 1\right]^{-1} = \frac{N_{\mathrm{upper}}}{N_{\mathrm{lower}} - N_{\mathrm{upper}}}\,. \tag{1.46}$$

A complete population inversion ($N_{\mathrm{lower}} = 0$) corresponds to T approaching zero from below and $f \to -1$. The quantity f for an amplifying medium is also referred to as the population inversion factor. Now we can understand why the effects of photon bunching are so much more pronounced in an amplifying medium than in an absorbing medium: f can be of order unity at room temperature for amplification, while $f \ll 1$ for absorption.

The formulas for grey-body radiation carry over to a linear amplifier, with the above definition of f. For example, the mean photocount is still given by

$$\overline{n} = \frac{t\delta\omega}{2\pi} f \,\mathrm{tr}(\mathbb{1} - SS^\dagger) \,. \tag{1.47}$$

It is positive, as it should, because $f < 0$ at negative temperature but also $\mathrm{tr}(\mathbb{1} - SS^\dagger) < 0$ (because S is super-unitary in an amplifying medium). The reduction of the number of degrees of freedom remains given by Eq. (1.45).

1.5 Random-matrix theory

To evaluate the photocount distribution of a given system we need to know its scattering matrix. In principle, that requires a solution of the classical wave equation, which in general can only be done numerically. In a random medium the scattering matrix depends sensitively on the location of the scattering centra. It is therefore natural to ask not for the scattering matrix of a given system, but for the statistical distribution of the scattering matrix in an ensemble of random media with different locations of the scattering centra.

Random-matrix theory is the theoretical tool than can give this information [Meh90, Bee97, Guh98]. It applies not only to random media, but more generally to systems in which scattering is chaotic. Chaotic scattering can result from randomly placed impurities, but it can also result from irregularly shaped boundaries. In fact, even scattering from simple regular shapes can lead to chaos. An example of a cavity with chaotic scattering is shown in Fig. 1.5.

In ray optics one can characterise chaotic scattering by the exponential divergence of rays starting at the same point in space in almost the same direction. In

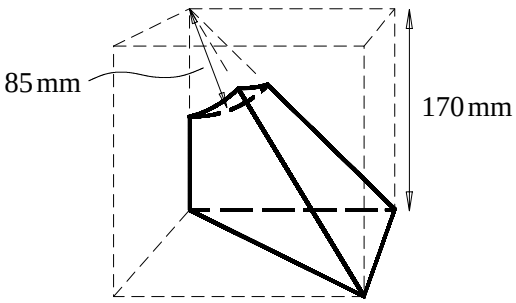

Figure 1.5: Cavity in which the scattering is chaotic. The dimensions are for the microwave cavity used in Ref. [Alt97].

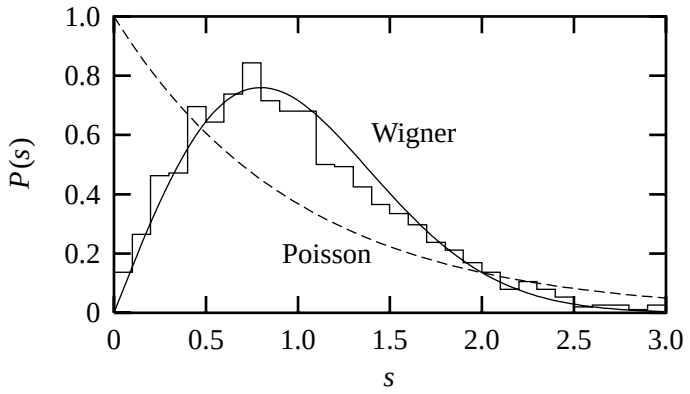

Figure 1.6: Comparison of the spacing of modes in the microwave cavity of Fig. 1.5 with Wigner's surmise (1.48) [solid line] and the Poisson distribution (1.49) [dashed line]. The mean level spacing has been set to $\Delta = 1$, and non-chaotic "bouncing-ball" modes have been eliminated from the experimental histogram. From Ref. [Alt97].

wave optics one should look at the spacing in frequency of cavity modes. Chaotic scattering leads to mode repulsion, meaning that the probability $P(s)$ to find a spacing s much smaller than the mean spacing Δ vanishes linearly with s. In contrast, for non-chaotic, or regular scattering $P(s)$ tends to a non-zero constant for $s \to 0$.

Random-matrix theory represents the spectrum of a chaotic cavity by the eigenvalues of a real symmetric matrix H with independent, Gaussian distributed elements [Boh84]. The distribution of the spacings is then given by Wigner's surmise [Wig56],

$$P(s) \propto s\mathrm{e}^{-\pi s^2/4\Delta^2} . \tag{1.48}$$

In contrast, for regular scattering the spectrum is represented by independent eigenvalues (*not* independent matrix elements). The distribution of spacings is then the Poisson distribution

$$P(s) \propto \mathrm{e}^{-s/\Delta} . \tag{1.49}$$

In Fig. 1.6 we show the experimental data [Alt97] for a chaotic microwave cavity that confirms Wigner's surmise.

1.5.1 Gaussian ensemble

The ensemble of random matrices H introduced in the previous subsection to describe a chaotic cavity is called the Gaussian ensemble. Its distribution is

$$P(H) \propto \exp\left(-a \operatorname{tr} H^2\right) . \tag{1.50}$$

The coefficient $a = M(\pi/\Delta)^2$ is determined by the mean spacing Δ of the modes and by the dimension M of the matrix H. (We take $M \to \infty$ at the end of the calculation.) By integrating out the eigenvectors, one arrives at the distribution of the eigenvalues,

$$P(\{E_n\}) \propto \prod_{i<j} |E_i - E_j| \prod_k \exp\left(-a E_k^2\right) . \tag{1.51}$$

The term $|E_i - E_j|$ is the Jacobian for the change of variables from matrix elements to eigenvalues. It is responsible for the level repulsion discussed in the previous subsection.

The eigenvectors constitute the matrix U that diagonalises $H = U \operatorname{diag}(E_1, E_2, \ldots, E_M) U^{-1}$. The matrix U is orthogonal, $UU^T = \mathbb{1}$. (For that reason the ensemble of H is also called the Gaussian orthogonal ensemble; if H is complex Hermitian, instead of real symmetric, the matrix U is unitary, instead of orthogonal, and one speaks of the Gaussian unitary ensemble.) In the limit $M \to \infty$ the elements of U become approximately uncorrelated Gaussian

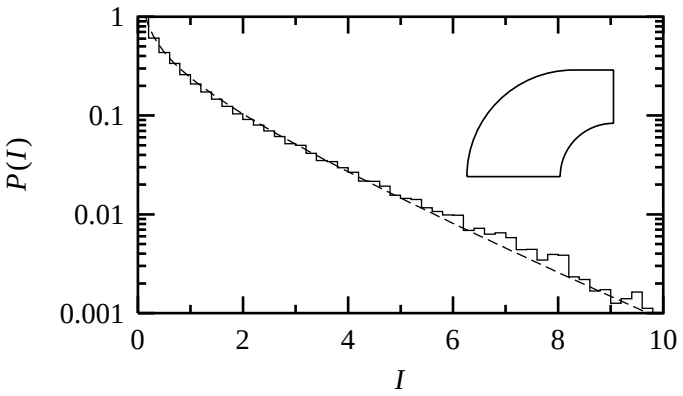

Figure 1.7: Comparison of the Porter-Thomas distribution (1.52) [dashed line] with the intensity distribution measured on the two-dimensional microwave cavity shown in the inset. From Ref. [Kud95].

distributed with zero mean and variance $1/M$. The corresponding distribution of the (normalised) intensity $I = M|U_{nm}|^2$ is known as the Porter-Thomas distribution [Por65],

$$P(I) \propto \frac{1}{\sqrt{I}} \mathrm{e}^{-I/2} \,. \tag{1.52}$$

Like Wigner's surmise, it has been verified experimentally, see Fig. 1.7.

1.5.2 Circular ensemble

A cavity can be coupled to the outside via an opening connected to a waveguide supporting N propagating modes (see Fig. 1.8). We introduce the waveguide as a theoretical device to obtain a finite-dimensional ($N \times N$) scattering matrix S. Qualitatively the results should be the same as without a waveguide, if one replaces N by the area A of the opening divided by λ^2/π.

Scattering inside the cavity remains chaotic if the opening to the outside is sufficiently small. The mean dwell time $\tau_{\mathrm{dwell}} \simeq 1/N\Delta$ of a photon inside the cavity should be long compared to the ergodic time τ_{erg} required for exploration of the chaotic phase space. In practice this is satisfied if the linear dimension of the opening is small compared to the linear dimension of the cavity.

From a random-matrix theory for H we can create a random-matrix theory for S. The matrices S and H are related by [Ver85]

$$S(\omega) = \mathbb{1} - 2\pi \mathrm{i} W^\dagger \frac{1}{H - \hbar\omega - \mathrm{i}\pi W W^\dagger} W \,, \tag{1.53}$$

$$W_{mn} = \pi^{-1/2} \delta_{mn} \,, \qquad m = 1, \ldots, M \,, \qquad n = 1, \ldots, N \,. \tag{1.54}$$

The resulting scattering matrix is unitary (because of flux conservation) and symmetric (because of time-reversal symmetry). The Gaussian ensemble for H im-

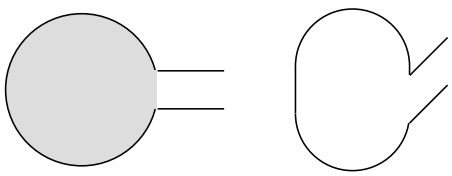

Figure 1.8: A chaotic cavity is connected to the outside by a waveguide. The dynamics can be chaotic due to scattering at randomly placed scattering centra (left) or due to the shape of the cacity (right).

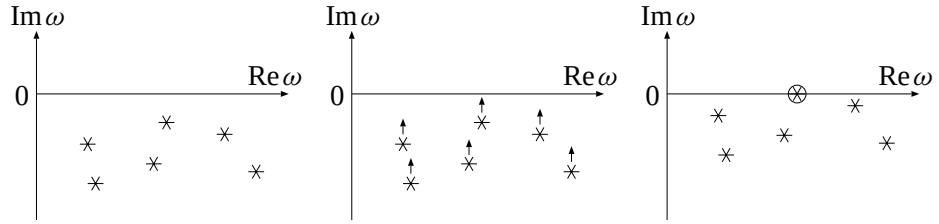

Figure 1.9: Poles of the scattering matrix in the complex frequency plane. In the absence of amplification, all poles lie in the lower half of the complex plane (left). Amplification shifts the poles upward by an amount $1/2\tau_a$ (centre). The lasing threshold is reached when the first pole hits the real axis (right).

plies that at any fixed frequency ω, the matrix S is uniformly distributed [Bro95],

$$P(S) = \text{constant}\,, \tag{1.55}$$

among the unitary symmetric $N \times N$ matrices. The distribution (1.55) represents the circular (orthogonal) ensemble.

The effects of absorption or amplification with rate $1/\tau_a$ are included in Eq. (1.53) by

$$S(\omega) = \mathbb{1} - 2\pi i W^\dagger \frac{1}{H - \hbar\omega - i\pi W W^\dagger \pm i/2\tau_a} W\,, \tag{1.56}$$

where the $+$ sign is for amplification and the $-$ sign for absorption. Causality requires that all the poles of $S(\omega)$ lie in the lower half of the complex plane (i. e., they should have a negative imaginary part). This is guaranteed if there is no amplification. Amplification pushes the poles upward by an amount $1/\tau_a$ (see Fig. 1.9). We have reached the laser threshold when the first pole crosses the real axis. Then the linear theory presented here breaks down.

1.5.3 Disordered waveguide

Imagine connecting many chaotic cavities in series, via segments of N-mode waveguides (see Fig. 1.10). Scattering in this structure is still chaotic, but the dwell time is in general not long enough to explore the entire available phase space. Most photons will explore only a fraction of the total length L of the structure. This represents a theorist's model for a waveguide geometry containing randomly placed scattering centra. In fact, one can show rigorously that the

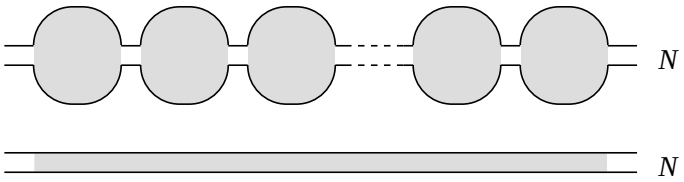

Figure 1.10: A series of chaotic cavities (top) is statistically equivalent to a disordered waveguide (bottom) provided the latter allows the same number N of propagating modes as the waveguides connecting the cavities. (For the series of cavities the mean free path is of the order of the linear dimension of the cavity.)

physics on long enough length scales (long compared to the mean free path l) is the same as for a true waveguide [Guh98].

The circular ensemble of the scattering matrix of one individual cavity allows one to construct the probability distribution of the scattering matrix of the entire structure. The result does not have a simple form (see Ref. [Bee97] for a review), so here we will restrict ourselves to a qualitative discussion of the three transport regimes.

- For $L \lesssim l$ the sample is ballistic. Scattering can be neglected and the transmission probability T through the waveguide is close to unity.

- For $l \lesssim L \lesssim Nl$ the sample is diffusive. The transmission probability decreases linearly with length, $T \propto l/L$. This regime exists only for $N \gg 1$. (There is no diffusive regime in a single-mode waveguide.)

- For $L \gtrsim Nl$ localisation takes place. The transmission probability drops exponentially $\propto \exp(-L/\xi_{\rm loc})$ where $\xi_{\rm loc} \simeq Nl$ is the localisation length.

In Fig. 1.11 we show the length dependence of the transmission probability through a disordered waveguide, computed by solving the Helmholtz equation numerically on a two-dimensional square lattice. We see the diffusive regime of linearly decreasing T followed by the localised regime of exponential decrease. The plot also shows another distinguishing feature of the diffusive and localised regimes. The relative fluctuations of T are much larger in the localised regime than in the diffusive regime. In the diffusive regime the root-mean-squared value of the fluctuations is smaller than the mean transmission probability by a factor $1/\sqrt{N}$. In the localised regime the fluctuations are of the same order of magnitude as the mean.

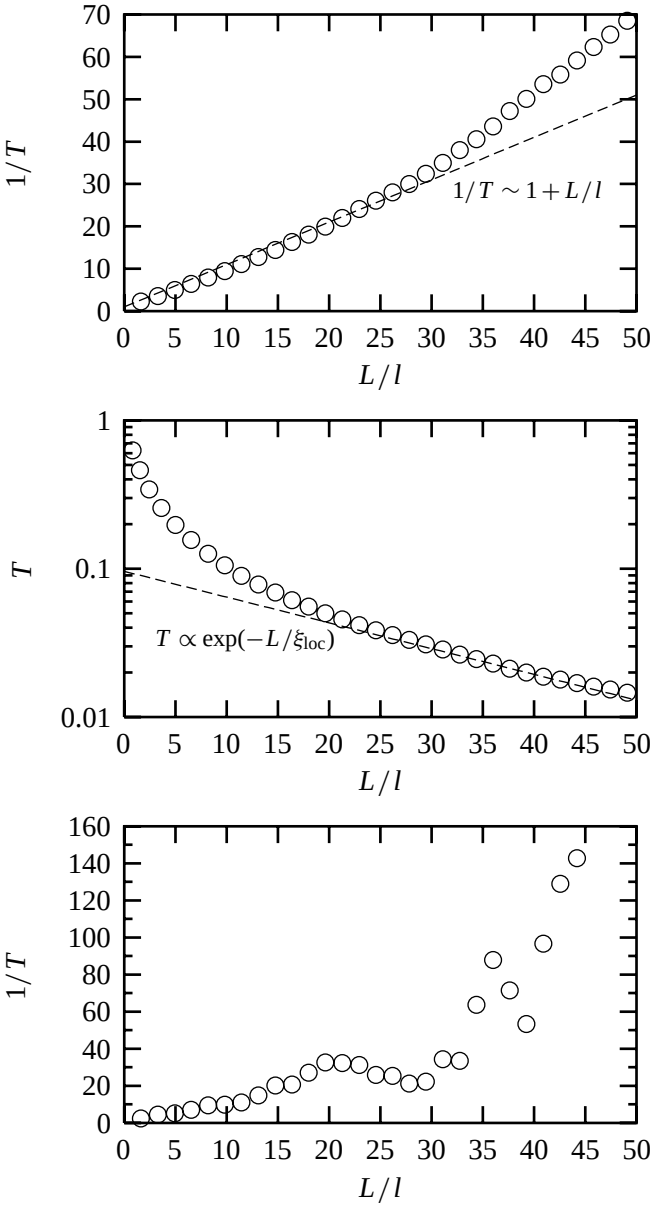

Figure 1.11: Numerically computed transmission probability T through a disordered waveguide allowing $N = 25$ propagating modes. The approximation $1/T \sim 1 + L/l$ is valid in the diffusive and ballistic regimes $L \lesssim Nl$ (top), the approximation $T \propto \exp(-L/\xi_{\rm loc})$ is valid in the localised regime $L \gtrsim Nl$ (centre). The top two panels are averages over many realisations of the disorder. The bottom panel is for a single realisation.Fluctuations are small in the diffusive regime and increase in the localised regime.

1.6 Random laser and Petermann factor

Although in this thesis we will not go beyond the laser threshold, our investigation was motivated by experiments on so called "random lasers" [Wie95]. We discuss the differences with "traditional lasers" in this section.

A traditional laser consists of a pumped, amplifying medium that is sandwiched between two mirrors (see Fig. 1.12, left). One of the two mirrors has a nonvanishing transmission probability γ so that the light generated in the medium can escape. The mirrors have two effects. Firstly, they lower the lasing threshold by increasing the average time spent by a photon in the amplifying medium. If L is the length of the laser, the effective length becomes $L_{\rm eff} \simeq 2L/\gamma$. Lasing occurs if the amplification rate $1/\tau_{\rm a}$ exceeds $c/L_{\rm eff}$, hence when L exceeds the critical length $L_{\rm c} \simeq \frac{1}{2}\gamma c\tau_{\rm a}$.

Secondly, the mirrors create narrow cavity modes that are responsible for a narrow linewidth Γ of the laser (much smaller than the amplification bandwidth). The quantum-limited linewidth is given by the Schawlow-Townes formula [Sch58]

$$\delta\omega = \frac{\Gamma_0^2}{2I}\,, \tag{1.57}$$

where I is the outgoing intensity (in photons/sec) and $\Gamma_0 \simeq c/L_{\rm eff}$ is the width of the lasing cavity mode.

In a random laser (Fig. 1.12, right), feedback is due to multiple scattering within the medium instead of being due to mirrors. For a medium with mean free path l (diffusion constant $D = \frac{1}{3}cl$) the typical time spent by a photon in the medium is L^2/D, so that the effective length becomes $L_{\rm eff} \simeq 3L^2/l$. The critical length is now $L_{\rm c} \simeq \sqrt{D\tau_{\rm a}}$. Such a mirrorless laser was first proposed by Letokhov [Let67] as a mechanism for laser action in interstellar clouds. The first laboratory experiments were carried out very recently [Cao99], see Fig. 1.13. An important distinction with traditional lasers is that the width Γ_0 of the cavity

Figure 1.12: In a traditional laser (left) mirrors at the ends of the amplifying medium reflect most of the intensity back into the medium. In a random laser (right) this feedback is provided by multiple scattering with disorder inside the medium.

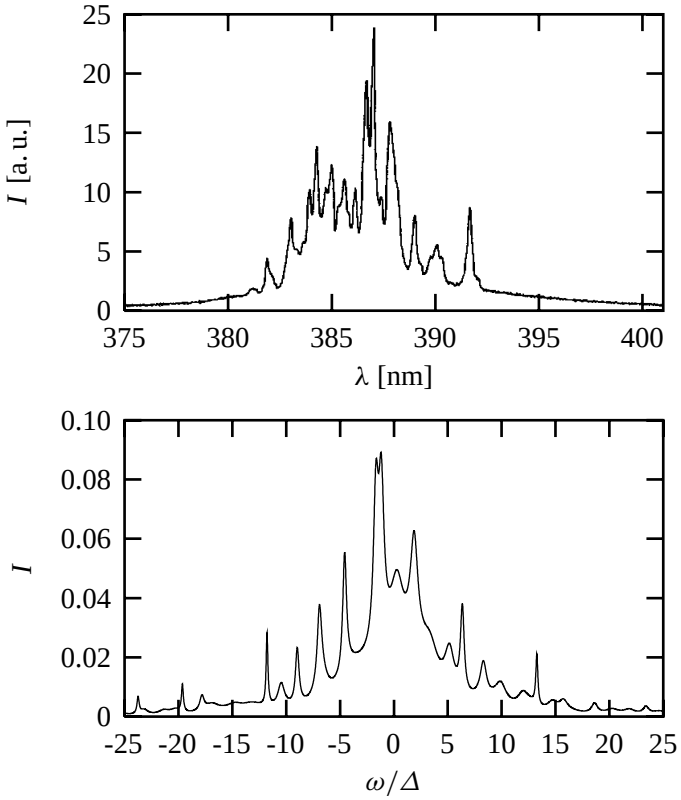

Figure 1.13: Top: Frequency dependence of the intensity $I = \overline{n}(Nt\delta\omega/2\pi)^{-1}$ of the radiation from a random laser, as measured by Cao et al. [Cao99]. The system consists of ZnO power film of thickness $5\,\mu$m, moderately pumped by a Nd:YAG laser. Bottom: Intensity calculated from Eqs. (1.47) and (1.56), with $f = -1$ (complete population inversion), $N = 5$, and a Lorentzian frequency profile for the amplification rate with width 5Δ and maximum $1/\tau_a = \Delta/40\pi$. In the experiment the medium was above the laser threshold, while in the calculation it was below so the comparison is not complete. (A complete comparison would require inclusion of the non-linear effects of mode competition.)

modes in a random laser is in general much larger than their spacing Δ, because the confinement by disorder is not as effective as the confinement by mirrors. (The ratio Γ_0/Δ is of order Nl/L, which is typically $\gg 1$.) Overlapping cavity modes lead to an increase of the laser linewidth above the Schawlow-Townes value (1.57), by an amount known as the Petermann factor K [Pet79, Sie89a, Sie89b],

$$\delta\omega = K\frac{\Gamma_0^2}{2I} \; . \tag{1.58}$$

Random-matrix theory is well suited to calculate the statistics of the Petermann factor in a random laser.

1.7 About this thesis

We conclude the introduction with an overview of the topics treated in this thesis.

Chapter 2: Excess noise for coherent radiation propagating through amplifying random media

Classically a signal can be amplified by an arbitrary factor without a deterioration of the signal-to-noise ratio. This is reflected in the classical input-output relation (1.8). Quantum-mechanically amplification introduces additional noise into the system — as demanded by the fluctuation-dissipation relation (1.19) and the quantum input-output relation (1.18).

A coherent state is the closest quantum-optical equivalent to a classical light beam. Its fluctuations have Poisson statistics, as for independent classical particles. If we are interested in the quantum-optical effects of interaction between light and an amplifying medium, a coherent state is thus the most obvious starting point.

Chapter 3: Propagation of squeezed radiation through amplifying or absorbing random media

After having examined the propagation of "classical" coherent radiation, the logical next step is an extension to states of the radiation field that are nonclassical by nature. Nonclassical states typically have an intensity noise that is smaller than for independent classical particles, a phenomenon referred to as "squeezing" of the state. The intensity fluctuations are "squeezed" (=reduced) at the expense of the phase fluctuations — which become larger.

In the previous chapter we have seen that a quantum-mechanical treatment introduces additional noise into the radiation field. This noise does not discriminate between intensity and phase and hence destroys the squeezing of the radiation, in a way which we will calculate.

Chapter 4: Photon shot noise of localised waves

The previous two chapters deal with the photodetection statistics of a disordered waveguide in the diffusive transport regime. The localised regime is addressed in Chapter 4. We calculate the noise power, which is proportional to the variance of the photocount distribution. For Poisson statistics the noise power P equals the mean current $\bar{I}$.

The ratio $P/\bar{I}$ is known as the Fano factor. We show that, for a coherent incident beam, the Fano factor reaches a universal limit of $1+\frac{3}{2}f$ once the length of the waveguide exceeds the absorption length. Localisation has no effect on this limiting value. This is the optical analogue of the universal $\frac{1}{3}$ suppression ($P/\bar{I} \to \frac{1}{3}$) of the shot noise in electronic systems [Bee92, Nag92].

Chapter 5: Long-range correlation of thermal radiation

So far we have considered the photocounting statistics measured by a single photodetector. The bosonic nature of the radiation leads to correlations in the photocount of two different photodetectors. This effect was discovered by Hanbury-Brown and Twiss [HB56], who used it to measure the angular aperture of a star. (The degree of correlation is sensitive to the aperture, even if the aperture cannot be resolved directly.) The correlation of radiation from a black body disappears if the detectors are separated by more than a coherence length. We have found that for a grey body a residual long-range correlation remains, that is negligibly small for the radiation from a star, but might well be observable in a laboratory setting.

Chapter 6: Quantum limit of the laser linewidth in chaotic cavities

We have introduced the notion of the Petermann factor in Sec. 1.6, as the excess noise of a laser due to overlapping cavity modes. Another, equivalent way of saying this is that the excess noise is due to non-orthogonality of the cavity modes. In the final chapter of this thesis we develop a complete theory for the statistical distribution of the Petermann factor in a chaotic cavity coupled to the outside via a small opening. The Petermann factor is found to scale as $\sqrt{N}$, with N the number of modes radiating through the opening.

Chapter 2

Excess noise for coherent radiation propagating through amplifying random media

2.1 Introduction

The coherent radiation emitted by a laser has a noise spectral density P equal to the time-averaged photocurrent $\bar{I}$. This noise is called photon shot noise, by analogy with electronic shot noise in vacuum tubes. If the radiation is passed through an amplifying medium, P increases more than $\bar{I}$ because of the excess noise due to spontaneous emission [Hen96]. For an ideal linear amplifier, the (squared) signal-to-noise ratio $\bar{I}^2/P$ drops by a factor of 2 as one increases the gain. One says that the amplifier has a noise figure of 2. This is a lower bound on the excess noise for a linear amplifier [Cav82].

Most calculations of the excess noise assume that the amplification occurs in a single propagating mode. (Recent examples include work by Loudon and his group [Jef93, Mat97].) The minimal noise figure of 2 refers to this case. Generalisation to amplification in a multimode waveguide is straightforward if there is no scattering between the modes. The recent interest in amplifying random media [Wie97] calls for an extension of the theory of excess noise to include intermode scattering. Here we present such an extension.

Our central result is an expression for the probability distribution of the photocount in terms of the transmission and reflection matrices t and r of the multimode waveguide. (The noise power P is determined by the variance of this distribution.) Single-mode results in the literature are recovered for scalar t and r. In the ab-

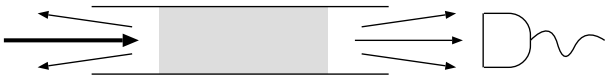

Figure 2.1: Coherent light (thick arrow) is incident on an amplifying medium (shaded), embedded in a waveguide. The transmitted radiation is measured by a photodetector.

sence of any incident radiation our expression reduces to the known photocount distribution for amplified spontaneous emission [Bee98]. We find that intermode scattering strongly increases the excess noise, resulting in a noise figure that is much larger than 2.

We present explicit calculations for two types of geometries, waveguide and cavity, distinguishing between photodetection in transmission and in reflection. We also discuss the parallel with absorbing media. We use the method of random-matrix theory [Bee97] to obtain the required information on the statistical properties of the transmission and reflection matrices of an ensemble of random media. Simple analytical results follow if the number of modes N is large (i.e., for high-dimensional matrices). Close to the laser threshold, the noise figure $\mathcal{F}$ exhibits large sample-to-sample fluctuations, such that the ensemble average diverges. We compute for arbitrary $N \geqslant 2$ the distribution $p(\mathcal{F})$ of $\mathcal{F}$ in the ensemble of disordered cavities, and show that $\mathcal{F} = N$ is the most probable value. This is the generalisation to multimode random media of the single-mode result $\mathcal{F} = 2$ in the literature.

2.2 Formulation of the problem

We consider an amplifying disordered medium embedded in a waveguide that supports $N(\omega)$ propagating modes at frequency ω (see Fig. 2.1). The amplification could be due to stimulated emission by an inverted atomic population or to stimulated Raman scattering [Hen96]. A negative temperature $T < 0$ describes the degree of population inversion in the first case or the density of the material excitation in the second case [Jef93]. A complete population inversion or vanishing density corresponds to the limit $T \to 0$ from below. The minimal noise figure mentioned in the introduction is reached in this limit. The amplification rate $1/\tau_{\rm a}$ is obtained from the (negative) imaginary part ε'' of the (relative) dielectric constant, $1/\tau_{\rm a} = \omega|\varepsilon''|$. Disorder causes multiple scattering with rate $1/\tau_{\rm s}$ and (transport) mean free path $l = c\tau_{\rm s}$ (with c the velocity of light in the medium).

We assume that τ_s and τ_a are both $\gg 1/\omega$, so that scattering as well as amplification occur on length scales large compared to the wavelength. The waveguide is illuminated from one end by monochromatic radiation (frequency ω_0, mean photocurrent I_0) in a coherent state. For simplicity, we assume that the illumination is in a single propagating mode (labelled m_0). At the other end of the waveguide, a photodetector detects the outcoming radiation. We assume, again for simplicity, that all N outgoing modes are detected with equal efficiency α. The case of single-mode detection is considered in Appendix 2.A.

We denote by $p(n)$ the probability to count n photons within a time τ. Its first two moments determine the mean photocurrent $\bar{I}$ and the noise power P, according to

$$\bar{I} = \frac{1}{\tau}\overline{n}\,, \qquad P = \lim_{\tau\to\infty}\frac{1}{\tau}\left(\overline{n^2} - \overline{n}^2\right)\,. \tag{2.1}$$

[The definition of P is equivalent to $P = \int_{-\infty}^{\infty} \mathrm{d}t\, \overline{\delta I(0)\delta I(t)}$, with $\delta I = I - \bar{I}$ the fluctuating part of the photocurrent.] It is convenient to compute the generating function $F(\xi)$ for the factorial cumulants κ_j, defined by

$$F(\xi) = \sum_{j=1}^{\infty}\frac{\kappa_j \xi^j}{j!} = \ln\Big[\sum_{n=0}^{\infty}(1+\xi)^n p(n)\Big]\,. \tag{2.2}$$

One has $\overline{n} = \kappa_1$, $\overline{n^2} = \kappa_2 + \kappa_1(1+\kappa_1)$.

The outgoing radiation in mode n is described by an annihilation operator $a_n^{\mathrm{out}}(\omega)$, using the convention that modes $1, 2, \ldots, N$ are on the left-hand side of the medium and modes $N+1, \ldots, 2N$ are on the right-hand side. The vector a^{out} consists of the operators $a_1^{\mathrm{out}}, a_2^{\mathrm{out}}, \ldots, a_{2N}^{\mathrm{out}}$. Similarly, we define a vector a^{in} for incoming radiation. These two sets of operators each satisfy the bosonic commutation relations

$$[a_n(\omega), a_m^\dagger(\omega')] = \delta_{nm}\delta(\omega-\omega')\,, \qquad [a_n(\omega), a_m(\omega')] = 0\,, \tag{2.3}$$

and are related by the input-output relations [Jef93, Mat95, Gru96b]

$$a^{\mathrm{out}}(\omega) = S(\omega)a^{\mathrm{in}}(\omega) + V(\omega)c^\dagger(\omega)\,. \tag{2.4}$$

We have introduced the $2N\times 2N$ scattering matrix S, the $2N\times 2N$ matrix V, and the vector c of $2N$ bosonic operators. The scattering matrix S can be decomposed into four $N\times N$ reflection and transmission matrices,

$$S = \begin{pmatrix} r' & t' \\ t & r \end{pmatrix}\,. \tag{2.5}$$

Reciprocity imposes the conditions $t' = t^T$, $r = r^T$, and $r' = r'^T$.

The operators c account for spontaneous emission in the amplifying medium. They satisfy the bosonic commutations relation (2.3), which implies that

$$VV^\dagger = SS^\dagger - \mathbb{1} \,. \tag{2.6}$$

Their expectation values are

$$\langle c_n(\omega) c_m^\dagger(\omega') \rangle = -\delta_{nm} \delta(\omega - \omega') \, f(\omega, T) \,, \tag{2.7}$$

with the Bose-Einstein function

$$f(\omega, T) = \left[\exp(\hbar\omega / k_\mathrm{B} T) - 1 \right]^{-1} \tag{2.8}$$

evaluated at negative temperature T (< 0).

2.3 Calculation of the generating function

The probability $p(n)$ that n photons are counted in a time τ is given by [Gla63, Kel64]

$$p(n) = \frac{1}{n!} \langle : W^n \mathrm{e}^{-W} : \rangle \,, \tag{2.9}$$

where the colons denote normal ordering with respect to $a^{\,\mathrm{out}}$, and

$$W = \alpha \int_0^\tau \mathrm{d}t \sum_{n=N+1}^{2N} a_n^{\mathrm{out}\,\dagger}(t) a_n^{\mathrm{out}}(t) \,, \tag{2.10}$$

$$a_n^{\mathrm{out}}(t) = (2\pi)^{-1/2} \int_0^\infty \mathrm{d}\omega \, \mathrm{e}^{-\mathrm{i}\omega t} a_n^{\mathrm{out}}(\omega) \,. \tag{2.11}$$

The generating function (2.2) becomes

$$F(\xi) = \ln \langle : \mathrm{e}^{\xi W} : \rangle \,. \tag{2.12}$$

Expectation values of a normally ordered expression are readily computed using the optical equivalence theorem [Man95]. Application of this theorem to our problem consists in discretising the frequency in infinitesimally small steps of Δ (so that $\omega_p = p\Delta$) and then replacing the annihilation operators $a_n^{\mathrm{in}}(\omega_p), c_n(\omega_p)$ by complex numbers a_{np}^{in}, c_{np} (or their complex conjugates for the corresponding creation operators). The coherent state of the incident radiation corresponds to a

non-fluctuating value of $a_{np}^{\rm in}$ with $|a_{np}^{\rm in}|^2 = \delta_{nm_0}\delta_{pp_0} 2\pi I_0/\Delta$ (with $\omega_0 = p_0\Delta$). The thermal state of the spontaneous emission corresponds to uncorrelated Gaussian distributions of the real and imaginary parts of the numbers c_{np}, with zero mean and variance $\langle(\mathrm{Re}\, c_{np})^2\rangle = \langle(\mathrm{Im}\, c_{np})^2\rangle = -\frac{1}{2} f(\omega_p, T)$. (Note that $f < 0$ for $T < 0$.) To evaluate the characteristic function (2.12) we need to perform Gaussian averages. The calculation is described in Appendix 2.B.

The result takes a simple form in the long-time regime $\omega_{\rm c}\tau \gg 1$, where $\omega_{\rm c}$ is the frequency within which $S(\omega)$ does not vary appreciably. We find

$$F(\xi) = F_{\rm exc}(\xi) - \frac{\tau}{2\pi}\int_0^\infty \ln\det\left[\mathbb{1} - \alpha\xi f(\mathbb{1} - rr^\dagger - tt^\dagger)\right] \mathrm{d}\omega\,, \tag{2.13}$$

$$F_{\rm exc}(\xi) = \alpha\xi\tau I_0 \left(t^\dagger\left[\mathbb{1} - \alpha\xi f(\mathbb{1} - rr^\dagger - tt^\dagger)\right]^{-1} t\right)_{m_0 m_0}\,, \tag{2.14}$$

where $\det(\cdots)$ denotes the determinant and $(\cdots)_{m_0m_0}$ the m_0,m_0 element of a matrix. In Eq. (2.14) the functions f, t, and r are to be evaluated at $\omega = \omega_0$. The integral in Eq. (2.13) is the generating function for the photocount due to amplified spontaneous emission obtained in Ref. [Bee98]. It is independent of the incident radiation and can be eliminated in a measurement by filtering the output through a narrow frequency window around ω_0. The function $F_{\rm exc}(\xi)$ describes the excess noise due to the beating of the coherent radiation with the spontaneous emission [Hen96]. The expression (2.14) is the central result of this chapter.

By expanding $F(\xi)$ in powers of ξ we obtain the factorial cumulants, in view of Eq. (2.2). In what follows we will consider only the contribution from $F_{\rm exc}(\xi)$, assuming that the contribution from the integral over ω has been filtered out as mentioned above. We find

$$\kappa_k = k!\alpha^k \tau f^{k-1} I_0 \left[t^\dagger(\mathbb{1} - rr^\dagger - tt^\dagger)^{k-1} t\right]_{m_0 m_0}\,, \tag{2.15}$$

where again $\omega = \omega_0$ is implied. The mean photocurrent $\bar{I} = \kappa_1/\tau$ and the noise power $P = (\kappa_2 + \kappa_1)/\tau$ become

$$\begin{aligned} \bar{I} &= \alpha I_0 (t^\dagger t)_{m_0 m_0}\,, \quad P = \bar{I} + P_{\rm exc}\,, \\ P_{\rm exc} &= 2\alpha^2 f I_0 \left[t^\dagger(\mathbb{1} - rr^\dagger - tt^\dagger)t\right]_{m_0 m_0}\,. \end{aligned} \tag{2.16}$$

The noise power P exceeds the shot noise $\bar{I}$ by the amount $P_{\rm exc}$.

The formulas above are easily adapted to a measurement in reflection by making the exchange $r \to t'$, $t \to r'$. For example, the mean reflected photocurrent is $\bar{I} = \alpha I_0 (r'^\dagger r')_{m_0 m_0}$, while the excess noise is

$$P_{\rm exc} = 2\alpha^2 f I_0 \left[r'^\dagger(\mathbb{1} - r'r'^\dagger - t't'^\dagger)r'\right]_{m_0 m_0}\,. \tag{2.17}$$

2.4 Noise figure

The noise figure $\mathcal{F}$ is defined as the (squared) signal-to-noise ratio at the input I_0^2/P_0, divided by the signal-to-noise ratio at the output, $\bar{I}^2/P$. Since $P_0 = I_0$ for coherent radiation at the input, one has $\mathcal{F} = (P_{\rm exc} + \bar{I})I_0/\bar{I}^2$, hence

$$\mathcal{F} = -2f\frac{\left(t^\dagger r r^\dagger t + t^\dagger t t^\dagger t\right)_{m_0m_0}}{\left(t^\dagger t\right)^2_{m_0m_0}} + \frac{1+2\alpha f}{\alpha\left(t^\dagger t\right)_{m_0m_0}}\,. \tag{2.18}$$

The noise figure is independent of I_0. For large amplification the second term on the right-hand side can be neglected relative to the first, and the noise figure becomes also independent of the detection efficiency α. The minimal noise figure for given r and t is reached for an ideal detector ($\alpha = 1$) and at complete population inversion ($f = -1$).

Since $(t^\dagger r r^\dagger t + t^\dagger t t^\dagger t)_{m_0m_0} = \sum_k |(t^\dagger r)_{m_0k}|^2 + \sum_k |(t^\dagger t)_{m_0k}|^2 \geqslant (t^\dagger t)^2_{m_0m_0}$, one has $\mathcal{F} \geqslant -2f$ for large amplification [when the second term on the right-hand side of Eq. (2.18) can be neglected]. The minimal noise figure $\mathcal{F} = 2$ at complete population inversion is reached in the absence of reflection [$(t^\dagger r)_{m_0k} = 0$] and in the absence of intermode scattering [$(t^\dagger t)_{m_0k} = 0$ if $k \neq m_0$]. This is realised in the single-mode theories of Refs. [Jef93, Mat97]. Our result (2.18) generalises these theories to include scattering between the modes, as is relevant for a random medium.

These formulas apply to detection in transmission. For detection in reflection one has instead

$$\mathcal{F} = -2f\frac{\left(r'^\dagger t' t'^\dagger r' + r'^\dagger r' r'^\dagger r'\right)_{m_0m_0}}{\left(r'^\dagger r'\right)^2_{m_0m_0}} + \frac{1+2\alpha f}{\alpha\left(r'^\dagger r'\right)_{m_0m_0}}\,. \tag{2.19}$$

Again, for large amplification the second term on the right-hand side may be neglected relative to the first. The noise figure then becomes smallest in the absence of transmission, when $\mathcal{F} = -2f(r'^\dagger r' r'^\dagger r')_{m_0m_0}(r'^\dagger r')^{-2}_{m_0m_0} \geqslant -2f$. The minimal noise figure of 2 at complete population inversion requires $(r'^\dagger r' r'^\dagger r')_{m_0m_0} = (r'^\dagger r')^2_{m_0m_0}$, which is possible only in the absence of intermode scattering.

To make analytical progress in the evaluation of $\mathcal{F}$, we will consider an ensemble of random media, with different realisations of the disorder. For large N and away from the laser threshold, the sample-to-sample fluctuations in numerators and denominators of Eqs. (2.18) and (2.19) are small, so we may average them separately. Furthermore, the "equivalent channel approximation" is accurate for random media [Mel92], which says that the ensemble averages are independent

of the mode index m_0. Summing over m_0, we may therefore write $\mathcal{F}$ as the ratio of traces, so the noise figure for a measurement in transmission becomes

$$\mathcal{F} = -2f N \frac{\prec \mathrm{tr}(t^\dagger r r^\dagger t + t^\dagger t t^\dagger t) \succ}{\prec \mathrm{tr}\, t^\dagger t \succ^2} + N \frac{1 + 2\alpha f}{\alpha \prec \mathrm{tr}\, t^\dagger t \succ}, \tag{2.20}$$

and similarly for a measurement in reflection. The brackets $\prec \cdots \succ$ denote the ensemble average.

2.5 Applications

2.5.1 Amplifying disordered waveguide

As a first example, we consider a weakly amplifying, strongly disordered waveguide of length L. Averages of the moments of $rr^\dagger$ and $tt^\dagger$ for this system have been computed by Brouwer [Bro98] as a function of the number of propagating modes N, the mean free path l, and the amplification length $\xi_\mathrm{a} = \sqrt{D\tau_\mathrm{a}}$, where $1/\tau_\mathrm{a}$ is the amplification rate and $D = cl/3$ is the diffusion constant. It is assumed that $1/N \ll l/\xi_\mathrm{a} \ll 1$ but the ratio $L/\xi_\mathrm{a} \equiv s$ is arbitrary. In this regime, sample-to-sample fluctuations are small, so the ensemble average is representative of a single system.

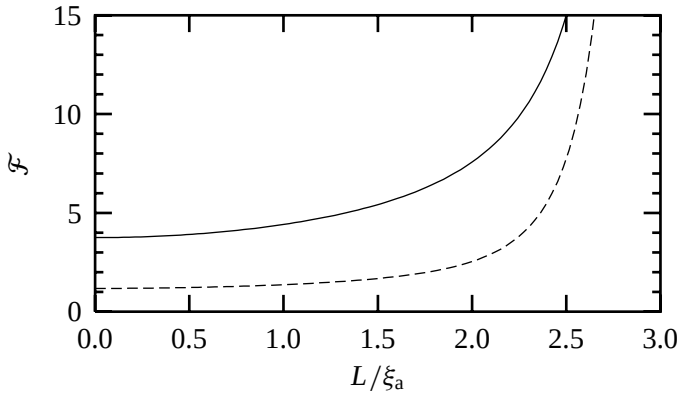

Figure 2.2: Noise figure of an amplifying disordered waveguide (length L, amplification length ξ_a) measured in transmission (solid line) and in reflection (dashed line). The curves are computed from Eqs. (2.21)–(2.24) for $\alpha = 1$, $f = -1$, and $L/l = 10$. The laser threshold is at $L/\xi_\mathrm{a} = \pi$.

The results for a measurement in transmission are

$$\bar{I} = \frac{4\alpha l}{3L} I_0 \frac{s}{\sin s} , \tag{2.21}$$

$$P_{\rm exc} = \frac{2\alpha^2 l}{3L} f I_0 s \left(\frac{3}{\sin s} - \frac{2s - \operatorname{cotan} s}{\sin^2 s} + \frac{s \operatorname{cotan} s - 1}{\sin^3 s} - \frac{s}{\sin^4 s} \right) . \tag{2.22}$$

For a measurement in reflection, one finds

$$\bar{I} = \alpha I_0 \left(1 - \frac{4l}{3L} s \operatorname{cotan} s \right) , \tag{2.23}$$

$$P_{\rm exc} = \frac{2\alpha^2 l}{3L} f I_0 s \left(2 \operatorname{cotan} s - \frac{1}{\sin s} + \frac{\operatorname{cotan} s}{\sin^2 s} + \frac{s \operatorname{cotan} s - 1}{\sin^3 s} - \frac{s}{\sin^4 s} \right) . \tag{2.24}$$

The noise figure $\mathcal{F}$ follows from $\mathcal{F} = (P_{\rm exc} + \bar{I}) I_0 / \bar{I}^2$. It is plotted in Fig. 2.2. One notices a strong increase in $\mathcal{F}$ on approaching the laser threshold at $s = \pi$.

2.5.2 Amplifying disordered cavity

Our second example is an optical cavity filled with an amplifying random medium. The radiation leaves the cavity through a waveguide supporting N modes. The formulas for a measurement in reflection apply with $t = 0$ because there is no transmission. The distribution of the eigenvalues of $r^\dagger r$ is known in the large-N limit [Bee99] as a function of the dimensionless amplification rate $\gamma = 2\pi / N \tau_a \Delta\omega$ (with $\Delta\omega$ the spacing of the cavity modes near frequency ω_0). The first two moments of this distribution are

$$N^{-1} \prec \operatorname{tr} r^\dagger r \succ = \frac{1}{1-\gamma} , \tag{2.25}$$

$$N^{-1} \prec \operatorname{tr} r^\dagger r r^\dagger r \succ = \frac{2\gamma^2 - 2\gamma + 1}{(1-\gamma)^4} . \tag{2.26}$$

The resulting photocurrent has mean and variance

$$\bar{I} = \alpha I_0 \frac{1}{1-\gamma} , \tag{2.27}$$

$$P_{\rm exc} = 2\alpha^2 f I_0 \gamma \frac{\gamma - \gamma^2 - 1}{(1-\gamma)^4} . \tag{2.28}$$

The resulting noise figure for $\alpha = 1$ and $f = -1$,

$$\mathcal{F} = \frac{1 - \gamma + \gamma^2 + \gamma^3}{(1-\gamma)^2} , \tag{2.29}$$

is plotted in Fig. 2.3. Again, we see a strong increase of $\mathcal{F}$ on approaching the laser threshold at $\gamma = 1$.

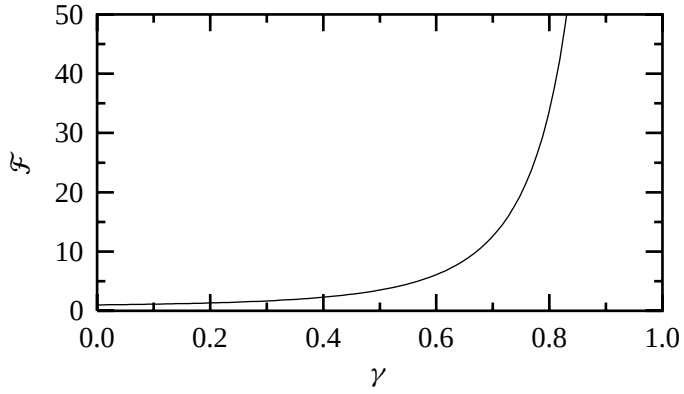

Figure 2.3: Noise figure of an amplifying disordered cavity, connected to a photodetector via an N-mode waveguide. The curve is the result (2.29), as a function of the dimensionless amplification rate γ. (Ideal detection efficiency, $\alpha = 1$, and full population inversion, $f = -1$, are assumed in this plot.) The laser threshold occurs at $\gamma = 1$.

2.6 Near the laser threshold

In the preceding section we have taken the large-N limit. In that limit the noise figure diverges on approaching the laser threshold. In this section we consider the vicinity of the laser threshold for arbitrary N.

The scattering matrix $S(\omega)$ has poles in the lower half of the complex plane. With increasing amplification, the poles shift upward. The laser threshold is reached when a pole reaches the real axis, say at resonance frequency $\omega_{\rm th}$. For ω near $\omega_{\rm th}$ the scattering matrix has the generic form

$$S_{nm} = \frac{\sigma_n \sigma_m}{\omega - \omega_{\rm th} + \frac{1}{2}{\rm i}\Gamma - {\rm i}/2\tau_{\rm a}} \,, \tag{2.30}$$

where σ_n is the complex coupling constant of the resonance to the nth mode in the waveguide, Γ is the decay rate, and $1/\tau_{\rm a}$ the amplification rate. The laser threshold is at $\Gamma\tau_{\rm a} = 1$.

We assume that the incident radiation has frequency $\omega_0 = \omega_{\rm th}$. Substitution of Eq. (2.30) into Eq. (2.18) or (2.19) gives the simple result

$$\mathcal{F} = \frac{-2f\Sigma}{|\sigma_{m_0}|^2} \,, \qquad \Sigma = \sum_{n=1}^{2N} |\sigma_n|^2 \,, \tag{2.31}$$

for the limiting value of the noise figure on approaching the laser threshold. The limit is the same for detection in transmission and in reflection. Since the coupling constant $|\sigma_{m_0}|^2$ to the mode m_0 of the incident radiation can be much smaller than the total coupling constant Σ, the noise figure (2.31) has large fluctuations. We need to consider the statistical distribution $p(\mathcal{F})$ in the ensemble of random media. The typical (or modal) value of $\mathcal{F}$ is the value $\mathcal{F}_{\rm typ}$ at which $p(\mathcal{F})$ is maximal. We will see that this remains finite although the ensemble average $\prec\mathcal{F}\succ$ of $\mathcal{F}$ diverges.

2.6.1 Waveguide geometry

We first consider the case of an amplifying disordered waveguide. The total coupling constant $\Sigma = \Sigma_{\rm l} + \Sigma_{\rm r}$ is the sum of the coupling constant $\Sigma_{\rm l} = \sum_{n=1}^{N} |\sigma_n|^2$ to the left end of the waveguide and the coupling constant $\Sigma_{\rm r} = \sum_{n=N+1}^{2N} |\sigma_n|^2$ to the right. The assumption of equivalent channels implies that

$$\prec 1/\mathcal{F}\succ = -\frac{1}{2fN}\prec \Sigma_{\rm l}/\Sigma\succ = -\frac{1}{4fN}\,. \tag{2.32}$$

Since the average of $1/\mathcal{F}$ is finite, it is reasonable to assume that $\mathcal{F}_{\rm typ} \approx \prec 1/\mathcal{F}\succ^{-1} = -4fN$, or $\mathcal{F}_{\rm typ} \approx 4N$ for complete population inversion. The scaling with N explains why the large-N theory of the preceding section found a divergent noise figure at the laser threshold. We conclude that the divergency of $\mathcal{F}$ at $L/\xi_{\rm a} = \pi$ in Fig. 2.2 is cut off at a value of order N, if $\mathcal{F}$ is identified with the typical value $\mathcal{F}_{\rm typ}$.

2.6.2 Cavity geometry

In the case of an amplifying disordered cavity, we can make a more precise statement on $p(\mathcal{F})$. Since there is only reflection, there is only one $\Sigma = \sum_{n=1}^{N} |\sigma_n|^2$. The assumption of equivalent channels now gives

$$\prec 1/\mathcal{F}\succ = -\frac{1}{2fN}\,. \tag{2.33}$$

Following the same reasoning as in the case of the waveguide, we would conclude that $\mathcal{F}_{\rm typ} \approx \prec 1/\mathcal{F}\succ^{-1} = -2fN$. We will see that this is correct within a factor of 2.

To compute $p(\mathcal{F})$ we need the distribution of the dimensionless coupling constants $u_n = \sigma_n/\sqrt{\Sigma}$. The N complex numbers u_n form a vector $\vec{u}$ of length 1. According to random-matrix theory [Bee97], the distribution $p(S)$ of the scattering

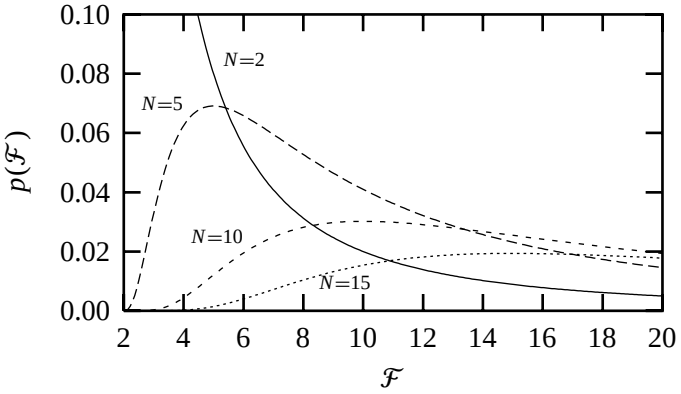

Figure 2.4: Probability distribution of the noise figure near the laser threshold for an amplifying disordered cavity, computed from Eq. (2.36) for $f = -1$. The most probable value is $\mathcal{F} = N$, while the average value diverges.

matrix is invariant under unitary transformations $S \to USU^T$ (with U an $N \times N$ unitary matrix). It follows that the distribution $p(\vec{u})$ of the vector $\vec{u}$ is invariant under rotations $\vec{u} \to U\vec{u}$, hence

$$p(u_1, u_2, \ldots, u_N) \propto \delta\Big(1 - \sum_n |u_n|^2\Big) \,. \tag{2.34}$$

In other words, the vector $\vec{u}$ has the same distribution as a column of a matrix that is uniformly distributed in the unitary group [Per83]. By integrating out $N-1$ of the u_n's we find the marginal distribution of u_{m_0},

$$p(u_{m_0}) = \frac{N-1}{\pi} \left(1 - |u_{m_0}|^2\right)^{N-2} \,, \tag{2.35}$$

for $N \geqslant 2$ and $|u_{m_0}|^2 \leqslant 1$.

The distribution of $\mathcal{F} = -2f|u_{m_0}|^{-2}$ becomes

$$p(\mathcal{F}) = -2f(N-1)\left(1 + \frac{2f}{\mathcal{F}}\right)^{N-2} \mathcal{F}^{-2} \,, \tag{2.36}$$

for $N \geqslant 2$ and $\mathcal{F} \geqslant -2f$. We have plotted $p(\mathcal{F})$ in Fig. 2.4 for complete population inversion ($f = -1$) and several choices of N. It is a broad distribution, all its moments are divergent. The typical value of the noise figure is the value at which $p(\mathcal{F})$ becomes maximal, hence

$$\mathcal{F}_{\text{typ}} = -fN \,, \qquad N \geqslant 2 \,. \tag{2.37}$$

In the single-mode case, in contrast, $\mathcal{F} = -2f$ for every member of the ensemble [hence $p(\mathcal{F}) = \delta(\mathcal{F} + 2f)$]. We conclude that the typical value of the noise figure near the laser threshold of a disordered cavity is larger than in the single-mode case by a factor $N/2$.

2.7 Absorbing media

The general theory of Sec. 2.2 can also be applied to an absorbing medium, in equilibrium at temperature $T > 0$. Eq. (2.4) then has to be replaced with

$$a^{\text{out}}(\omega) = S(\omega)a^{\text{in}}(\omega) + Q(\omega)b(\omega)\,, \tag{2.38}$$

where the bosonic operator b has the expectation value

$$\langle b_n^\dagger(\omega)b_m(\omega')\rangle = \delta_{nm}\delta(\omega-\omega')\,f(\omega,T)\,, \tag{2.39}$$

and the matrix Q is related to S by

$$QQ^\dagger = \mathbb{1} - SS^\dagger\,. \tag{2.40}$$

The formulas for $F(\xi)$ of Sec. 2.3 remain unchanged.

Ensemble averages for absorbing systems follow from the corresponding results for amplifying systems by substitution $\tau_{\text{a}} \to -\tau_{\text{a}}$. The results for an absorbing disordered waveguide with detection in transmission are

$$\bar{I} = \frac{4\alpha l}{3L} I_0 \frac{s}{\sinh s}\,, \tag{2.41}$$

$$P_{\text{exc}} = \frac{2\alpha^2 l}{3L}\, f I_0 s \left(\frac{3}{\sinh s} - \frac{2s + \operatorname{cotanh} s}{\sinh^2 s} - \frac{s\operatorname{cotanh} s - 1}{\sinh^3 s} + \frac{s}{\sinh^4 s} \right), \tag{2.42}$$

where $s = L/\xi_{\text{a}}$ with ξ_{a} the absorption length. Similarly, for detection in reflection one has

$$\bar{I} = \alpha I_0 \left(1 - \frac{4l}{3L} s \operatorname{cotanh} s \right), \tag{2.43}$$

$$P_{\text{exc}} = \frac{2\alpha^2 l}{3L}\, f I_0 s \left(2\operatorname{cotanh} s - \frac{1}{\sinh s} - \frac{\operatorname{cotanh} s}{\sinh^2 s} - \frac{s\operatorname{cotanh} s - 1}{\sinh^3 s} + \frac{s}{\sinh^4 s} \right). \tag{2.44}$$

These formulas follow from Eqs. (2.21)–(2.24) upon substitution of $s \to is$.

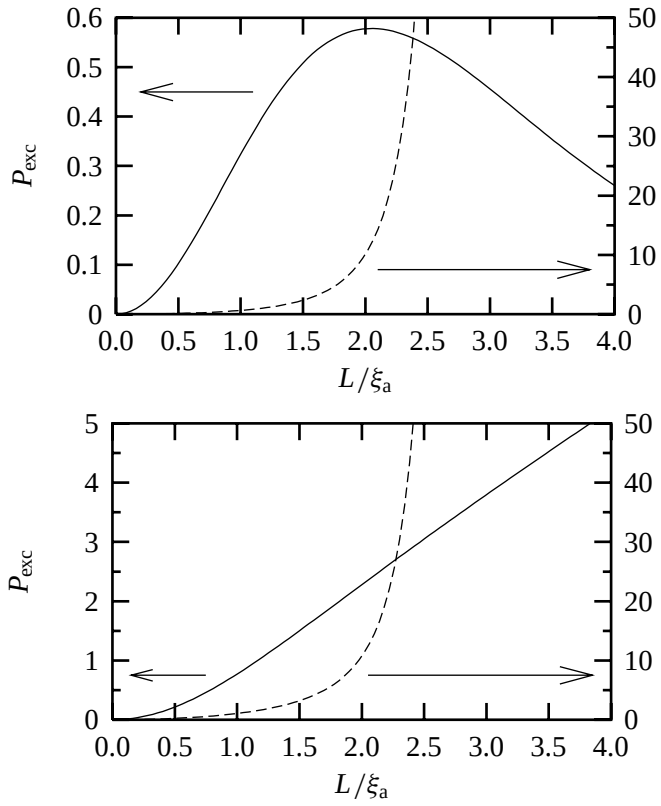

Figure 2.5: Excess noise power $P_{\rm exc}$ for an absorbing (solid line, left axis) and amplifying disordered waveguide (dashed line, right axis), in units of $\alpha^2 l|f|I_0/L$. The top panel is for detection in transmission, the bottom panel for detection in reflection.

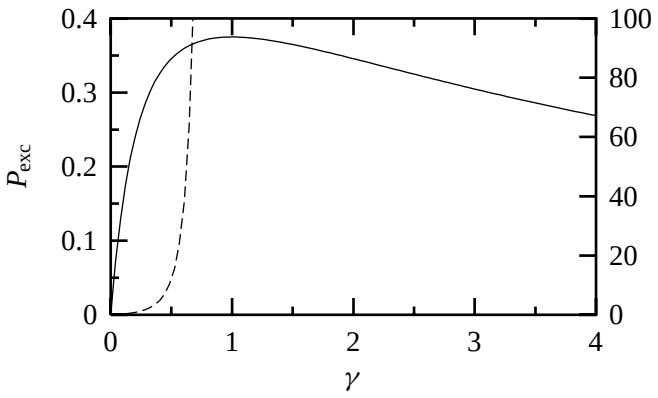

Figure 2.6: Excess noise power $P_{\rm exc}$ for an absorbing (solid line, left axis) and amplifying disordered cavity (dashed line, right axis), in units of $\alpha^2|f|I_0$.

For an absorbing disordered cavity, we find [substituting $\gamma \to -\gamma$ in Eqs. (2.27) and (2.28)],

$$\bar{I} = \alpha I_0 \frac{1}{1+\gamma}\,, \tag{2.45}$$

$$P_{\rm exc} = 2\alpha^2 f I_0 \gamma \frac{\gamma^2+\gamma+1}{(1+\gamma)^4}\,, \tag{2.46}$$

with γ the dimensionless absorption rate.

Since typically $f \ll 1$ in absorbing systems, the noise figure $\mathcal{F}$ is dominated by shot noise, $\mathcal{F} \approx I_0/\bar{I}$. Instead of $\mathcal{F}$ we therefore plot the excess noise power $P_{\rm exc}$ in Figs. 2.5 and 2.6. In contrast to the monotonic increase of $P_{\rm exc}$ with $1/\tau_{\rm a}$ in amplifying systems, the absorbing systems show a maximum in $P_{\rm exc}$ for certain geometries. The maximum occurs near $L/\xi_{\rm a} = 2$ for the disordered waveguide with detection in transmission, and near $\gamma = 1$ for the disordered cavity. For larger absorption rates the excess noise power decreases because $\bar{I}$ becomes too small for appreciable beating with the spontaneous emission.

2.8 Conclusion

In summary, we have studied the photodetection statistics of coherent radiation that has been transmitted or reflected by an amplifying or absorbing random medium. The cumulant generating function $F(\xi)$ is the sum of two terms. The first

term is the contribution from spontaneous emission obtained in Ref. [Bee98]. The second term $F_{\rm exc}$ is the excess noise due to beating of the coherent radiation with the spontaneous emission. Equation (2.14) relates $F_{\rm exc}$ to the transmission and reflection matrices of the medium.

In the applications of our general result for the cumulant generating function we have concentrated on the second cumulant, which gives the spectral density $P_{\rm exc}$ of the excess noise. We have found that $P_{\rm exc}$ increases monotonically with increasing amplification rate, while it has a maximum as a function of absorption rate in certain geometries.

In amplifying systems we studied how the noise figure $\mathcal{F}$ increases on approaching the laser threshold. Near the laser threshold the noise figure shows large sample-to-sample fluctuations, such that its statistical distribution in an ensemble of random media has divergent first and higher moments. The most probable value of $\mathcal{F}$ is of the order of the number N of propagating modes in the medium, independent of material parameters such as the mean free path. It would be of interest to observe this universal limit in random lasers.

2.A Single-mode detection

We have assumed throughout this chapter that all N modes propagating through the waveguide are detected at either the left or the right end. At the opposite extreme one can consider the case of single-mode detection. This is particularly relevant in a slab geometry, where the cross-sectional area of the photodetector is much less than the area of the random medium (see Fig. 2.7). The number of detected modes is then much smaller than the number of modes N propagating through the medium. The limit of single-mode detection is reached when the

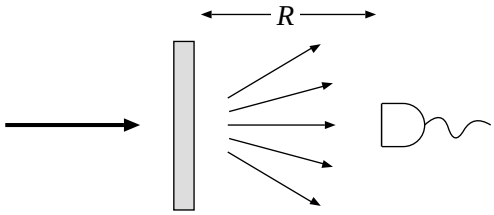

Figure 2.7: Schematic diagram of detection of radiation propagating through a slab. Single-mode detection occurs when the area of the photodetector becomes less than R^2/N.

photodetector covers an area comparable to the area of one speckle or smaller.

Single-mode detection of thermal radiation was considered in Ref. [Bee98]. Denoting the detected mode by the index n_0, the mean photocurrent was found to be

$$\bar{I}_{\text{thermal}} = \int_0^\infty \frac{\mathrm{d}\omega}{2\pi} j_{\text{thermal}}(\omega)\,, \tag{2.47}$$

$$j_{\text{thermal}}(\omega) = \alpha f (\mathbb{1} - rr^\dagger - tt^\dagger)_{n_0 n_0}\,, \tag{2.48}$$

and the noise power

$$P_{\text{thermal}} = \int_0^\infty \frac{\mathrm{d}\omega}{2\pi} j^2_{\text{thermal}}(\omega)\,. \tag{2.49}$$

In this case of single-mode detection the noise power contains no information beyond what is contained in the photocurrent.

The same holds for the excess noise considered in this chapter. The mean transmitted photocurrent in a narrow frequency interval around ω_0 is given by

$$\bar{I} = \alpha I_0 |t_{n_0 m_0}|^2\,, \tag{2.50}$$

and the excess noise

$$P_{\text{exc}} = 2\bar{I}\, j_{\text{thermal}}(\omega_0) \tag{2.51}$$

is simply the product of the mean transmitted photocurrent and thermal current density. Noise measurements in single-mode detection are thus not nearly as interesting as in multi-mode detection, since the latter give information on the scattering properties that is not contained in the mean photocurrent.

2.B Derivation of Eq. (2.14)

To evaluate the Gaussian averages that lead to Eq. (2.14), it is convenient to use a matrix notation. We replace the summation in Eq. (2.10) by a multiplication of the vector a^{out} with the projection $\mathcal{P}a^{\text{out}}$, where the projection matrix $\mathcal{P}$ has zero elements except $\mathcal{P}_{nn} = 1$, $N+1 \leqslant n \leqslant 2N$. We thus write

$$W = \alpha \int_0^\tau \mathrm{d}t\, a^{\text{out}\dagger}(t) \mathcal{P} a^{\text{out}}(t)\,. \tag{2.52}$$

Insertion of Eqs. (2.4) and (2.11) gives

$$W = \frac{\alpha}{2\pi}\int_0^\tau \mathrm{d}t \int_0^\infty \mathrm{d}\omega \int_0^\infty \mathrm{d}\omega' \big[a^{\mathrm{in}^\dagger}(\omega)S^\dagger(\omega) + c(\omega)V^\dagger(\omega)\big] \times \mathcal{P}\big[S(\omega')a^{\mathrm{in}}(\omega') + V(\omega')c^\dagger(\omega')\big]\mathrm{e}^{\mathrm{i}(\omega-\omega')t} \,. \quad (2.53)$$

As explained in Sec. 2.3, we discretise the frequency as $\omega_p = p\Delta$, $p = 1,2,3,\ldots$. The integral over frequency is then replaced with a summation,

$$\int_0^\infty \mathrm{d}\omega\, g(\omega) \to \Delta \sum_{p=1}^\infty g(\omega_p) \,. \quad (2.54)$$

We write Eq. (2.53) as a matrix multiplication,

$$\xi W = a^{\mathrm{in}^\dagger} A a^{\mathrm{in}} + cBc^\dagger + a^{\mathrm{in}^\dagger} C^\dagger c^\dagger + cCa^{\mathrm{in}} \,, \quad (2.55)$$

with the definitions

$$\begin{aligned}
A_{np,n'p'} &= \frac{\alpha\Delta\xi}{2\pi}\int_0^\tau \mathrm{d}t \left[S^\dagger(\omega_p)\mathcal{P}S(\omega_{p'})\right]_{nn'} \mathrm{e}^{\mathrm{i}\Delta(p-p')t} \,, \\
B_{np,n'p'} &= \frac{\alpha\Delta\xi}{2\pi}\int_0^\tau \mathrm{d}t \left[V^\dagger(\omega_p)\mathcal{P}V(\omega_{p'})\right]_{nn'} \mathrm{e}^{\mathrm{i}\Delta(p-p')t} \,, \\
C_{np,n'p'} &= \frac{\alpha\Delta\xi}{2\pi}\int_0^\tau \mathrm{d}t \left[V^\dagger(\omega_p)\mathcal{P}S(\omega_{p'})\right]_{nn'} \mathrm{e}^{\mathrm{i}\Delta(p-p')t} \,, \\
a^{\mathrm{in}}_{np} &= \Delta^{1/2} a^{\mathrm{in}}_n(\omega_p) \,, \qquad c_{np} = \Delta^{1/2} c_n(\omega_p) \,.
\end{aligned} \quad (2.56)$$

We now apply the optical equivalence theorem [Man95], as discussed in Sec. 2.3. The operators a^{in}_{np} are replaced by constant numbers $\delta_{nm_0}\delta_{pp_0}(2\pi I_0/\Delta)^{1/2}$. The operators c_{np} are replaced by independent Gaussian variables, such that the expectation value (2.12) takes the form of a Gaussian integral,

$$\begin{aligned}
\langle : \mathrm{e}^{\xi W} : \rangle &= \int \mathrm{d}\{c_{np}\} \exp\left[\xi W + \sum_{np} |c_{np}|^2 / f(\omega_p, T)\right] \\
&= \int d\{c_{np}\} \exp\left[a^{\mathrm{in}^*} A a^{\mathrm{in}} - cMc^* + a^{\mathrm{in}^*} C^\dagger c^* + cCa^{\mathrm{in}}\right] \,,
\end{aligned} \quad (2.57)$$

where we have defined

$$M_{np,n'p'} = -B_{np,n'p'} - \frac{\delta_{nn'}\delta_{pp'}}{f(\omega_p)} \,. \quad (2.58)$$

We eliminate the cross-terms of $a^{\rm in}$ and c in Eq. (2.57) by the substitution

$$c'^{*} = c^{*} - M^{-1} C a^{\rm in} , \tag{2.59}$$

leading to

$$\langle : \mathrm{e}^{\xi W} : \rangle = \exp\left[a^{\rm in *} (A + C^{\dagger} M^{-1} C) a^{\rm in} \right] \int d\left\{ c'_{np} \right\} \exp\left(-c' M c'^{*} \right) . \tag{2.60}$$

The integral is proportional to the determinant of M^{-1}, giving the generating function

$$\begin{aligned} F(\xi) &= \text{const} - \ln\det M + a^{\rm in *} \left(A + C^{\dagger} M^{-1} C \right) a^{\rm in} \\ &= \text{const} - \ln\det M + \frac{2\pi I_0}{\Delta} \left(A + C^{\dagger} M^{-1} C \right)_{m_0 p_0, m_0 p_0} . \end{aligned} \tag{2.61}$$

The additive constant follows from $F(0) = 0$. The term $-\ln\det M$ is the contribution from amplified spontaneous emission calculated in Ref. [Bee98]. The term proportional to I_0 is the excess noise of the coherent radiation, termed $F_{\rm exc}$ in Sec. 2.3.

Eq. (2.61) can be simplified in the long-time regime, $\omega_{\rm c}\tau \gg 1$. We may then set $\Delta = 2\pi/\tau$ and use

$$\int_0^{\tau} \mathrm{e}^{\mathrm{i}\Delta(p-p')t} \, \mathrm{d}t = \tau \delta_{pp'} . \tag{2.62}$$

The matrices defined in Eq. (2.56) thus become diagonal in the frequency index,

$$A_{np,n'p'} = \frac{\alpha \Delta \tau \xi}{2\pi} \left[S^{\dagger}(\omega_p) \mathcal{P} S(\omega_p) \right]_{nn'} \delta_{pp'} \tag{2.63}$$

and similarly for B and C. We then find

$$(A + C^{\dagger} M^{-1} C)_{np,n'p'} = \frac{\alpha \xi \Delta \tau}{2\pi} \left[S^{\dagger} \mathcal{P} (\mathbb{1} + \alpha \xi f V V^{\dagger} \mathcal{P})^{-1} S \right]_{nn'} \delta_{pp'} , \tag{2.64}$$

where f, S, and V are evaluated at $\omega = \omega_p$. Substitution into Eq. (2.61) gives the result (2.14) for $F_{\rm exc}(\xi)$.

Simplification of Eq. (2.61) is also possible in the short-time regime, when $\Omega_{\rm c}\tau \ll 1$, with $\Omega_{\rm c}$ the frequency range over which $SS^{\dagger}$ differs appreciably from the unit matrix. The generating function then is

$$\begin{aligned} F_{\rm exc}(\xi) = \alpha \xi \tau I_0 \Bigg[t^{\dagger}(\omega_0) \Big(\mathbb{1} - \frac{\alpha \xi \tau}{2\pi} \int_0^{\infty} \mathrm{d}\omega \, f(\omega, T) \\ \times \left[\mathbb{1} - r(\omega) r^{\dagger}(\omega) - t(\omega) t^{\dagger}(\omega) \right] \Big)^{-1} t(\omega_0) \Bigg]_{m_0 m_0} . \end{aligned} \tag{2.65}$$

Chapter 3

Propagation of squeezed radiation through amplifying or absorbing random media

3.1 Introduction

Squeezed radiation is in a state in which one of the quadratures of the electric field fluctuates less than the other [Wal94, Man95]. Such a nonclassical state is useful, because the fluctuations in the photon flux can be reduced below that of a Poisson process — at the expense of enhanced fluctuations in the phase. Sub-Poissonian noise is a delicate feature of the radiation, it is easily destroyed by the interaction with an absorbing or amplifying medium [Hen96]. The noise from spontaneous emission events is responsible for the degradation of the squeezing.

Because of the fundamental and practical importance, there exists a considerable literature on the propagation of squeezed and other nonclassical states of light through absorbing or amplifying media. We cite some of the most recent papers on this topic [Leo93, Jef94, Sch96, Bar98, Art99, Knö99, Abd99]. The main simplification of these investigations is the restriction to systems in which the scattering is one-dimensional, such as parallel dielectric layers. Each propagating mode can then be treated separately from any other mode. It is the purpose of the present paper to remove this restriction, by presenting a general theory for three-dimensional scattering, and to apply it to a medium with randomly located scattering centra.

This chapter builds on the previous one, in which we considered the propagation of a coherent state through such a random medium. Physically, the problem

considered here is different because a coherent state has Poisson noise, so that the specific nonclassical features of squeezed radiation do not arise in Ch. 2. Technically, the difference is that a squeezed state, as most other nonclassical states, lacks a diagonal representation in terms of coherent states [Wal94, Man95]. We cannot therefore directly extend the theory of the previous chapter to the propagation of squeezed states. The basic idea of our approach remains the same: The photodetection statistics of the transmitted radiation is related to that of the incident radiation by means of the scattering matrix of the medium. The method of random-matrix theory [Bee97] is then used to evaluate the noise properties of the transmitted radiation, averaged over an ensemble of random media with different positions of the scatterers.

The outline of this chapter is as follows. In Sec. 3.2 we first summarise the scattering formalism, and then show how the characteristic function of the state of the transmitted radiation can be obtained from that of the incident state. This allows us to compute the photocount statistics as measured in direct detection (Sec. 3.3), and in homodyne photodetection measurements (Sec. 3.4). The expressions in Secs. 3.2–3.4 are generally valid for any incident state. In Sec. 3.5 we specialise to the case that the incident radiation is in an ideal squeezed state (also known as a squeezed state of minimal uncertainty, or as a two-photon coherent state [Wal94, Man95]). The statistics of direct and homodyne measurements are expressed in terms of the degree of squeezing of the incident state. The Fano factor, introduced in Sec. 3.6, quantifies the degree to which the squeezing has been destroyed by the propagation through an amplifying or absorbing medium. The ensemble average of the Fano factor is then computed using random-matrix theory in Sec. 3.7. We conclude in Sec. 3.8.

3.2 Scattering formulation

We consider an amplifying or absorbing disordered medium embedded in a waveguide that supports $N(\omega)$ propagating modes at frequency ω. The conceptual advantage of embedding the medium in a waveguide is that we can give a scattering formulation in terms of a finite-dimensional matrix. The outgoing radiation in mode n is described by an annihilation operator $a_n^{\rm out}(\omega)$, using the convention that modes $1,2,\ldots,N$ are on the left-hand-side of the medium and modes $N+1,\ldots,2N$ are on the right-hand-side. The vector $a^{\rm out}$ consists of the operators $a_1^{\rm out}, a_2^{\rm out}, \ldots, a_{2N}^{\rm out}$. Similarly, we define a vector $a^{\rm in}$ for incoming radiation.

These two sets of operators each satisfy the bosonic commutation relations

$$[a_n(\omega), a_m^\dagger(\omega')] = \delta_{nm}\delta(\omega-\omega')\,, \qquad [a_n(\omega), a_m(\omega')] = 0\,. \tag{3.1}$$

They are related by the input-output relations [Jef93, Gru96b, Bee98]

$$a^{\rm out}(\omega) = S(\omega)a^{\rm in}(\omega) + Q(\omega)b(\omega)\,, \tag{3.2a}$$
$$a^{\rm out}(\omega) = S(\omega)a^{\rm in}(\omega) + V(\omega)c^\dagger(\omega)\,, \tag{3.2b}$$

where the first equation is for an absorbing medium and the second for an amplifying medium. We have introduced the $2N\times 2N$ scattering matrix S, the $2N\times 2N$ matrices Q and V, and the vectors b and c of $2N$ bosonic operators. The scattering matrix can be decomposed into four $N\times N$ reflection and transmission matrices,

$$S = \begin{pmatrix} r' & t' \\ t & r \end{pmatrix}\,. \tag{3.3}$$

Reciprocity imposes the conditions $t' = t^T$, $r = r^T$, and $r' = r'^T$.

The operators b and c account for spontaneous emission in the medium. They satisfy the bosonic commutation relations (3.1), hence

$$QQ^\dagger = \mathbb{1} - SS^\dagger\,, \qquad VV^\dagger = SS^\dagger - \mathbb{1}\,. \tag{3.4}$$

Their expectation values are

$$\langle b_n^\dagger(\omega)b_m(\omega')\rangle = \delta_{nm}\delta(\omega-\omega')\,f(\omega,T)\,, \tag{3.5a}$$
$$\langle c_n(\omega)c_m^\dagger(\omega')\rangle = -\delta_{nm}\delta(\omega-\omega')\,f(\omega,T)\,. \tag{3.5b}$$

The Bose-Einstein function

$$f(\omega,T) = \left[\exp(\hbar\omega/k_{\rm B}T) - 1\right]^{-1} \tag{3.6}$$

is evaluated at positive temperature T for an absorbing medium and at negative temperature for an amplifying medium.

It is convenient to discretise the frequency in infinitesimally small steps of Δ, so that $\omega_p = p\Delta$, and treat the frequency index p as a separate vector index (in addition to the mode index n). For example, $a_{np}^{\rm out} = a_n^{\rm out}(\omega_p)$ and $S_{np,n'p'} = S_{nn'}(\omega_p)\delta_{pp'}$.

The state of the outgoing radiation is described by the characteristic function

$$\chi_{\rm out}(\eta) = \langle : \exp\Big(\Delta^{1/2} \sum_{n,p} \big[a_n^{\rm out\dagger}(\omega_p)\eta_n(\omega_p) - \eta_n^*(\omega_p) a_n^{\rm out}(\omega_p) \big] \Big) : \rangle$$
$$= \langle : \exp\big[\Delta^{1/2} (a^{\rm out\dagger}\eta - \eta^\dagger a^{\rm out}) \big] : \rangle \,, \tag{3.7}$$

where $\langle : \cdots : \rangle$ indicates the expectation value of a normally ordered product of operators $a^{\rm out}$ and $a^{\rm out\dagger}$ (creation operators to the left of the annihilation operators). The vector η has elements $\eta_{np} = \eta_n(\omega_p)$. The density operator of the outgoing radiation is uniquely defined by the characteristic function $\chi_{\rm out}$ [Wal94]. Similarly, the incoming state has characteristic function

$$\chi_{\rm in}(\eta) = \langle : \exp\big[\Delta^{1/2} (a^{\rm in\dagger}\eta - \eta^\dagger a^{\rm in}) \big] : \rangle \,. \tag{3.8}$$

The characteristic function of the thermal radiation inside an absorbing medium is given by

$$\chi_{\rm abs}(\eta) = \langle : \exp\big[\Delta^{1/2} (b^\dagger \eta - \eta^\dagger b) \big] : \rangle = \exp\Big(- \sum_{n,p} \eta_{np}^* \, f(\omega_p, T) \eta_{np} \Big)$$
$$\equiv \exp(-\eta^\dagger f \eta) \,. \tag{3.9}$$

In the final equality f denotes the matrix with elements $f_{np,n'p'} = \delta_{nn'}\delta_{pp'} f(\omega_p, T)$. For an amplifying medium, replacing b by $c^\dagger$ and normal ordering by anti-normal ordering, one finds instead

$$\chi_{\rm amp}(\eta) = \exp(\eta^\dagger f \eta) \,. \tag{3.10}$$

Combination of Eqs. (3.2) and (3.4) with Eqs. (3.7–3.10) yields a relationship between the characteristic functions of the incoming and outgoing states,

$$\chi_{\rm out}(\eta) = \exp\left(-\eta^\dagger [\mathbb{1} - SS^\dagger] f \eta \right) \chi_{\rm in}(S^\dagger \eta) \,. \tag{3.11}$$

This relation holds both for absorbing and amplifying media, because the difference in sign in the exponent of Eqs. (3.9) and (3.10) is cancelled by the difference in sign between $QQ^\dagger = \mathbb{1} - SS^\dagger$ and $VV^\dagger = -(\mathbb{1} - SS^\dagger)$.

3.3 Photocount distribution

The photocount distribution is the probability $p(n)$ that n photons are absorbed by a photodetector within a certain time τ (see Fig. 3.1). The factorial cumulants

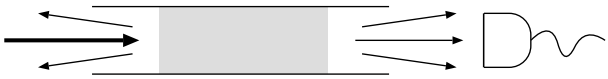

Figure 3.1: Schematic illustration of direct detection: Radiation is incident on a random medium (shaded). The transmitted radiation is absorbed by a photodetector.

κ_j of $p(n)$ (the first two being $\kappa_1 = \overline{n}$ and $\kappa_2 = \overline{n(n-1)} - \overline{n}^2$) are most easily obtained from the generating function [Man95]

$$F(\xi) = \sum_{j=1}^{\infty} \frac{\kappa_j \xi^j}{j!} = \ln\left(\sum_{n=0}^{\infty} (1+\xi)^n p(n)\right) . \tag{3.12}$$

The generating function is determined by a normally ordered expectation value [Gla63, Kel64],

$$\mathrm{e}^{F(\xi)} = \langle : \mathrm{e}^{\xi W} : \rangle , \qquad W = \int_0^{\tau} \mathrm{d}t \sum_{n=1}^{2N} d_n a_n^{\mathrm{out}\dagger}(t) a_n^{\mathrm{out}}(t) . \tag{3.13}$$

Here $d_n \in [0,1]$ is the detection efficiency of the nth mode and the time-dependent operators are defined as

$$a_n^{\mathrm{out}}(t) = (2\pi)^{-1/2} \int_0^{\infty} \mathrm{d}\omega \, \mathrm{e}^{-\mathrm{i}\omega t} a_n^{\mathrm{out}}(\omega) . \tag{3.14}$$

Discretising the frequencies as described in Sec. 3.2, one can write

$$W = \frac{\Delta^2}{2\pi} \int_0^{\tau} \mathrm{d}t \sum_n d_n \sum_{p,p'} \mathrm{e}^{\mathrm{i}\Delta(p-p')t} a_n^{\mathrm{out}\dagger}(\omega_p) a_n^{\mathrm{out}}(\omega_{p'}) . \tag{3.15}$$

This expression can be simplified in the limit $\tau \to \infty$ of long counting times, when one can set $\Delta = 2\pi/\tau$ and use

$$\int_0^{\tau} \mathrm{e}^{\mathrm{i}\Delta(p-p')t} \, \mathrm{d}t = \tau \delta_{pp'} . \tag{3.16}$$

Hence, in the long-time limit the generating function is given by

$$\mathrm{e}^{F(\xi)} = \langle : \exp\left(\xi \Delta \sum_{n,p} d_n a_n^{\mathrm{out}\dagger}(\omega_p) a_n^{\mathrm{out}}(\omega_p)\right) : \rangle \equiv \langle : \exp(\xi \Delta a^{\mathrm{out}\dagger} \mathcal{D} a^{\mathrm{out}}) : \rangle , \tag{3.17}$$

where we have defined the matrix of detector efficiencies $\mathcal{D}_{np,n'p'} = d_n \delta_{nn'} \delta_{pp'}$.

Comparing Eqs. (3.7) and (3.17) we see that the generating function $F(\xi)$ can be obtained from the characteristic function $\chi_{\rm out}$ by convolution with a Gaussian,

$$\mathrm{e}^{F(\xi)} = \frac{1}{\det(-\xi\,\pi\mathcal{D})} \int \mathrm{d}\eta\, \chi_{\rm out}(\eta) \exp\left(\frac{1}{\xi}\eta^\dagger \mathcal{D}^{-1}\eta\right), \tag{3.18}$$

where $\int \mathrm{d}\eta$ is an integration over the real and imaginary parts of η. We now substitute the relation (3.11) between $\chi_{\rm out}$ and $\chi_{\rm in}$, to arrive at a relation between $F(\xi)$ and $\chi_{\rm in}$:

$$\mathrm{e}^{F(\xi)} = \frac{1}{\det(-\xi\,\pi\mathcal{D})} \int \mathrm{d}\eta\, \chi_{\rm in}(S^\dagger\eta) \exp\left(\frac{1}{\xi}\eta^\dagger \mathcal{D}^{-1}\eta - \eta^\dagger(\mathbb{1} - SS^\dagger) f\,\eta\right). \tag{3.19}$$

The fluctuations in the photocount are partly due entirely to thermal fluctuations, which would exist even without any incident radiation. If we denote by $F_{\rm th}(\xi)$ the generating function of these thermal fluctuations, then Eq. (3.19) can be written in the form

$$F(\xi) = F_{\rm th}(\xi) + \ln\Big[\frac{1}{\det(\pi M)} \int \mathrm{d}\eta\, \chi_{\rm in}(\eta) \exp\left(-\eta^\dagger M^{-1}\eta\right)\Big], \tag{3.20}$$

$$F_{\rm th}(\xi) = -\ln\det\big[\mathbb{1} - \xi\,\mathcal{D}(\mathbb{1} - SS^\dagger) f\big]. \tag{3.21}$$

We have defined the Hermitian matrix

$$M = -\xi S^\dagger\big[\mathbb{1} - \xi\,\mathcal{D}(\mathbb{1} - SS^\dagger) f\big]^{-1} \mathcal{D} S, \tag{3.22}$$

and we have performed a change of integration variables from η to $S^\dagger\eta$ [with Jacobian $\det(SS^\dagger)$].

The expression (3.21) generalises the result of Ref. [Bee98] to arbitrary detection-efficiency matrix $\mathcal{D}$. Returning to a continuous frequency, it can be written as (recall that $\Delta = 2\pi/\tau$)

$$F_{\rm th}(\xi) = -\frac{\tau}{2\pi} \int_0^\infty \mathrm{d}\omega \ln\det\Big(\mathbb{1} - \xi\, D\big[\mathbb{1} - S(\omega)S^\dagger(\omega)\big] f(\omega, T)\Big), \tag{3.23}$$

where D is a $2N \times 2N$ diagonal matrix containing the detection efficiencies d_n on the diagonal ($D_{nm} = d_n \delta_{nm}$). The first two factorial cumulants are

$$\kappa_1^{\rm th} = \tau \int_0^\infty \frac{\mathrm{d}\omega}{2\pi} f(\omega, T)\, \mathrm{tr}\, D\big[\mathbb{1} - S(\omega)S^\dagger(\omega)\big], \tag{3.24}$$

$$\kappa_2^{\rm th} = \tau \int_0^\infty \frac{\mathrm{d}\omega}{2\pi} f^2(\omega, T)\, \mathrm{tr}\left(D[\mathbb{1} - S(\omega)S^\dagger(\omega)]\right)^2. \tag{3.25}$$

Note that all factorial cumulants depend linearly on the detection time τ in the long-time limit.

If only the N modes at one side of the waveguide are detected (with equal efficiency d), then $d_n = 0$ for $1 \leqslant n \leqslant N$ and $d_n = d$ for $N+1 \leqslant n \leqslant 2N$, hence

$$F_{\rm th}(\xi) = -\frac{\tau}{2\pi}\int_0^\infty {\rm d}\omega \ln\det\Big(\mathbb{1} - \xi d\big[\mathbb{1} - r(\omega)r^\dagger(\omega) - t(\omega)t^\dagger(\omega)\big] f(\omega,T)\Big)\,, \tag{3.26}$$

in agreement with Ref. [Bee99].

The difference $F(\xi) - F_{\rm th}(\xi)$ contains the noise from the incident radiation by itself as well as the excess noise due to beating of the incident radiation with the vacuum fluctuations. If the incident radiation is in a coherent state, then $\chi_{\rm in}(\eta) = \exp(\alpha^\dagger\eta - \eta^\dagger\alpha)$ for some vector α (called the displacement vector) with elements $\alpha_{np} = \alpha_n(\omega_p)$. Substitution into Eq. (3.20) gives the generating function

$$\begin{aligned} F(\xi) &= F_{\rm th}(\xi) - \alpha^\dagger M\alpha\,, \\ &= F_{\rm th}(\xi) + \frac{\tau\xi}{2\pi}\int_0^\infty {\rm d}\omega\, \alpha^\dagger(\omega)S^\dagger(\omega)\Big[\mathbb{1} - \xi D\big[\mathbb{1} - S(\omega)S^\dagger(\omega)\big] f(\omega,T)\Big]^{-1} \\ &\qquad\qquad \times DS(\omega)\alpha(\omega)\,. \end{aligned} \tag{3.27}$$

The first two factorial cumulants are

$$\kappa_1 = \tau\int_0^\infty \frac{{\rm d}\omega}{2\pi}\alpha^\dagger(\omega)S^\dagger(\omega)DS(\omega)\alpha(\omega) + \kappa_1^{\rm th}\,, \tag{3.28}$$

$$\kappa_2 = 2\tau\int_0^\infty \frac{{\rm d}\omega}{2\pi} f(\omega,T)\alpha^\dagger(\omega)S^\dagger(\omega)D\big[\mathbb{1} - S(\omega)S^\dagger(\omega)\big]DS(\omega)\alpha(\omega) + \kappa_2^{\rm th}\,. \tag{3.29}$$

If the incident coherent radiation is in a single mode m_0 and monochromatic with frequency ω_0, then Eqs. (3.27–3.29) simplify for detection in transmission to

$$F(\xi) = F_{\rm th}(\xi) + \tau\xi d I_0\Big(t^\dagger\big[\mathbb{1} - \xi d(\mathbb{1} - rr^\dagger - tt^\dagger) f(\omega_0,T)\big]^{-1}t\Big)_{m_0m_0}\,, \tag{3.30}$$

$$\kappa_1 = I_0\tau d[t^\dagger t]_{m_0m_0} + \kappa_1^{\rm th}\,, \tag{3.31}$$

$$\kappa_1^{\rm th} = \tau d\int_0^\infty \frac{{\rm d}\omega}{2\pi} f(\omega,T)\,{\rm tr}\big[\mathbb{1} - r(\omega)r^\dagger(\omega) - t(\omega)t^\dagger(\omega)\big]\,, \tag{3.32}$$

$$\kappa_2 = 2I_0\tau d^2 f(\omega_0,T)\big[t^\dagger(\mathbb{1} - rr^\dagger - tt^\dagger)t\big]_{m_0m_0} + \kappa_2^{\rm th}\,, \tag{3.33}$$

$$\kappa_2^{\rm th} = \tau d^2\int_0^\infty \frac{{\rm d}\omega}{2\pi} f^2(\omega,T)\,{\rm tr}\big[\mathbb{1} - r(\omega)r^\dagger(\omega) - t(\omega)t^\dagger(\omega)\big]^2\,. \tag{3.34}$$

Here $I_0 = (2\pi)^{-1}\int_0^\infty d\omega\,|\alpha|^2$ is the incident photon flux and the matrices r and t without frequency argument are to be evaluated at frequency ω_0. These are the results of Ch. 2.

3.4 Homodyne detection

The photocount measurement described in Sec. 3.3 (known as direct detection) cannot distinguish between the two quadratures of the electric field. Such phase dependent information can be retrieved by homodyne detection, i.e. by superimposing a strong probe beam (described by operators $a^{\rm probe}$) onto the signal beam (see Fig. 3.2). The total radiation incident on the detector is described by the operator

$$a^{\rm total} = \kappa^{1/2} a^{\rm out} + (1-\kappa)^{1/2} a^{\rm probe}\,, \tag{3.35}$$

where the factor $\sqrt{\kappa}$ accounts for the attenuation of the signal beam by the beam splitter that superimposes it onto the probe beam. (For simplicity we assume a real scalar κ, more generally κ would be a complex coupling matrix.)

The characteristic function of $a^{\rm total}$ is the product of the characteristic functions of $a^{\rm out}$ and $a^{\rm probe}$. We assume that the probe beam is in the coherent state with displacement vector β, having elements $\beta_{np} = \beta_n(\omega_p)$. From Eq. (3.11) one gets

$$\chi_{\rm total}(\eta) = \exp\left[-\kappa\eta^\dagger(\mathbb{1} - SS^\dagger)\,f\,\eta + (1-\kappa)^{1/2}(\beta^\dagger\eta - \eta^\dagger\beta)\right]\chi_{\rm in}(S^\dagger\kappa^{1/2}\eta)\,. \tag{3.36}$$

The generating function $F_{\rm homo}(\xi)$ of the photocount distribution in homodyne de-

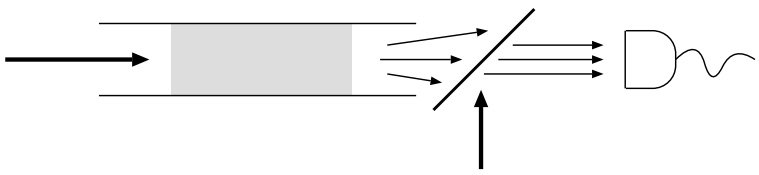

Figure 3.2: Schematic illustration of homodyne detection: At the left, radiation is incident on a random medium (shaded). At the right, a strong coherent beam is superimposed onto the transmitted radiation, and the combined radiation is absorbed by a photodetector.

tection is given by [cf. Eq. (3.17)]

$$\begin{aligned}\exp[F_{\rm homo}(\xi)] &= \langle{:}\exp(\xi\,\Delta a^{\rm total\dagger}\mathcal{D}a^{\rm total}){:}\rangle \\ &\approx \exp\bigl[\xi(1-\kappa)\beta^\dagger\mathcal{D}\beta\bigr]\langle{:}\exp\Bigl(\Delta^{1/2}\sqrt{\kappa(1-\kappa)}\xi\bigl[a^{\rm out\dagger}\mathcal{D}\beta+\beta^\dagger\mathcal{D}a^{\rm out}\bigr]\Bigr){:}\rangle\,.\end{aligned} \tag{3.37}$$

In the second approximate equality we have linearised the exponent with respect to $a^{\rm out}$, which is justified if the probe beam is much stronger than the signal beam. The remaining expectation value has the form of a characteristic function if we take ξ purely imaginary, so that $\xi^* = -\xi$. The result is

$$\begin{aligned}F_{\rm homo}(\xi) &= \xi(1-\kappa)\beta^\dagger\mathcal{D}\beta + \ln\chi_{\rm out}(\sqrt{\kappa(1-\kappa)}\xi\,\mathcal{D}\beta) \\ &= \xi(1-\kappa)\beta^\dagger\mathcal{D}\beta + \kappa(1-\kappa)\xi^2\beta^\dagger\mathcal{D}(\mathbb{1}-SS^\dagger)\,f\,\mathcal{D}\beta \\ &\qquad + \ln\chi_{\rm in}(\sqrt{\kappa(1-\kappa)}\xi\,S^\dagger\mathcal{D}\beta)\,.\end{aligned} \tag{3.38}$$

In the second equation we have substituted the relation (3.11) between $\chi_{\rm out}$ and $\chi_{\rm in}$.

3.5 Squeezed radiation

We consider the case that the incident radiation is in the ideal squeezed state $|\epsilon,\alpha\rangle = \mathcal{C}\mathcal{S}|0\rangle$ [Wal94, Man95], obtained from the vacuum state $|0\rangle$ by subsequent action of the squeezing operator

$$\mathcal{S} = \exp\bigl[\tfrac{1}{2}\Delta(a^{\rm in}\epsilon^* a^{\rm in} - a^{\rm in^\dagger}\epsilon a^{\rm in^\dagger})\bigr] \tag{3.39}$$

and the displacement operator

$$\mathcal{C} = \exp\bigl[\Delta^{1/2}(a^{\rm in^\dagger}\alpha - \alpha^\dagger a^{\rm in})\bigr]\,. \tag{3.40}$$

As in the previous sections, we have discretised the frequency, $\omega_p = p\Delta$, and used the vector of operators $a^{\rm in}_{np} = a^{\rm in}_n(\omega_p)$. The complex squeezing parameters $\epsilon_n(\omega) = \rho_n(\omega)\mathrm{e}^{\mathrm{i}\phi_n(\omega)}$ are contained in the diagonal matrix ϵ with elements $\epsilon_{np,n'p'} = \epsilon_n(\omega_p)\delta_{nn'}\delta_{pp'}$. Similarly, the vector α with elements $\alpha_{np} = \alpha_n(\omega_p)$ contains the displacement parameters.

The characteristic function of the incident radiation is given by [Wal94, Yue76]

$$\begin{aligned}\chi_{\rm in}(\eta) = \exp\Bigl[&\alpha^\dagger\eta - \eta^\dagger\alpha - \tfrac{1}{4}\eta^T(\mathrm{e}^{-\mathrm{i}\phi}\sinh 2\rho)\eta - \tfrac{1}{4}\eta^\dagger(\mathrm{e}^{\mathrm{i}\phi}\sinh 2\rho)\eta^* \\ &- \eta^\dagger(\sinh^2\rho)\eta\Bigr]\,.\end{aligned} \tag{3.41}$$

According to Eq. (3.11), we thus find for the characteristic function of the outgoing radiation

$$\chi_{\rm out}(\eta) = \exp\Bigg(\alpha^\dagger S^\dagger \eta - \eta^\dagger S\alpha - \frac{1}{4}\eta^T S^*(\mathrm{e}^{-\mathrm{i}\phi}\sinh 2\rho)S^\dagger\eta \\ -\frac{1}{4}\eta^\dagger S(\mathrm{e}^{\mathrm{i}\phi}\sinh 2\rho)S^T\eta^* - \eta^\dagger\big[f - S(f-\sinh^2\rho)S^\dagger\big]\eta\Bigg)\,. \quad (3.42)$$

The generating function $F(\xi)$ of the photocount distribution is obtained from $\chi_{\rm in}$ by convolution with a Gaussian, cf. Eq. (3.18). We find

$$F(\xi) = F_{\rm th}(\xi) - \tfrac{1}{2}\ln\det X - \tfrac{1}{2}\begin{pmatrix}\alpha^*\\ \alpha\end{pmatrix}^T X^{-1}\begin{pmatrix}M\alpha\\ M^*\alpha^*\end{pmatrix}, \quad (3.43)$$

where the matrix X is defined in terms of the matrix M by

$$X = \mathbb{1} + \begin{pmatrix} M\sinh\rho & -M\mathrm{e}^{\mathrm{i}\phi}\cosh\rho \\ -M^*\mathrm{e}^{-\mathrm{i}\phi}\cosh\rho & M^*\sinh\rho\end{pmatrix}\begin{pmatrix}\sinh\rho & 0\\ 0 & \sinh\rho\end{pmatrix}. \quad (3.44)$$

If squeezing is absent, $\rho = 0$, hence $X = \mathbb{1}$ and Eq. (3.43) reduces to the result (3.27) for coherent radiation. For a squeezed vacuum ($\alpha = 0$) one has simply $F(\xi) = F_{\rm th}(\xi) - \frac{1}{2}\ln\det X$.

If the radiation is incident only in mode m_0, then we may compute the matrix inverse and the determinant in Eq. (3.43) explicitly. The matrix $M(\omega)$ defined in Eq. (3.22) may be replaced by its m_0, m_0 element,

$$M_{m_0m_0}(\omega) \equiv m = -\xi\Big[S^\dagger\big(\mathbb{1} - \xi D[\mathbb{1} - SS^\dagger]f\big)^{-1}DS\Big]_{m_0m_0}. \quad (3.45)$$

Note that m is real, since it is the diagonal element of a Hermitian matrix. The resulting generating function is

$$F(\xi) = F_{\rm th}(\xi) - \tfrac{1}{2}\tau\int_0^\infty\frac{\mathrm{d}\omega}{2\pi}\ln(1+2m\sinh^2\rho - m^2\sinh^2\rho) \\ -\tau\int_0^\infty\frac{\mathrm{d}\omega}{2\pi}m|\alpha|^2\frac{1+m\sinh\rho[\sinh\rho+\cosh\rho\cos(2\arg\alpha-\phi)]}{1+2m\sinh^2\rho-m^2\sinh^2\rho}\,. \quad (3.46)$$

The first two factorial cumulants, for detection in transmission, are

$$\kappa_1 = \kappa_1^{\rm th} + \tau d \int_0^\infty \frac{{\rm d}\omega}{2\pi}(|\alpha|^2 + \sinh^2\rho)[t^\dagger t]_{m_0 m_0} \,, \tag{3.47}$$

$$\begin{aligned}\kappa_2 = \kappa_2^{\rm th} &+ 2\tau d^2 \int_0^\infty \frac{{\rm d}\omega}{2\pi}(|\alpha|^2 + \sinh^2\rho)\, f[t^\dagger(\mathbb{1} - rr^\dagger - tt^\dagger)t]_{m_0 m_0} \\ &+ \tau d^2 \int_0^\infty \frac{{\rm d}\omega}{2\pi}[t^\dagger t]^2_{m_0 m_0}\big[|\alpha\cosh\rho - \alpha^* {\rm e}^{{\rm i}\phi}\sinh\rho|^2 - |\alpha|^2 \\ &+ \sinh^2\rho(\cosh^2\rho + \sinh^2\rho)\big] \,,\end{aligned} \tag{3.48}$$

where $\kappa_1^{\rm th}$ and $\kappa_2^{\rm th}$ are given by Eqs. (3.32) and (3.34).

The generating function for homodyne detection follows from Eqs. (3.38) and (3.42),

$$\begin{aligned}F_{\rm homo}(\xi) &= \xi(1-\kappa)\beta^\dagger \mathcal{D}\beta + \xi\sqrt{\kappa(1-\kappa)}(\alpha^\dagger S^\dagger \mathcal{D}\beta + \beta^\dagger \mathcal{D} S\alpha) \\ &- \frac{1}{4}\xi^2\kappa(1-\kappa)\big[\beta\mathcal{D}S^*({\rm e}^{-{\rm i}\phi}\sinh 2\rho)S^\dagger\mathcal{D}\beta + \beta^\dagger\mathcal{D}S({\rm e}^{{\rm i}\phi}\sinh 2\rho)S^T\mathcal{D}\beta^*\big] \\ &+ \xi^2\kappa(1-\kappa)\beta^\dagger\mathcal{D}\big[f - S(f - \sinh^2\rho)S^\dagger\big]\mathcal{D}\beta \,.\end{aligned} \tag{3.49}$$

All factorial cumulants except for the first two vanish in the strong-probe approximation. We may simplify the generating function by assuming that the signal beam is incident in a single mode m_0 and that the probe beam is also in a single mode n_0. For detection in transmission one then has the factorial cumulants

$$\kappa_1 = \tau d \int_0^\infty \frac{{\rm d}\omega}{2\pi}\Big((1-\kappa)|\beta|^2 + 2\sqrt{\kappa(1-\kappa)}\,{\rm Re}[\alpha\beta^* t_{n_0 m_0}]\Big) \,, \tag{3.50}$$

$$\begin{aligned}\kappa_2 &= -\tau\kappa(1-\kappa)d^2\int_0^\infty\frac{{\rm d}\omega}{2\pi}{\rm Re}\big[\beta^{*2}{\rm e}^{{\rm i}\phi}t^2_{n_0 m_0}\big]\sinh 2\rho \\ &+ 2\tau\kappa(1-\kappa)d^2\int_0^\infty\frac{{\rm d}\omega}{2\pi}|\beta|^2\big[|t_{n_0 m_0}|^2\sinh^2\rho + f(\mathbb{1} - rr^\dagger - tt^\dagger)_{n_0 n_0}\big] \,.\end{aligned} \tag{3.51}$$

3.6 Fano factor

For the application of these general formulas we focus our attention on the Fano factor $\mathcal{F}$, defined as the ratio of the noise power $P = \tau^{-1}\,{\rm var}\, n$ and the mean current $\bar{I} = \tau^{-1}\bar{n}$:

$$\mathcal{F} = P/\bar{I} = 1 + \kappa_2/\kappa_1 \,. \tag{3.52}$$

(We have assumed the limit $\tau \to \infty$.) For coherent radiation $\mathcal{F} = 1$, corresponding to Poisson statistics. Thermal radiation has $\mathcal{F} > 1$ (super-Poissonian). Nonclassical states, such as squeezed states, can have $\mathcal{F} < 1$.

We assume that the radiation is incident in a single mode m_0 and is detected in transmission (equal efficiency d per transmitted mode). We consider a frequency-resolved measurement, covering a narrow frequency interval around the central frequency ω_0 of the incident radiation. The thermal contributions $\kappa_1^{\rm th}$ and $\kappa_2^{\rm th}$ may then be neglected, since they are spread out over a wide frequency range. The incident radiation has Fano factor $\mathcal{F}_{\rm in}$, measured in direct detection with unit efficiency. For squeezed radiation, one has

$$\mathcal{F}_{\rm in} = 1 + \frac{|\alpha\cosh\rho - \alpha^* \mathrm{e}^{\mathrm{i}\phi}\sinh\rho|^2 - |\alpha|^2 + \sinh^2\rho(\cosh^2\rho + \sinh^2\rho)}{|\alpha|^2 + \sinh^2\rho} \,. \quad (3.53)$$

We seek the Fano factor of the transmitted radiation, both for direct detection ($\mathcal{F}_{\rm direct}$) and for homodyne detection ($\mathcal{F}_{\rm homo}$). Combining Eqs. (3.47) and (3.48), we find for direct detection

$$\mathcal{F}_{\rm direct} - 1 = d(t^\dagger t)_{m_0m_0}(\mathcal{F}_{\rm in} - 1) + 2d\ f(\omega_0, T)\frac{[t^\dagger(\mathbb{1} - rr^\dagger - tt^\dagger)t]_{m_0m_0}}{(t^\dagger t)_{m_0m_0}} \,. \quad (3.54)$$

The first term is due entirely to the incident radiation. It is absent for coherent radiation (because then $\mathcal{F}_{\rm in} = 0$). The second term is due to the beating of the incident radiation with the vacuum fluctuations. It is independent of the incident radiation and was studied in detail in Ch. 2. Sub-Poissonian counting statistics, i.e. $\mathcal{F}_{\rm direct} < 1$, is in an amplifying medium ($f \leqslant -1$) only possible when

$$2(t^\dagger t t^\dagger t)_{m_0m_0} < (t^\dagger t)^2_{m_0m_0} + 2(t^\dagger t)_{m_0m_0} - 2(t^\dagger r r^\dagger t)_{m_0m_0} \,. \quad (3.55)$$

In the absence of reflection ($r = 0$) and inter-mode scattering (t diagonal), this reduces to the well-known condition [Cav82, Lou84, Ste86] $(t^\dagger t)_{m_0m_0} < 2$. Since $(t^\dagger t t^\dagger t)_{m_0m_0} = \sum_k |(t^\dagger t)_{m_0k}|^2 \geqslant (t^\dagger t)^2_{m_0m_0}$, the presence of inter-mode scattering decreases the maximally allowed amplification factor $(t^\dagger t)_{m_0m_0}$.

The Fano factor in the strong-probe approximation ($|\beta| \to \infty$) follows from Eqs. (3.50) and (3.51), with the result

$$\mathcal{F}_{\rm homo} - 1 = 2d\kappa|t_{n_0m_0}|^2\sinh^2\rho + 2d\kappa f(\omega_0, T)(\mathbb{1} - rr^\dagger - tt^\dagger)_{n_0n_0} - d\kappa\,\mathrm{Re}\big[\mathrm{e}^{\mathrm{i}(\phi - 2\arg\beta)}t^2_{n_0m_0}\big]\sinh 2\rho \,. \quad (3.56)$$

In the strong-probe approximation, it is independent of α and $|\beta|$. Similarly to Eq. (3.54), the first term is entirely due to the incident radiation, vanishing for

coherent radiation ($\rho = 0$), and the second term is due the beating with vacuum fluctuations. The additional third term describes the effect of the phase of the probe beam on the measurement. Typically, in a measurement one would vary the phase of the probe beam until the Fano factor is minimised, which occurs when $\arg\beta = \frac{1}{2}\phi + \arg t_{n_0 m_0}$. The resulting Fano factor $\mathcal{F}^{\min}_{\text{homo}}$ is given by

$$\mathcal{F}^{\min}_{\text{homo}} = 1 - 2d\kappa |t_{n_0 m_0}|^2 \mathrm{e}^{-\rho} \sinh\rho + 2d\kappa f(\omega_0, T)(\mathbb{1} - rr^\dagger - tt^\dagger)_{n_0 n_0} \,. \quad (3.57)$$

Squeezing in the outgoing radiation for an amplifying medium is only possible when $|t_{n_0 m_0}|^2 < 2 - 2(rr^\dagger)_{n_0 n_0} - \sum_{k \neq m_0} |t_{n_0 k}|^2$. The single-mode limit $|t_{n_0 m_0}|^2 = 2$ is thus decreased by both reflection and inter-mode scattering.

3.7 Ensemble averages

The expressions for the Fano factor given in the previous section contain the reflection and transmission matrices of the waveguide. These are N-dimensional matrices that depend on the positions of the scatterers inside the waveguide. The distribution of these matrices in an ensemble of disordered waveguides is described by random-matrix theory [Bee97]. Ensemble averages of moments of $rr^\dagger$ and $tt^\dagger$ for $N \gg 1$ have been computed by Brouwer [Bro98], as a function of the mean free path l and the amplification (absorption) length $\xi_{\text{a}} = \sqrt{D\tau_{\text{a}}}$, where $1/\tau_{\text{a}}$ is the amplification (absorption) rate and $D = cl/3$ is the diffusion constant. It is assumed that both ξ_{a} and L are small compared to the localisation length Nl but large compared to the mean free path l. Obviously, this requires a large number N of propagating modes. The relative size of L and ξ_{a} is arbitrary.

As sample-to-sample fluctuations are small for $N \gg 1$, we can take in Eq. (3.54) the averages of numerator and denominator separately. The dependence on the index m_0 of the incident mode drops out on averaging, $\langle \cdots \rangle_{m_0 m_0} = N^{-1} \langle \mathrm{tr} \cdots \rangle$. For an absorbing disordered waveguide, we find

$$\begin{aligned} \mathcal{F}_{\text{direct}} = 1 &+ \frac{4ld}{3\xi_{\text{a}} \sinh s} (\mathcal{F}_{\text{in}} - 1) \\ &+ \frac{d}{2} f(\omega_0, T) \left[3 - \frac{2s + \operatorname{cotanh} s}{\sinh s} - \frac{s \operatorname{cotanh} s - 1}{\sinh^2 s} + \frac{s}{\sinh^3 s} \right] . \end{aligned} \quad (3.58)$$

We have abbreviated $s = L/\xi_{\text{a}}$. In the limit of strong absorption, $s \to \infty$, the Fano factor approaches the universal limit $\mathcal{F}_{\text{direct}} = 1 + \frac{3}{2} df$ (see Sec. 4.4). The Fano factor $\mathcal{F}_{\text{in}}$ is given by Eq. (3.53) for an incident squeezed state, but Eq. (3.58) is more generally valid for any state of the incident radiation.

The result for an amplifying disordered waveguide follows by the replacement $\tau_a \to -\tau_a$, hence $\xi_a \to i\xi_a$:

$$\mathcal{F}_{\rm direct} = 1 + \frac{4ld}{3\xi_a \sin s}(\mathcal{F}_{\rm in} - 1) + \frac{d}{2} f(\omega_0, T)\left[3 - \frac{2s - \cot an\, s}{\sin s} + \frac{s\, \cot an\, s - 1}{\sin^2 s} - \frac{s}{\sin^3 s}\right]. \quad (3.59)$$

The Fano factor diverges at the laser threshold $s = \pi$. The function $f(\omega_0, T)$ now has to be evaluated at a negative temperature. For a complete population inversion of the atomic states $f \to -1$.

The minimal Fano factor in homodyne detection is given by Eq. (3.57). The average $\langle |t_{n_0 m_0}|^2 \rangle$ is again independent of the mode indices, hence it can be replaced by $N^{-2}\langle {\rm tr}\, tt^\dagger \rangle$. For an absorbing waveguide we find

$$\mathcal{F}^{\rm min}_{\rm homo} = 1 - \frac{8ld\kappa}{3N\xi_a \sinh s} e^{-\rho} \sinh\rho + \frac{8ld\kappa}{3\xi_a} f(\omega_0, T)\left[{\rm cotanh}\, s + \frac{1}{\sinh s}\right], \quad (3.60)$$

and for an amplifying waveguide

$$\mathcal{F}^{\rm min}_{\rm homo} = 1 - \frac{8ld\kappa}{3N\xi_a \sin s} e^{-\rho} \sinh\rho + \frac{8ld\kappa}{3\xi_a} f(\omega_0, T)\left[\cot an\, s - \frac{1}{\sin s}\right]. \quad (3.61)$$

Measurement of the ensemble average $\mathcal{F}^{\rm min}_{\rm homo}$ requires that for every sample the phase of the probe beam is re-adjusted so as to minimise the Fano factor. This is common practice in a homodyne measurement. If the phase of the probe beam is fixed, the random phase of $t_{n_0 m_0}$ will average to zero the third term in Eq. (3.56). In Eqs. (3.60) and (3.61) this amounts to the substitution $e^{-\rho} \to -\sinh\rho$.

A graphical presentation of the results (3.58)–(3.61) is given in Figs. 3.3–3.5. For the absorbing case we have taken $f = 0$ (appropriate for optical frequencies at room temperature). For the amplifying case we have taken $f = -1$ (complete population inversion). The formulas above cannot be used for $L \lesssim l$. The values of $\mathcal{F}_{\rm direct}$, $\mathcal{F}_{\rm homo}$, and $\mathcal{F}^{\rm min}_{\rm homo}$ for $L = 0$ can be read off from Eqs. (3.54)–(3.57), $\mathcal{F}_{\rm direct} \to 1 + d(\mathcal{F}_{\rm in} - 1)$, $\mathcal{F}_{\rm homo} = 1 + 2\delta_{n_0 m_0} d\kappa \sinh^2\rho$, and $\mathcal{F}^{\rm min}_{\rm homo} = 1 - 2\delta_{n_0 m_0} d\kappa e^{-\rho} \sinh\rho$. An extrapolation to $L = 0$ is shown dashed in Fig. 3.3.

The common feature of the Fano factors plotted in Figs. 3.3–3.5 is a convergence as the length of the waveguide becomes longer and longer. For an absorbing medium the $L \to \infty$ limit is independent of the state of the incident radiation. For an amplifying medium complete convergence is pre-empted by the laser threshold at $L = \pi\xi_a$.

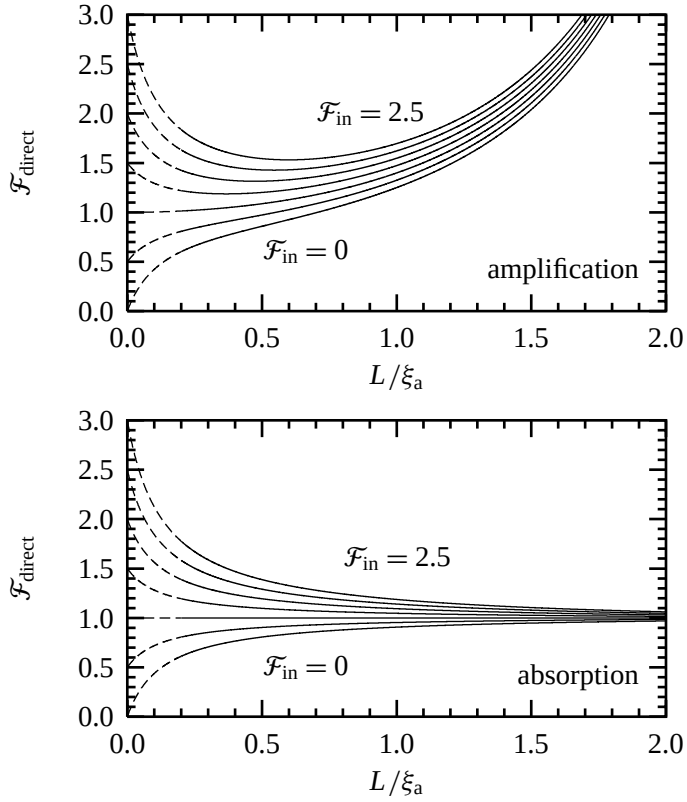

Figure 3.3: Average Fano factor $\mathcal{F}_{\rm direct}$ for direct detection as a function of the length of the waveguide. The left panel is for an amplifying medium [Eq. (3.59), $f = -1$], the right panel for an absorbing medium [Eq. (3.58), $f = 0$]. In both cases we took $l/\xi_{\rm a} = 0.1$, $d = 1$, and values of $\mathcal{F}_{\rm in}$ increasing from 0 to 3 in steps of 0.5. The dotted parts of the curves are extrapolations in the range $L \lesssim l$ that is not covered by Eqs. (3.58) and (3.59).

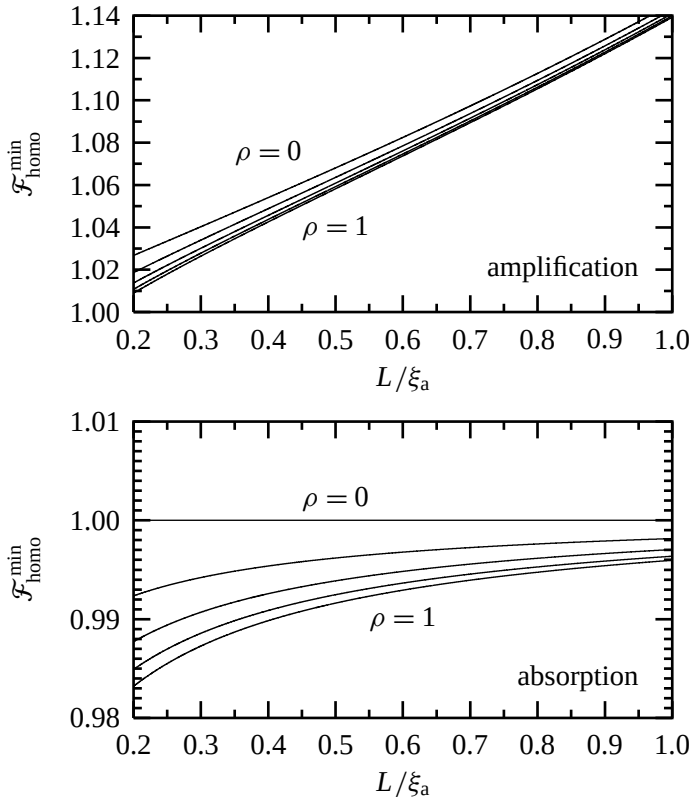

Figure 3.4: Average minimal Fano factor for homodyne detection, from Eqs. (3.60) and (3.61). Same parameter values as in Fig. 3.3, with $N = 10$, $\kappa = \frac{1}{2}$, and ρ increasing from 0 to 1 in steps of 0.25. For $L \lesssim l$ the curves extrapolate either to 1 (if $n_0 \neq m_0$) or to $1 - \mathrm{e}^{-\rho} \sinh \rho$ (if $n_0 = m_0$). (This extrapolation is not shown in the figure.)

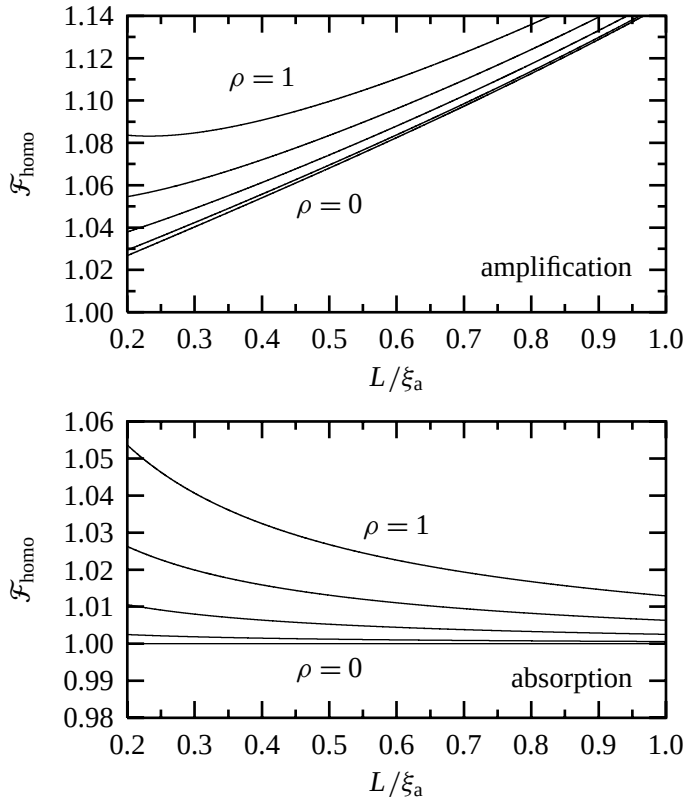

Figure 3.5: Average Fano factor for homodyne detection, from Eqs. (3.60) and (3.61) after the substitution $e^{-\rho} \to -\sinh\rho$, otherwise identical to Fig. 3.4. For $L \lesssim l$ the curves extrapolate either to 1 (if $n_0 \neq m_0$) or to $1 + \sinh^2\rho$ (if $n_0 = m_0$). (This extrapolation is not shown in the figure.)

3.8 Conclusions

In conclusion, we have derived general expressions for the photodetection statistics in terms of the scattering matrix of the medium through which the radiation has propagated. These expressions are particularly well suited for evaluation by means of random-matrix theory, as we have shown by an explicit example, the propagation of squeezed radiation through an amplifying or absorbing waveguide. The sub-Poissonian noise that can occur in a squeezed state (characterised by a Fano factor smaller than unity) is destroyed by thermal fluctuations in an absorbing medium or by spontaneous emission in an amplifying medium. The theory presented here describes this interaction of nonclassical radiation with matter in a quantitative way, without the restriction to one-dimensional scattering of earlier investigations.

Chapter 4

Photon shot noise of localised waves

4.1 Introduction

Analogies in the behaviour of photons and electrons provide a continuing source of inspiration in mesoscopic physics [Büt99]. Two familiar examples are the analogies between weak localisation of electrons and enhanced backscattering of light and between conductance fluctuations and optical speckle [Alt91]. The basis for these analogies is the similarity between the single-electron Schrödinger equation and the Helmholtz equation. The Helmholtz equation is a classical wave equation, and indeed the study of mesoscopic phenomena for light has been limited mostly to *classical* optics. A common theme in these studies is the interplay of interference and multiple scattering by disorder. The extension to *quantum* optics adds the interplay with vacuum fluctuations as a new ingredient.

Recently a theoretical approach to the quantum optics of disordered media was proposed [Bee98], that utilises the methods of the random-matrix theory of quantum transport [Bee97, Guh98]. The random matrix under consideration is the scattering matrix. The basic result of Ref. [Bee98] is a relationship between the scattering matrix and the photocount distribution. It was applied there to the statistics of blackbody radiation and amplified spontaneous emission. This work was reviewed in Ref. [Bee99]. Chapter 2 of this thesis discussed the optical analogue of electronic shot noise.

Shot noise is the time-dependent fluctuation of the current $I(t) = \bar{I} + \delta I(t)$ (measured in units of particles/s) resulting from the discreteness of the particles. The noise power

$$P = \int_{-\infty}^{\infty} \mathrm{d}t \, \overline{\delta I(0) \delta I(t)} \tag{4.1}$$

quantifies the size of the fluctuations. (The bar $\overline{\cdots}$ indicates an average over many measurements on the same system.) For independent particles the current fluctuations form a Poisson process, with power $P_{\text{Poisson}} = \bar{I}$ equal to the mean current. The ratio P/P_{Poisson} (called the Fano factor $\mathcal{F}$ [Fan47]) is a measure of the correlations between the particles.

For electrons, correlations resulting from the Pauli exclusion principle reduce P below P_{Poisson}. (See Ref. [Jon99] for a review.) The ratio P/P_{Poisson} is expressed in terms of traces of the transmission matrix t at the Fermi energy by [Büt90]

$$\mathcal{F} \equiv P/P_{\text{Poisson}} = 1 - \frac{\text{tr}(tt^\dagger)^2}{\text{tr}\, tt^\dagger} \,. \tag{4.2}$$

This formula holds at zero temperature (no thermal noise). In the absence of scattering all eigenvalues of the transmission-matrix product $tt^\dagger$ are equal to unity, hence $P = 0$. This absence of shot noise is realised in a ballistic point contact [Khl87, Les89]. At the other extreme, in a tunnel junction all transmission eigenvalues are $\ll 1$, hence $P = P_{\text{Poisson}}$ [Sch18]. A disordered metallic conductor is intermediate between these two extremes, having $P = \frac{1}{3} P_{\text{Poisson}}$ [Bee92, Nag92].

For the optical analogue we consider a monochromatic laser beam (frequency ω_0) incident in a single mode (labelled m_0) on a waveguide containing a disordered medium (at temperature T). The radiation from a laser is in a coherent state. The photostatistics of coherent radiation is that of a Poisson process [Man95], hence $P = P_{\text{Poisson}}$ for the incident beam. The question addressed in this work is: How does the ratio P/P_{Poisson} change as the radiation propagates through the random medium? We saw that, for electrons, scattering increases this ratio. In contrast, in the optical analogue scattering by itself has no effect: P remains equal to P_{Poisson} if the incident beam is only partially transmitted — provided the scattering matrix remains unitary. A non-unitary scattering matrix, resulting from absorption or amplification of radiation by the medium, increases the ratio P/P_{Poisson}. This excess noise can be understood as the beating of coherent radiation with vacuum fluctuations of the electromagnetic field [Hen96].

Photon shot noise has been studied extensively in systems where the scattering is one-dimensional (for example, randomly layered media) [Jef93, Mat97]. No formula of the generality of Eq. (4.2) was needed for those investigations. In order to go beyond the one-dimensional case, we have derived the optical analogue of Eq. (4.2). The result is

$$\mathcal{F} = 1 + 2\, f(\omega_0, T) \frac{[t^\dagger(\mathbb{1} - rr^\dagger - tt^\dagger)t]_{m_0 m_0}}{[t^\dagger t]_{m_0 m_0}} \,, \tag{4.3}$$

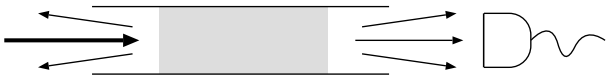

Figure 4.1: Coherent light (thick arrow) is incident on an absorbing or amplifying medium (shaded), embedded in a waveguide. The transmitted radiation is measured by a photodetector.

where $f(\omega,T) = [\exp(\hbar\omega/k_{\rm B}T) - 1]^{-1}$ is the Bose-Einstein function. Eq. (4.3) contains both the transmission matrix t and the reflection matrix r (evaluated at frequency ω_0). For a unitary scattering matrix, $rr^\dagger + tt^\dagger$ equals the unit matrix $\mathbb{1}$, hence the term proportional to f in Eq. (4.3) vanishes and $P = P_{\rm Poisson}$. Absorption and amplification both lead to an enhancement of P above $P_{\rm Poisson}$. For an absorbing system the matrix $\mathbb{1} - rr^\dagger - tt^\dagger$ is positive definite and $f > 0$, so $P/P_{\rm Poisson} > 1$. In an amplifying system $\mathbb{1} - rr^\dagger - tt^\dagger$ is negative definite but f is also negative (because $T < 0$ in an amplifying system), so $P/P_{\rm Poisson}$ is still > 1.

We will review the derivation of the optical shot-noise formula (4.3), and the application to absorbing and amplifying disordered waveguides. The amplifying case is of particular interest in view of the recent experiments on random lasers [Wie97, Cao99], which are amplifying media in which the feedback required for a laser threshold is provided by scattering from disorder rather than by mirrors.

4.2 Optical shot-noise formula

In this section we summarise the scattering formulation of the photodetection problem [Bee98], and derive the formula (4.3) for the excess noise. We consider an absorbing or amplifying disordered medium embedded in a waveguide that supports $N(\omega)$ propagating modes at frequency ω (see Fig. 4.1). The absorbing medium is in thermal equilibrium at temperature $T > 0$. In the amplifying medium, the amplification could be due to stimulated emission by an inverted atomic population or to stimulated Raman scattering [Hen96]. A negative temperature $T < 0$ describes the degree of population inversion in the first case or the density of the material excitation in the second case [Jef93]. A complete population inversion or vanishing density corresponds to the limit $T \to 0$ from below. The Bose-Einstein function $f(\omega,T)$ is > 0 for $T > 0$ and < -1 for $T < 0$.[1] The

[1]The quantity $f(\omega,T)$ is called the "population inversion factor" in the laser literature, because if ω is close to the laser frequency Ω one can express $f = (N_{\rm lower}/N_{\rm upper} - 1)^{-1}$ in terms

absorption or amplification rate $1/\tau_a = \omega|\varepsilon''|$ is obtained from the imaginary part ε'' of the (relative) dielectric constant ($\varepsilon'' > 0$ for absorption, $\varepsilon'' < 0$ for amplification). Disorder causes multiple scattering with rate $1/\tau_s$ and (transport) mean free path $l = c\tau_s$ (with c the velocity of light in the medium). The diffusion constant is $D = \frac{1}{3}cl$. The absorption or amplification length is defined by $\xi_a = \sqrt{D\tau_a}$.

The waveguide is illuminated from one end by monochromatic radiation (frequency ω_0, mean photocurrent I_0) in a coherent state. For simplicity, we assume that the illumination is in a single propagating mode (labelled m_0). At the other end of the waveguide, a photodetector detects the outcoming radiation. We assume, again for simplicity, that all N outgoing modes are detected with unit quantum efficiency. We denote by $p(n)$ the probability to count n photons within a time t. Its first two moments determine the mean photocurrent $\bar{I}$ and the noise power P, according to[2]

$$\bar{I} = \frac{1}{t}\bar{n}\,, \qquad P = \lim_{t\to\infty}\frac{1}{t}\left(\overline{n^2} - \bar{n}^2\right)\,. \tag{4.4}$$

The outgoing radiation in mode n is described by an annihilation operator $a_n^{\rm out}(\omega)$, using the convention that modes $1,2,\ldots,N$ are on the left-hand-side of the medium and modes $N+1,\ldots,2N$ are on the right-hand-side. The vector $a^{\rm out}$ consists of the operators $a_1^{\rm out}, a_2^{\rm out}, \ldots, a_{2N}^{\rm out}$. Similarly, we define a vector $a^{\rm in}$ for incoming radiation. These two sets of operators each satisfy the bosonic commutation relations

$$[a_n(\omega), a_m^\dagger(\omega')] = \delta_{nm}\delta(\omega-\omega')\,, \qquad [a_n(\omega), a_m(\omega')] = 0\,, \tag{4.5}$$

and are related by the input-output relations [Jef93, Mat95, Gru96b]

$$a^{\rm out} = Sa^{\rm in} + Ub + Vc^\dagger\,. \tag{4.6}$$

We have introduced the $2N\times 2N$ scattering matrix S, the $2N\times 2N$ matrices U, V, and the vectors b, c of $2N$ bosonic operators. The reflection and transmission matrices are $N\times N$ submatrices of S,

$$S = \begin{pmatrix} r' & t' \\ t & r \end{pmatrix}\,. \tag{4.7}$$

of the ratio $N_{\rm lower}/N_{\rm upper} = \exp(\hbar\Omega/k_{\rm B}T)$ of the population of the lower and upper atomic levels, with $f = -1$ corresponding to a complete population inversion.

[2]This definition of P is equivalent to Eq. (4.1); In some papers the noise power is defined with an extra factor of 2.

The operators b, c account for vacuum fluctuations. In order for these operators to satisfy the bosonic commutation relations (4.5), it is necessary that

$$UU^\dagger - VV^\dagger = \mathbb{1} - SS^\dagger \,. \tag{4.8}$$

In an absorbing medium $c \equiv 0$ and b has the expectation value

$$\langle b_n^\dagger(\omega) b_m(\omega')\rangle = \delta_{nm}\delta(\omega-\omega')\, f(\omega,T)\,, \qquad T>0\,. \tag{4.9}$$

Conversely, in an amplifying medium $b \equiv 0$ and c has the expectation value

$$\langle c_n(\omega) c_m^\dagger(\omega')\rangle = -\delta_{nm}\delta(\omega-\omega')\, f(\omega,T)\,, \qquad T<0\,. \tag{4.10}$$

The contributions from thermal emission to $\bar{I}$ and P can be eliminated by filtering the output through a narrow frequency window around ω_0. Only terms proportional to the incident current I_0 remain, and we arrive at Eq. (2.16),

$$\bar{I} = I_0 (t^\dagger t)_{m_0 m_0}\,, \tag{4.11}$$

$$P = \bar{I} + 2I_0\, f(\omega_0,T)\big[t^\dagger(\mathbb{1} - rr^\dagger - tt^\dagger)t\big]_{m_0 m_0}\,. \tag{4.12}$$

This yields the optical shot noise formula (4.3) discussed in the introduction.

4.3 Diffusive random medium

We consider an ensemble of absorbing disordered waveguides, with different realisations of the disorder, and evaluate the ensemble averages of Eqs. (4.11) and (4.12). For a random medium the dependence on the index m_0 of the incident radiation is insignificant on average, so we may replace the average of a matrix element $[\cdots]_{m_0 m_0}$ by the average of the normalised trace $N^{-1}\,\mathrm{tr}$. Moments of $rr^\dagger$ and $tt^\dagger$ in the presence of absorption have been computed by Brouwer [Bro98] using the methods of random-matrix theory, in the regime that both the length L of the waveguide and the absorption length ξ_a are much greater than the mean free path l but much less than the localisation length Nl. This is the large-N regime $N \gg L/l, \xi_\mathrm{a}/l \gg 1$. The ratio $L/\xi_\mathrm{a} \equiv s$ is arbitrary.

The result is given by Eqs. (2.41) and (2.42),

$$\bar{I} = \frac{4l}{3L} I_0 \frac{s}{\sinh s}\,, \tag{4.13}$$

$$P = \bar{I} + \frac{2l}{3L} I_0\, f s \left(\frac{3}{\sinh s} - \frac{2s + \cosh s \tanh s}{\sinh^2 s} - \frac{s\cosh s \tanh s - 1}{\sinh^3 s} + \frac{s}{\sinh^4 s} \right)\,. \tag{4.14}$$

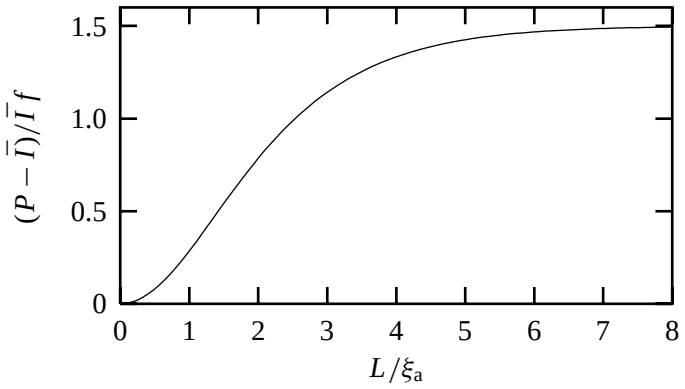

Figure 4.2: Excess noise power for an absorbing disordered waveguide, computed from Eqs. (4.13) and (4.14). The ratio $P/\bar{I}$ tends to $1+\frac{3}{2}f$ for $L \gg \xi_a$.

The ratio $P/P_{\rm Poisson} \equiv P/\bar{I}$ increases from 1 to $1+\frac{3}{2}f$ with increasing s, see Fig. 4.2. The limiting value $P/P_{\rm Poisson} \to 1+\frac{3}{2}f(\omega_0,T)$ for $L \gg \xi_a$ depends on temperature and frequency through the Bose-Einstein function, but is independent of the scattering or absorption rates. This might be seen as the optical analogue of the universal limiting value $P/P_{\rm Poisson} \to \frac{1}{3}$ for $L \gg l$ of the electronic shot noise [Bee92, Nag92].

4.4 Near and above the localisation length

For $L \gg \xi_a$ we may neglect the matrix $tt^\dagger$ with respect to $\mathbb{1}$ in Eq. (4.12), so that the expression for the Fano factor takes the form

$$\mathcal{F} = 1+2f(1-C_1)\,, \qquad C_p \equiv \frac{[t^\dagger (rr^\dagger)^p t]_{m_0 m_0}}{[t^\dagger t]_{m_0 m_0}}\,. \tag{4.15}$$

In the absence of localisation, for $L \ll \xi$, one can simplify the calculation of $\langle \mathcal{F} \rangle$ by averaging separately the numerator and denominator in the coefficient C_1, since the sample-to-sample fluctuations are small. This diffusive regime was studied above. Such a simplification is no longer possible in the localised regime and we should proceed differently.

We follow the general approach of Ref. [Bro98], by considering the change in $\mathcal{F}$ upon attaching a short segment of length δL to one end of the waveguide. Transmission and reflection matrices are changed to leading order in δL according

to

$$t \to t_{\delta L}(1+rr_{\delta L})t\,, \qquad r \to r'_{\delta L} + t_{\delta L}(1+rr_{\delta L})rt^T_{\delta L}\,, \tag{4.16}$$

where the superscript T indicates the transpose of a matrix. (Because of reciprocity the transmission matrix from left to right equals the transpose of the transmission matrix from right to left.) The transmission matrix $t_{\delta L}$ of the short segment may be chosen proportional to the unit matrix,

$$t_{\delta L} = (1-\delta L/2l - \delta L/2l_{\rm a})\mathbb{1}\,, \tag{4.17}$$

where $l_{\rm a} = 2\xi_{\rm a}^2/l$ is the ballistic absorption length. Unitarity of the scattering matrix then dictates that the reflection matrix from the left of the short segment is related to the reflection matrix from the right by $r'_{\delta L} = -r^\dagger_{\delta L}$. The reflection matrix $r_{\delta L}$ is symmetric (because of reciprocity), with zero mean and variance

$$\langle [r_{\delta L}]_{kl}[r_{\delta L}]^*_{mn}\rangle = (\delta_{km}\delta_{ln} + \delta_{kn}\delta_{lm})\delta L/\xi\,. \tag{4.18}$$

Substituting Eq. (4.16) into Eq. (4.15) and averaging we find the evolution equation

$$\begin{aligned}\xi\frac{d\langle C_1\rangle}{dL} = -2\langle C_1\rho_1\rangle + \langle\rho_2\rangle - \frac{\xi l}{\xi_{\rm a}^2}\langle C_1\rangle + 1 + 2\langle C_2 - C_1\rangle - \langle C_1^2\rangle \\ - 4\,{\rm Re}\big\langle [t^\dagger t]^{-2}_{m_0m_0}[t^\dagger r t^*]_{m_0m_0}[t^T r^\dagger r r^\dagger t]_{m_0m_0}\big\rangle \\ + 2\big\langle (1+C_1)[t^\dagger t]^{-2}_{m_0m_0}\big|[t^\dagger r t^*]_{m_0m_0}\big|^2\big\rangle\,,\end{aligned} \tag{4.19}$$

where we have defined $\rho_p = {\rm tr}(1-rr^\dagger)^p$.

For $L \gg \xi_{\rm a}$ we may replace the average of the product $\langle C_1\rho_1\rangle$ by the product of averages $\langle C_1\rangle\langle\rho_1\rangle$, because [Bro98] statistical correlations with traces that involve reflection matrices only are of relative order $\xi_{\rm a}/\xi$ — which we have assumed to be $\ll 1$. The moments of the reflection matrix are given for $L \gg \xi_{\rm a}$ by [3]

$$\langle\rho_p\rangle = \frac{\Gamma(p-1/2)}{\sqrt{\pi}\,\Gamma(p)}\,\frac{\xi}{\xi_{\rm a}}\,, \tag{4.20}$$

hence they are $\gg 1$ and also $\gg \xi l/\xi_{\rm a}^2$. We may therefore neglect the terms in the second, third, and fourth line of Eq. (4.19). What remains is the differential equation

$$\xi\frac{d\langle C_1\rangle}{dL} = -2\langle C_1\rangle\langle\rho_1\rangle + \langle\rho_2\rangle\,, \tag{4.21}$$

[3] These moments follow from the Laguerre distribution of the reflection eigenvalues, cf. Ref. [Bee96].

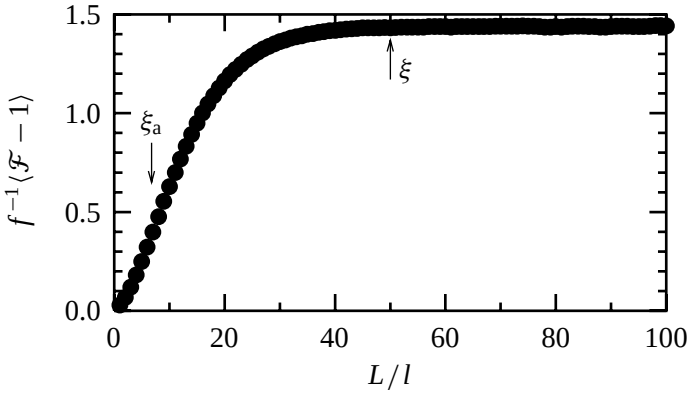

Figure 4.3: Length dependence of the average Fano factor, computed from Eq. (4.3). The data points result from a numerical simulation for an absorbing disordered waveguide with $N = 50$ propagating modes. Arrows indicate the absorption length ξ_a and the localisation length ξ. The average Fano factor is not affected by localisation.

which for $L \gg \xi_a$ has the solution

$$\langle C_1\rangle = \frac{\langle\rho_2\rangle}{2\langle\rho_1\rangle} = \frac{1}{4}\,. \tag{4.22}$$

We conclude that the average Fano factor $\langle\mathcal{F}\rangle = 1 + 2f(1-\langle C_1\rangle) \to 1 + \frac{3}{2}f$ for $L \gg \xi_a$, regardless of whether L is small or large compared to ξ.

To support this analytical calculation we have carried out numerical simulations. The absorbing disordered waveguide is modelled by a two-dimensional square lattice (lattice constant a). The dielectric constant ε has a real part that fluctuates from site to site and a non-fluctuating imaginary part. The multiple scattering of a scalar wave Ψ is described by discretising the Helmholtz equation $[\nabla^2 + (\omega_0/c)^2\varepsilon]\Psi = 0$ and computing the transmission and reflection matrices using the recursive Green function technique [Bar91]. The mean free path $l = 20a$ and the absorption length $\xi_a = 135a$ are determined from the average transmission probability $N^{-1}\langle \mathrm{tr}\, tt^\dagger\rangle = l/\xi_a \sinh(L/\xi_a)$ in the diffusive regime [Bro98]. Averages were performed over the $N/2$ modes m_0 near normal incidence and over some $10^2 - 10^3$ realisations of the disorder. Results are shown in Figs. 4.3 and 4.4.

The length dependence of the average Fano factor is plotted in Fig. 4.3, for $N = 50$ and L ranging from 0 to 2ξ. Clearly, localisation has no effect. The limiting value of $f^{-1}\langle\mathcal{F}-1\rangle$ resulting from this simulation is slightly smaller than

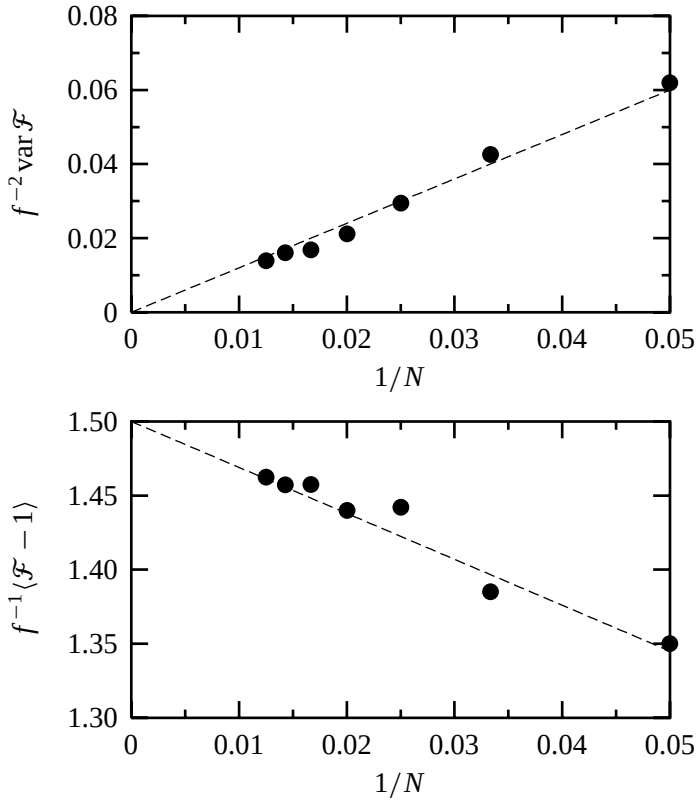

Figure 4.4: Dependence of the average and variance of the Fano factor on the number N of propagating modes, for fixed length $L = 260\,l = 38.5\,\xi_{\mathrm{a}}$ of the waveguide. The length is larger than the localisation length $\xi = (N+1)l$ for all data points. The dashed lines extrapolate to the theoretical expectation for $1/N \to 0$.

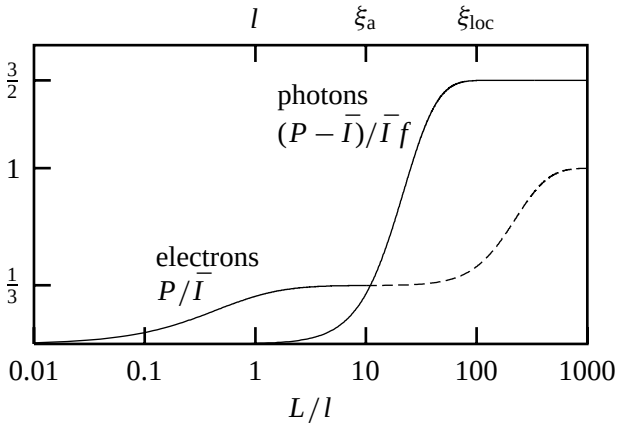

Figure 4.5: Different dependence for electrons and photons of the shot-noise power P on the length L of the waveguide. The curve for photons is the same as in Fig. 4.2, the solid curve for electrons has been calculated in Ref. [Jon92, Jon95], the dashed curve is a qualitative interpolation. We have assumed a factor of 10 between the mean free path l, the absorption length ξ_a, and the localisation length $\xi_{loc} = Nl$. (For electrons, the absorption length should be ignored.) The electronic P increases from 0 to $\frac{1}{3}$ of the Poisson value $\bar{I}$ when L becomes larger than l, and then increases further to full Poisson noise at $\xi_{loc} = Nl$. The photonic P has only a single transition, at ξ_a, from $\bar{I}$ to $(1+\frac{3}{2})\bar{I}$. Nothing happens at $L = l$ or $L = \xi_{loc}$ to the shot noise of coherent radiation.

the value $3/2$ predicted by the analytical theory for $N \gg 1$. The N-dependence of $\langle \mathcal{F} \rangle$ in the localized regime is shown in Fig. 4.4. A line through the data points extrapolates to the theoretical expectation $f^{-1}\langle \mathcal{F} - 1 \rangle \to 3/2$ for $N \to \infty$. Fig. 4.4 also shows the variance of the Fano factor. The variance extrapolates to 0 for $N \to \infty$, indicating that $\mathcal{F} = P/\bar{I}$ becomes self-averaging for large N. This is in contrast to P and $\bar{I}$ themselves, which fluctuate strongly in the localized regime.

It is interesting to compare this length dependence of the Fano factor with the electronic analogue, where P becomes equal to the Poisson noise $\bar{I}$ in the localised regime. The difference between shot noise for electrons and photons in summarised in Fig. 4.5.

4.5 Amplifying random medium

The results for an amplifying disordered waveguide in the large-N regime follow from Eqs. (4.13) and (4.14) for the absorbing case by the substitution $\tau_a \to -\tau_a$, or equivalently $s \to is$. One then finds Eqs. (2.21) and (2.22),

$$\bar{I} = \frac{4l}{3L} I_0 \frac{s}{\sin s} , \tag{4.23}$$

$$P = \bar{I} + \frac{2l}{3L} I_0 f s \left(\frac{3}{\sin s} - \frac{2s - \cot\!\operatorname{an} s}{\sin^2 s} + \frac{s \cot\!\operatorname{an} s - 1}{\sin^3 s} - \frac{s}{\sin^4 s} \right) . \tag{4.24}$$

Recall that the Bose-Einstein function $f < -1$ in an amplifying medium. As shown in Fig. 4.6, the ratio $P/\bar{I}$ increases without bound as the length $L \to \pi\xi_a$ or, equivalently, the amplification rate $1/\tau_a \to \pi^2 D/L^2$. This is the laser threshold.

To understand better the behaviour close to the laser threshold, we consider the scattering matrix $S(\omega)$ as a function of complex frequency ω. In the absence of amplification all poles (resonances) of S are in the lower half of the complex plane, as required by causality. Amplification shifts the poles upward by an amount $1/2\tau_a$. The laser threshold is reached when the first pole hits the real axis, say at resonance frequency Ω. For ω near Ω the scattering matrix has the generic form

$$S_{nm} = \frac{\sigma_n \sigma_m}{\omega - \Omega + \frac{1}{2} i\Gamma - i/2\tau_a} , \tag{4.25}$$

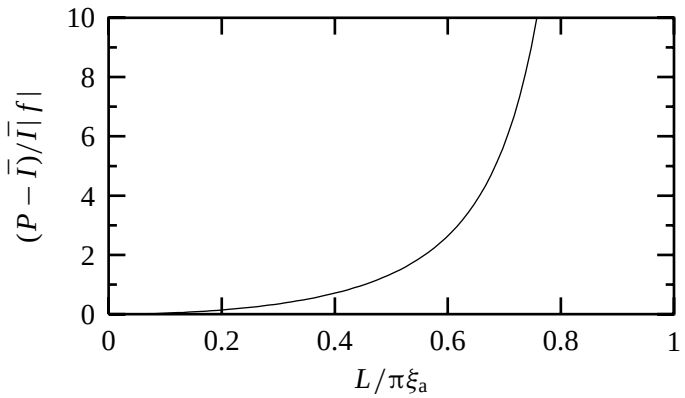

Figure 4.6: Excess noise power for an amplifying disordered waveguide, computed from Eqs. (4.23) and (4.24). The ratio $P/\bar{I}$ diverges at the laser threshold $L = \pi\xi_a$.

where σ_n is the complex coupling constant of the resonance to the nth mode in the waveguide and Γ is the decay rate. The laser threshold is at $\Gamma\tau_a = 1$. We will now show that, while P and $\bar{I}$ diverge at the laser threshold, the signal-to-noise ratio $\mathcal{S} = \bar{I}^2/P$ has a finite limit — independent of σ_n, Γ, or τ_a. The signal-to-noise ratio $\mathcal{S}$ is, up to a prefactor $\bar{I}$, the inverse of the noise figure discussed in Sec. 2.6.

We assume that the incident radiation has frequency $\omega_0 = \Omega$. Substitution of Eq. (4.25) into Eqs. (4.23) and (4.24) gives the simple result

$$\mathcal{S} = \frac{I_0|\sigma_{m_0}|^2}{2|f|\Sigma}, \qquad \Sigma = \sum_{n=1}^{2N}|\sigma_n|^2. \tag{4.26}$$

The total coupling constant $\Sigma = \Sigma_l + \Sigma_r$ is the sum of the coupling constant $\Sigma_l = \sum_{n=1}^{N}|\sigma_n|^2$ to the left end of the waveguide and the coupling constant $\Sigma_r = \sum_{n=N+1}^{2N}|\sigma_n|^2$ to the right. The ensemble average $\langle|\sigma_{m_0}|^2/\Sigma\rangle$ is independent of $m_0 \in [1, N]$, hence

$$\langle\mathcal{S}\rangle = \frac{I_0}{2|f|N}\langle\Sigma_l/\Sigma\rangle = \frac{I_0}{4|f|N}, \tag{4.27}$$

since $\langle\Sigma_l/\Sigma\rangle = \langle\Sigma_r/\Sigma\rangle \Rightarrow \langle\Sigma_l/\Sigma\rangle = 1/2$. The signal-to-noise ratio of the incident coherent radiation (with noise power $P_0 = I_0$) is given by $\mathcal{S}_0 = I_0^2/P_0 = I_0$. The ratio $\mathcal{S}/\mathcal{S}_0$ is the reciprocal of the noise figure of the amplifier. The signal-to-noise ratio of the transmitted radiation is maximal for complete population inversion, when $|f| = 1$ and $\langle\mathcal{S}\rangle$ is smaller than $\mathcal{S}_0$ by a factor $4N$. This universal limit $\langle\mathcal{S}/\mathcal{S}_0\rangle \to 1/4N$ does not require large N, but holds for any $N = 1, 2, \ldots$. It is the multi-mode generalisation of a theorem for the minimal noise figure of a single-mode linear amplifier [Hen96, Cav82].

4.6 Outlook

We conclude by mentioning some directions for future research. In the electronic case it is known that the result $P/\bar{I} = 1/3$ for the Fano factor of a diffusive conductor can be either computed from the scattering matrix [Bee92] (using random-matrix theory) or from a kinetic equation known as the Boltzmann-Langevin equation [Nag92]. Here we have shown using the former approach that the optical analogue is a Fano factor of $1 + \frac{3}{2}f$ for a disordered waveguide longer than the absorption length. To obtain this result from a kinetic equation one needs a Boltzmann-Langevin equation for bosons. Work in this direction is in progress [Mis99].

The effect of localisation on the Fano factor is strikingly different for electrons and photons. In the electronic case the average $\langle P/\bar{I}\rangle$ goes to 1 in the localised regime, but we have found for the optical case that this average is unchanged as the length of the waveguide becomes longer than the localisation length and approaches the universal value $1+\frac{3}{2}f$.

In the case of an amplifying disordered waveguide we have restricted ourselves to the linear regime below the laser threshold. Above threshold the fluctuations in the amplitude of the electromagnetic field are strongly suppressed and only phase fluctuations remain [Man95]. These determine the quantum-limited linewidth of the radiation, see Ch. 6. The application to a disordered waveguide would require a knowledge of the statistics of the poles of the scattering matrix in such a system, which is currently lacking.[4]

The recent interest in the Hanbury-Brown and Twiss experiment for electrons in a disordered metal (for a recent example see [Büt99]) suggests a study of the optical case. The formalism presented here for auto-correlations of the photocurrent can be readily extended to cross-correlations (see Ch. 5), but it has not yet been applied to a random medium.

We do not know of any experiments on photon shot noise in a random medium, and hope that the theoretical predictions reviewed here will stimulate work in this direction. The universal limits of the Fano factor in the absorbing case and the signal-to-noise ratio in the amplifying case seem particularly promising for an experimental study.

[4]Since in Sec. 4.5 the laser threshold was found to be at $1/\tau_a = \pi^2 D/L^2$ in the large-N limit, we conclude that $\Gamma = \pi^2 D/L^2$ is the minimal decay rate in that limit. In other words, the density of S-matrix poles for a disordered waveguide without amplification should vanish for $\mathrm{Im}\,\omega > -\pi^2 D/2L^2$ if $N \to \infty$. This density is unknown, but a similar gap in the density of poles has been found for the scattering matrix of a chaotic cavity [Fyo97].

Chapter 5

Long-range correlation of thermal radiation

5.1 Introduction

The Hanbury Brown-Twiss effect is the existence of spatial correlations in the intensity of thermal radiation by a distant source. It was originally proposed as an intensity-interferometric method to measure the angular opening of a star [HB56], far less susceptible to atmospheric distortion than amplitude-interferometric methods [Boa90]. Two photodetectors at equal distance r from a source (diameter a) will measure a correlated current if their separation d is smaller than the transverse coherence length $d_c \simeq \lambda r/a$ of the radiation from the source at wavelength λ. The correlation function decays with increasing d in an oscillatory way, with amplitude $\propto (d_c/d)^3$ [Man95].

The textbook results assume that the source of the thermal radiation is a black body, meaning that at each frequency any incident radiation is either fully absorbed or fully reflected. In a realistic system there will be a frequency range where only partial absorption occurs. The purpose of this paper is to show that in general for thermal radiation the correlation function does not decay completely to zero, but to a non-zero d-independent background value. This long-range correlation is smaller than the short-range correlation by a factor $(\lambda/a)^2$, and becomes dominant for $d \gtrsim r(\lambda/a)^{1/3}$. It contains information on deviations of the thermal radiation from the black-body limit.

The new information contained in the long-range correlation is most easily described when the source is embedded in a waveguide (see Fig. 5.1). The waveguide has length L, cross-sectional area $A \simeq a^2$, and supports $N = 2\pi A/\lambda^2$

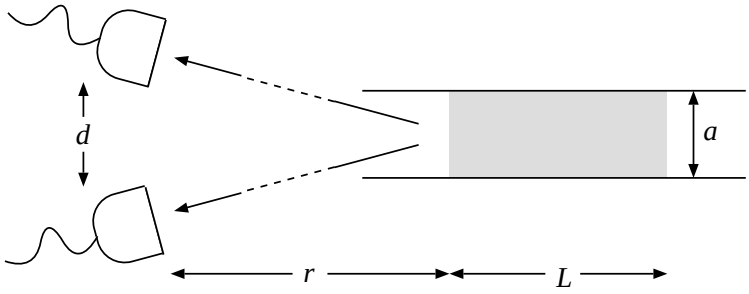

Figure 5.1: Schematic diagram of a source (length L, diameter a) radiating into an N-mode waveguide that is open at both ends. The radiation leaving the waveguide at one end is detected by two photodetectors at a distance r from the source and separated by a distance d. The photocathodes have an area below the transverse coherence area $d_c^2 \simeq r^2/N$. We find that the photocurrents are correlated even if the two detectors are separated by more than d_c.

propagating modes at frequency ω, counting both polarisations. In the far-field, and near normal incidence, each mode corresponds to a transverse coherence area $(r\lambda)^2/A \equiv d_c^2$. The source is in thermal equilibrium at temperature T. The radiation emitted through the left end of the waveguide is incident on a pair of photodetectors, one detecting the photocurrent $I_k(t)$ in mode k, the other detecting $I_l(t)$. Each photocathode has an area equal to the coherence area or smaller. The photocount $n_k = \overline{n}_k + \delta n_k$ (number of photons counted in a time t) and the photocurrent $I_k = \mathrm{d}n_k/\mathrm{d}t = \overline{I}_k + \delta I_k$ fluctuate around their time-averaged values $\overline{n}_k$ and $\overline{I}_k = \overline{n}_k/t$. We seek the correlation function

$$C_{kl} = \int_{-\infty}^{\infty} \overline{\delta I_k(t+\tau)\delta I_l(t)}\,\mathrm{d}\tau = \lim_{t\to\infty} \frac{1}{t}\overline{\delta n_k(t)\delta n_l(t)}\,. \tag{5.1}$$

The overline indicates an average over many measurements on the same sample.

5.2 Random-matrix formulation

The advantage of embedding the source in a waveguide is that we can characterise it by a finite-dimensional scattering matrix $S(\omega)$, consisting of four blocks of dimension $N \times N$,

$$S = \begin{pmatrix} r & t \\ t' & r' \end{pmatrix}\,. \tag{5.2}$$

A mode l incident from the left is reflected into mode k with amplitude r_{kl} and transmitted with amplitude t'_{kl}. Similarly, r'_{kl} and t_{kl} are the reflection and transmission amplitudes for a mode l incident from the right. Reciprocity relates these amplitudes by $r_{kl} = r_{lk}$, $r'_{kl} = r'_{lk}$, and $t_{kl} = t'_{lk}$.

It has been shown recently [Bee98], using the method of "input-output relations" [Jef93, Mat95, Gru96b], how the photocount distribution can be expressed in terms of the scattering matrix. The expressions in Ref. [Bee98] are for a single multi-mode photodetector. The corresponding formulas for two single-mode photodetectors are

$$\begin{aligned} C_{kl} &= \alpha_k \alpha_l \int_0^\infty |(QQ^\dagger)_{kl}(\omega)|^2 \big[f(\omega,T)\big]^2 \frac{\mathrm{d}\omega}{2\pi} + \delta_{kl}\bar{I}_k \,, \\ I_k &= \alpha_k \int_0^\infty (QQ^\dagger)_{kk}(\omega) f(\omega,T) \frac{\mathrm{d}\omega}{2\pi} \,, \end{aligned} \tag{5.3}$$

where α_k is the detector efficiency (the fraction of the photocurrent in mode k that is detected) and f is the Bose-Einstein function

$$f(\omega,T) = \big[\exp(\hbar\omega/k_{\mathrm{B}}T) - 1\big]^{-1} \,. \tag{5.4}$$

The $N \times N$ matrix Q is related to the reflection and transmission matrices by

$$QQ^\dagger = \mathbb{1} - rr^\dagger - tt^\dagger \,. \tag{5.5}$$

The integral over ω extends over a range Ω_{c} set by the absorption line width, centered at ω_0. Typically, $\Omega_{\mathrm{c}} \ll \omega_0$, so we can neglect the frequency dependence of N and f. The matrix $Q(\omega)$ for a random medium fluctuates on a scale ω_{c} much smaller than Ω_{c}. The integration over ω then averages out the fluctuations, so that we may replace the integrand by its ensemble average, indicated by $\langle \ldots \rangle$,

$$C_{kl} = \alpha_k \alpha_l f^2 \int_0^\infty \langle |(QQ^\dagger)_{kl}(\omega)|^2 \rangle \frac{\mathrm{d}\omega}{2\pi} + \delta_{kl}\bar{I}_k \,. \tag{5.6}$$

We evaluate the ensemble average using results from random-matrix theory [Bee97]. For a medium with randomly placed scatterers, the "equivalent channel approximation" [Mel92] has proven to be reliable. According to this approximation, all N modes are statistically equivalent. As a consequence, for any $k \neq l$ one has

$$\begin{aligned} \langle \mathrm{tr}(QQ^\dagger)^2 \rangle &= N \sum_{j=1}^N \langle (QQ^\dagger)_{kj} (QQ^\dagger)_{jk} \rangle \\ &= N(N-1)\langle |(QQ^\dagger)_{kl}|^2 \rangle + N \langle (QQ^\dagger)_{kk}^2 \rangle \,. \end{aligned} \tag{5.7}$$

The average of $(QQ^\dagger)^2_{kk}$ factorises in the large-N limit [Bee97],

$$\langle (QQ^\dagger)^2_{kk}\rangle = \langle (QQ^\dagger)_{kk}\rangle^2 \left[1+\mathcal{O}(N^{-1})\right] = N^{-2}\langle \mathrm{tr}\, QQ^\dagger\rangle^2 . \tag{5.8}$$

Combination of Eqs. (5.7) and (5.8) gives us

$$\langle |(QQ^\dagger)_{kl}|^2\rangle = N^{-2}\langle \mathrm{tr}(QQ^\dagger)^2\rangle - N^{-3}\langle \mathrm{tr}\, QQ^\dagger\rangle^2 + \mathcal{O}(N^{-2}) . \tag{5.9}$$

The eigenvalues $\sigma_1, \sigma_2, \ldots, \sigma_N$ of the matrix $rr^\dagger + tt^\dagger$ are the "scattering strengths" of the random medium. We denote by $\overline{\sigma^p} \equiv N^{-1}\sum_n \sigma_n^p$ the pth spectral moment of the scattering strengths. According to Eqs. (5.5), (5.6) and (5.9), the cross-correlator C_{kl} ($k \neq l$) then takes the form of a variance,

$$C_{kl} = \frac{\alpha_k \alpha_l f^2}{N} \int_0^\infty \left(\langle \overline{\sigma^2}\rangle - \langle \overline{\sigma}\rangle^2 \right) \frac{\mathrm{d}\omega}{2\pi} . \tag{5.10}$$

This is our basic result for the long-range correlation announced in the introduction. The new information contained in the cross-correlator is the variance of the scattering strengths. The auto-correlator, in contrast, depends entirely on the first spectral moment,

$$C_{kk} = \alpha_k^2 f^2 \int_0^\infty \langle 1-\overline{\sigma}\rangle^2 \frac{\mathrm{d}\omega}{2\pi} + \bar{I}_k , \tag{5.11a}$$

$$\bar{I}_k = \alpha_k f \int_0^\infty \langle 1-\overline{\sigma}\rangle \frac{\mathrm{d}\omega}{2\pi} , \tag{5.11b}$$

where we have used Eq. (5.8).

The long-range correlation C_{kl} of two photodetectors separated by more than a coherence length is an order N smaller than the short-range correlation $C_{kk} - \bar{I}_k$ of two photodetectors separated by less than a coherence length. (The full value C_{kk} is measured in a single-detector experiment.) The long-range correlation vanishes if all N scattering strengths are the same, as they would be for an idealised "step-function model" of a black body ($\sigma_n = 0$ for $|\omega - \omega_0| < \Omega_\mathrm{c}$ and $\sigma_n = 1$ otherwise). A random, partially absorbing medium, in contrast, has a broad distribution of scattering strengths [Bee97], hence a substantial long-range correlation of the photocurrent.

5.3 Applications

5.3.1 Disordered medium

As first example, we compute the correlation for a weakly absorbing, strongly disordered medium. The moments of $rr^\dagger$ and $tt^\dagger$ appearing in Eqs. (5.10) and

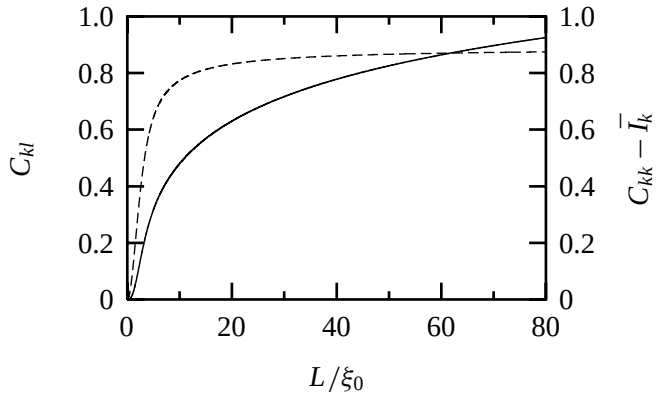

Figure 5.2: Long-range correlation $\bar{C}_{kl}$ (solid line), in units of $\Omega_c l f^2 \alpha_k \alpha_l / N \xi_0$, and short-range correlation $C_{kk} - \bar{I}_k$ (dashed line), in units of $\Omega_c (l f \alpha_k / \xi_0)^2$, of the radiation emitted from a disordered waveguide. A Lorentzian frequency dependence is assumed for the dielectric function, with width Ω_c and absorption length ξ_0 at the centre of the absorption line. The mean free path l is assumed to be $\ll \xi_0$. The short-range correlation saturates in the limit $L/\xi_0 \to \infty$, while the long-range correlation keeps increasing $\propto \ln L/\xi_0$.

(5.11) have been calculated by Brouwer [Bro98] as a function of the number of modes N, the sample length L, the mean free path l, and the absorption length $\xi_a = \sqrt{D\tau_a}$ (τ_a is the absorption time and $D = cl/3$ the diffusion constant). It is assumed that $1/N \ll l/\xi_a \ll 1$, but the ratio $L/\xi_a \equiv s$ is arbitrary. The result is

$$\left\langle \overline{\sigma^2} \right\rangle - \langle \overline{\sigma} \rangle^2 = \frac{2l}{3\xi_a} \left(\coth^3 s - \frac{3}{\sinh s} + \frac{s}{\sinh^2 s} + \frac{s \coth s - 1}{\sinh^3 s} - \frac{s}{\sinh^4 s} \right), \tag{5.12a}$$

$$\langle 1 - \overline{\sigma} \rangle = \frac{4l}{3\xi_a} \tanh \frac{s}{2}. \tag{5.12b}$$

To compute the correlators (5.10) and (5.11) it remains to carry out the integrations over ω. The frequency dependence is governed by the imaginary part of the dielectric function $\varepsilon''(\omega)$, for which take the Lorentzian $\varepsilon''(\omega) = \varepsilon_0''[1 + (\omega - \omega_0)^2/\Omega_c^2]^{-1}$. Since $\tau_a = 1/\omega_0 \varepsilon''$, the corresponding ω-dependence of ξ_a and s is $\xi_a/\xi_0 = s_0/s = [1 + (\omega - \omega_0)^2/\Omega_c^2]^{1/2}$, with ξ_0 and s_0 the values of ξ and s at $\omega = \omega_0$. Results are plotted in Fig. 5.2. In the limit $L/\xi_0 \to 0$ of a thin sample,

we have

$$C_{kl} = \frac{1}{45}\Omega_c \frac{l f^2 \alpha_k \alpha_l}{N\xi_0} (L/\xi_0)^3 \,, \tag{5.13a}$$

$$C_{kk} = \frac{4}{9\pi}\Omega_c \left(\frac{l f \alpha_k}{\xi_0}\right)^2 (L/\xi_0)^2 + \bar{I}_k \,, \tag{5.13b}$$

$$\bar{I}_k = \frac{1}{3}\Omega_c \frac{l f \alpha_k}{\xi_0} (L/\xi_0) \,. \tag{5.13c}$$

In the opposite limit $L/\xi_0 \to \infty$ of a thick sample, the cross-correlator C_{kl} and the mean current $\bar{I}_k$ both diverge logarithmically $\propto \ln L/\xi_0$. The ratio $C_{kl}/(\bar{I}_k \bar{I}_l)^{1/2}$ tends to $(1/2N)\, f\sqrt{\alpha_k \alpha_l}$ in the large-L limit, and the short-range correlation $C_{kk} - \bar{I}_k$ to $\frac{8}{9}\Omega_c (l f \alpha_k/\xi_0)^2$, remaining larger than the long-range correlation because the limit $N \to \infty$ has to be taken before $L \to \infty$.

5.3.2 Chaotic cavity

Our second example is an optical cavity filled with an absorbing random medium. The radiation leaves the cavity through a waveguide supporting N modes. The general formula (5.3) applies with $QQ^\dagger = \mathbb{1} - rr^\dagger$ (since there is no transmission). The scattering strengths $\sigma_1, \sigma_2, \ldots, \sigma_N$ in this case are eigenvalues of $rr^\dagger$. Their distribution is known in the large-N limit [Bee99] as a function of the dimensionless absorption rate $\gamma = 2\pi/N\tau_a \Delta\omega$, with $\Delta\omega$ the spacing of the cavity modes near frequency ω_0. (The quantity γ is the ratio of the mean dwell time in the cavity without absorption and the absorption time.) The moments $\langle\overline{\sigma}\rangle$ and $\langle\overline{\sigma^2}\rangle$ can then be computed by numerical integration. Results are shown in Fig. 5.3, again for a Lorentzian frequency dependence of $\varepsilon''(\omega)$. Unlike in the first example, we are now not restricted to weak absorption but can let the absorption rate γ_0 at the central frequency ω_0 become arbitrarily large. For weak absorption, $\gamma_0 \ll 1$, we have

$$C_{kl} = \frac{1}{4}\Omega_c \frac{f^2 \alpha_k \alpha_l}{N} \gamma_0^2 \,, \tag{5.14a}$$

$$C_{kk} = \frac{1}{4}\Omega_c (f \alpha_k \gamma_0)^2 + \bar{I}_k \,, \tag{5.14b}$$

$$\bar{I}_k = \frac{1}{2}\Omega_c f \alpha_k \gamma_0 \,. \tag{5.14c}$$

For strong absorption, $\gamma_0 \gg 1$, all three quantities C_{kl}, C_{kk} and $\bar{I}_k$ diverge $\propto \sqrt{\gamma_0}$ (see Fig. 5.3, top). The ratio $C_{kl}/(\bar{I}_k \bar{I}_l)^{1/2}$ tends to $0.062\, f(\alpha_k \alpha_l)^{1/2}/N$, and the

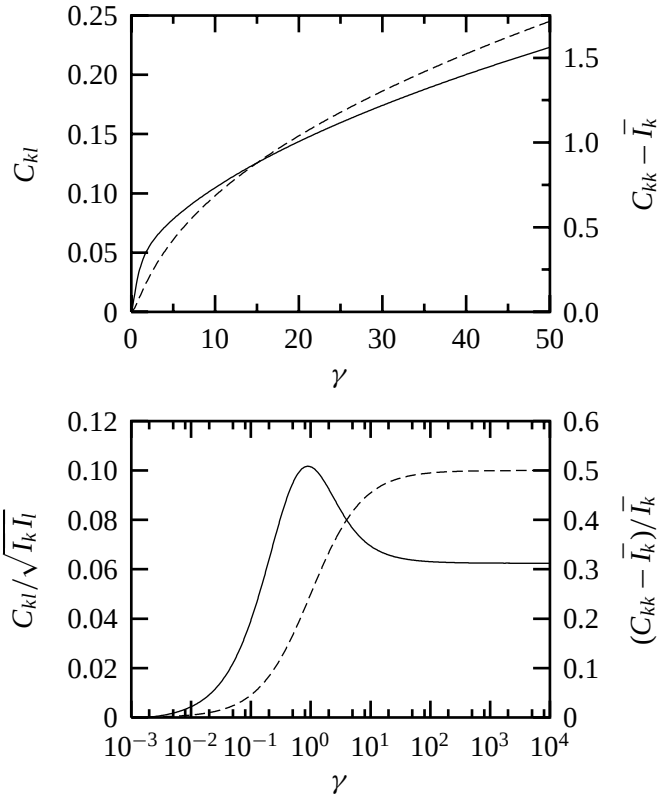

Figure 5.3: Correlators of the radiation emitted from a disordered optical cavity as a function of the absorption rate γ_0 at the centre of the absorption line with Lorentzian profile. (The absorption rate is normalised to the mean dwell time.) Top: Long-range correlation C_{kl} (solid line), in units of $\Omega_c f^2 \alpha_k \alpha_l / N$, and short-range correlation $C_{kk} - \bar{I}_k$ (dashed line), in units of $\Omega_c f^2 \alpha_k^2$. Bottom: Same correlators, but now normalised by the mean photocurrent. (The left axis is in units of $f\sqrt{\alpha_k \alpha_l}/N$, the right axis in units of $f\alpha_k$.) The long-range correlation persists in the limit $\gamma_0 \to \infty$ because of partial absorption in the tails of the absorption line.

ratio $(C_{kk} - \bar{I}_k)/\bar{I}_k$ to $\frac{1}{2} f \alpha_k$ (see Fig. 5.3, bottom). The long-range correlation does not vanish as $\gamma_0 \to \infty$, because there remains a tail of frequencies with moderate absorption and thus a wide distribution of scattering strengths, even if the system behaves like an ideal black body for frequencies near ω_0.

5.4 Conclusion

In summary, we have shown that the thermal radiation emitted by random media contains long-range spatial correlations in the intensity. The long-range correlation has information on the spectral variation of the scattering strengths that is not accessible from the luminosity. We have analysed two types of systems in detail, providing specific predictions that we hope will motivate an experimental search for the long-range correlation.

Chapter 6

Quantum limit of the laser linewidth in chaotic cavities

6.1 Introduction

Laser action selects a mode in a cavity and enhances the output intensity in this mode by a nonlinear feedback mechanism. Vacuum fluctuations of the electromagnetic field ultimately limit the narrowing of the emission spectrum [Sch58]. The quantum-limited linewidth, or Schawlow-Townes linewidth,

$$\delta\omega_{\mathrm{ST}} = \frac{1}{2}\Gamma^2/I \ , \tag{6.1}$$

is proportional to the square of the decay rate Γ of the lasing cavity mode and inversely proportional to the output power I (in units of photons/s). This is a lower bound for the linewidth when Γ is much less than the linewidth of the atomic transition and when the lower level of the transition is unoccupied. Many years after the work of Schawlow and Townes it was realised [Pet79, Sie89a, Sie89b] that the true fundamental limit is larger than Eq. (6.1) by a factor K that characterises the non-orthogonality of the cavity modes. This excess noise factor, or Petermann factor, has generated an extensive literature [Che96, Eij96, Eij97, Bru97, Gra98, Sie98].

Apart from its importance for cavity lasers, the Petermann factor is of fundamental significance in the more general context of scattering theory. A lasing cavity mode is associated with a pole of the scattering matrix in the complex frequency plane. We will show that the Petermann factor is proportional to the squared modulus of the residue of this pole. Poles of the scattering matrix

also determine the position and height of resonances of nuclei, atoms, and molecules [Mah69]. Powerful numerical tools that give access to poles even deep in the complex plane have been developed recently [Man97]. They can be used to determine the residues of the poles as well. Our work is of relevance for these more general studies, beyond the original application to cavity lasers.

Existing theories of the Petermann factor usually deal with cavities that have a high degree of symmetry. They factorise $K = K_{\rm l} K_{\rm r}$ into longitudinal and transverse factors, assuming that the cavity mode is separable into longitudinal and transverse modes, each of which is basically one-dimensional. For such regular cavities the framework of ray optics provides a simple way to solve the problem in a good approximation [Eij96, Eij97]. This approach breaks down if the light propagation in the cavity becomes chaotic, either because of an irregular shape of the boundaries or because of randomly placed scatterers. In the language of dynamical systems, one crosses over from integrable to chaotic dynamics [Haa91]. The method of random-matrix theory is well-suited for such chaotic cavities [Haa91, Meh90]. Instead of considering a single cavity, one studies an ensemble of cavities with small variations in shape and size, or in position of the scatterers. The distribution of the scattering matrix in this ensemble is known. Recent work has provided a detailed knowledge on the statistics of the poles [Sok88, Sok89, Fyo96, Fyo97, Som99]. Much less is known about the residues [Jan99, Cha98, Meh00]. In this chapter we fill the remaining gap to a considerable extent.

The outline of this chapter is as follows. In Section 6.2 we derive the connection between the Petermann factor and the residue of the pole of the lasing mode. The residue in turn is seen to be characteristic for the degree of nonorthogonality of the modes. In this way we make contact with the existing literature on the Petermann factor [Gra98, Sie98].

In Section 6.3 we study the single-channel case of a scalar scattering matrix. This applies to a cavity that is coupled to the outside via a small opening of area $\mathcal{A} \lesssim \lambda^2/2\pi$ (with λ the wavelength of the lasing mode). For preserved time-reversal symmetry (the relevant case in optics) we find that the ensemble average of $K-1$ depends *non-analytically* $\propto T \ln T^{-1}$ on the transmission probability T through the opening, so that it is beyond the reach of perturbation theory even if $T \ll 1$. We present a complete resummation of the perturbation series that overcomes this obstacle. We derive the conditional distribution $P(K)$ of the Petermann factor at a given decay rate Γ of the lasing mode, valid for any value of T. The most probable value of $K-1$ is $\propto T$, hence it is parametrically smaller than the average.

In a cavity with such a small opening the deviations of K from unity are very small. We contrast this in Sec. 6.4 with the multi-channel case of an $N \times N$ scattering matrix, which corresponds to an opening of area $\mathcal{A} \approx N\lambda^2/2\pi$. The lasing mode acquires a decay rate Γ of order $\Gamma_0 = NT\Delta/2\pi$ (with Δ the mean spacing of the cavity modes), and the mean Petermann factor is $K \propto \sqrt{N}$.

6.2 Relationship between Petermann factor and residue

Modes of a closed cavity, in the absence of absorption or amplification, are eigenvalues ω_n of a Hermitian operator H_0. This operator can be chosen real if the system possesses time-reversal symmetry (symmetry index $\beta = 1$), otherwise it is complex ($\beta = 2$). For a chaotic cavity, H_0 can be modelled by an $M \times M$ Hermitian matrix with independent Gaussian distributed elements,

$$P(H_0) \propto \exp\left(-\frac{\beta M}{4\mu^2}\,\mathrm{tr}\,H_0^2\right) . \tag{6.2}$$

(For $\beta = 1$ (2), this is the Gaussian orthogonal (unitary) ensemble [Meh90].) The mean density of eigenvalues is the Wigner semicircle

$$\varrho(\omega) = \frac{M}{2\pi\mu^2}\sqrt{4\mu^2 - \omega^2} . \tag{6.3}$$

The mean mode spacing at the centre $\omega = 0$ is $\Delta = \pi\mu/M$. (The limit $M \to \infty$ at fixed spacing Δ of the modes is taken at the end of the calculation.)

A small opening in the cavity is described by a real, non-random $M \times N$ coupling matrix W, with N the number of scattering channels transmitted through the opening. (For an opening of area $\mathcal{A}$, $N \simeq 2\pi\mathcal{A}/\lambda^2$ at wavelength λ.) Modes of the open cavity are complex eigenvalues (with negative imaginary part) of the non-Hermitian matrix

$$H = H_0 - \mathrm{i}\pi W W^\dagger . \tag{6.4}$$

In absence of amplification or absorption, the scattering matrix S at frequency ω is related to H by [Mah69, Ver85]

$$S = \mathbb{1} - 2\pi\mathrm{i}W^\dagger(\omega - H)^{-1}W . \tag{6.5}$$

The scattering matrix is a unitary (and symmetric, for $\beta = 1$) random $N \times N$ matrix, with poles at the eigenvalues of H. It enters the input-output relation

$$a_m^{\mathrm{out}}(\omega) = \sum_{n=1}^{N} S_{mn}(\omega)a_n^{\mathrm{in}}(\omega) , \tag{6.6}$$

which relates the annihilation operators $a_m^{\rm out}$ of the scattering states that leave the cavity to the annihilation operators $a_n^{\rm in}$ of states that enter the cavity. The indices n, m label the scattering channels.

We now assume that the cavity is filled with a homogeneous amplifying medium (constant amplification rate $1/\tau_{\rm a}$ over a large frequency window $\Omega_{\rm a} = L\Delta$, $L \gg N$). This adds a term $\mathrm{i}/2\tau_{\rm a}$ to the eigenvalues, shifting them upward towards the real axis. The scattering matrix

$$S = \mathbb{1} - 2\pi \mathrm{i} W^\dagger (\omega - H - \mathrm{i}/2\tau_{\rm a})^{-1} W \tag{6.7}$$

is then no longer unitary, and the input-output relation changes to [Jef93, Bee98]

$$a_m^{\rm out}(\omega) = \sum_{n=1}^{N} S_{mn}(\omega) a_n^{\rm in}(\omega) + \sum_{n=1}^{N} V_{mn}(\omega) c_n^\dagger(\omega)\,. \tag{6.8}$$

All operators fulfil the canonical bosonic commutation relations $[a_n(\omega), a_m^\dagger(\omega')] = \delta_{nm}\delta(\omega-\omega')$. As a consequence,

$$V(\omega)V^\dagger(\omega) = S(\omega)S^\dagger(\omega) - \mathbb{1}\,. \tag{6.9}$$

The operators c describe the spontaneous emission of photons in the cavity and have expectation value

$$\langle c_n^\dagger(\omega) c_m(\omega')\rangle = \delta_{nm}\delta(\omega-\omega')\, f(\omega, T)\,, \tag{6.10}$$

with $f(\omega,T) = [\exp(\hbar\omega/k_{\rm B}T) - 1]^{-1}$ the Bose-Einstein distribution function at frequency ω and temperature T.[1]

In the absence of external illumination ($\langle a^{\rm in\,\dagger} a^{\rm in}\rangle = 0$), the photon current per frequency interval,

$$I(\omega) = \frac{1}{2\pi} \sum_{m=1}^{N} \langle a_m^{\rm out\,\dagger}(\omega) a_m^{\rm out}(\omega)\rangle\,, \tag{6.11}$$

is related to the scattering matrix by Kirchhoff's law [Jef93, Bee98]

$$I(\omega) = f(\omega,T)\frac{1}{2\pi}\,\mathrm{tr}\big[\mathbb{1} - S^\dagger(\omega)S(\omega)\big]\,. \tag{6.12}$$

For ω near the laser transition we may replace f by the population inversion factor $N_{\rm up}/(N_{\rm low} - N_{\rm up})$, where $N_{\rm up}$ and $N_{\rm low}$ are the mean occupation numbers of the

[1] The temperature T defined in this way is positive for an amplifying medium.

upper and lower levels of the transition. In this way the photon current can be written in the form

$$I(\omega) = \frac{1}{2\pi} \frac{N_{\rm up}}{N_{\rm up} - N_{\rm low}} \,{\rm tr}\big[S^\dagger(\omega) S(\omega) - \mathbb{1}\big] \,, \tag{6.13}$$

that is suitable for an amplifying medium.

The lasing mode is the eigenvalue $\Omega - {\rm i}\Gamma/2$ closest to the real axis, and the laser threshold is reached when the decay rate Γ of this mode equals the amplification rate $1/\tau_{\rm a}$. Near the laser threshold we need to retain only the contribution from the lasing mode (say mode number l) to the scattering matrix (6.7),

$$S_{nm} = -2\pi{\rm i} \frac{(W^\dagger U)_{nl} (U^{-1} W)_{lm}}{\omega - \Omega + {\rm i}\Gamma/2 - {\rm i}/2\tau_{\rm a}} , \tag{6.14}$$

where U is the matrix of right eigenvectors of H (no summation over l is implied). The photon current near threshold takes the form

$$I(\omega) = \frac{2\pi N_{\rm up}}{N_{\rm up} - N_{\rm low}} \frac{(U^\dagger W W^\dagger U)_{ll} (U^{-1} W W^\dagger U^{-1\dagger})_{ll}}{(\omega - \Omega)^2 + \frac{1}{4}(\Gamma - 1/\tau_{\rm a})^2} \,. \tag{6.15}$$

This is a Lorentzian with full width at half maximum $\delta\omega = \Gamma - 1/\tau_{\rm a}$.

The coupling matrix W can be eliminated by writing

$$-\pi (U^\dagger W W^\dagger U)_{ll} = {\rm Im}\big(U^\dagger H U\big)_{ll} = -\frac{\Gamma}{2} (U^\dagger U)_{ll} \,, \tag{6.16a}$$

$$-\pi (U^{-1} W W^\dagger U^{-1\dagger})_{ll} = {\rm Im}\big(U^{-1} H U^{-1\dagger}\big)_{ll} = -\frac{\Gamma}{2} (U^{-1} U^{-1\dagger})_{ll} \,. \tag{6.16b}$$

The total output current is found by integrating over frequency,

$$I = (U^\dagger U)_{ll} (U^{-1} U^{-1\dagger})_{ll} \frac{N_{\rm up}}{N_{\rm up} - N_{\rm low}} \frac{\Gamma^2}{\delta\omega} \,. \tag{6.17}$$

Comparison with the Schawlow-Townes value (6.1) shows that

$$\delta\omega = 2K \frac{N_{\rm up}}{N_{\rm up} - N_{\rm low}} \delta\omega_{\rm ST} \,, \tag{6.18}$$

where the Petermann factor K is identified as

$$K = (U^\dagger U)_{ll} (U^{-1} U^{-1\dagger})_{ll} \geqslant 1 \,. \tag{6.19}$$

For time-reversal symmetry, we can choose $U^{-1} = U^T$, and find $K = [(UU^\dagger)_{ll}]^2$. The factor of 2 in the relation between $\delta\omega$ and $\delta\omega_{\rm ST}$ occurs because we have computed the laser linewidth in the linear regime just below the threshold, instead of far above the threshold. The effect of the nonlinearities above threshold is to suppress the amplitude fluctuations while leaving the phase fluctuations intact [Gol91], hence the simple factor of 2 reduction of the linewidth. The factor $N_{\rm up}/(N_{\rm up} - N_{\rm low})$ accounts for the extra noise due to an incomplete population inversion. The remaining factor K is due to the non-orthogonality of the cavity modes [Sie89a, Sie89b], since $K = 1$ if U is unitary.

6.3 Single scattering channel

The relation (6.19) serves as the starting point for a calculation of the statistics of the Petermann factor in an ensemble of chaotic cavities. In this section we consider the case $N = 1$ of a single scattering channel, for which the coupling matrix W reduces to a vector $\vec{\alpha} = (W_{11}, W_{21}, \ldots, W_{M1})$. The magnitude $|\vec{\alpha}|^2 = (M\Delta/\pi^2)w$, where $w \in [0,1]$ is related to the transmission probability T of the single scattering channel by $T = 4w(1+w)^{-2}$ [Bee97]. We assume a basis in which H_0 is diagonal (eigenvalues ω_q, right eigenvectors $|q\rangle$, left eigenvectors $\langle q|$). In this basis the entries α_q remain real for $\beta = 1$, but become complex numbers for $\beta = 2$. Since the eigenvectors $|q\rangle$ point into random directions, and since the fixed length of $\vec{\alpha}$ becomes an irrelevant constraint in the limit $M \to \infty$, each real degree of freedom in α_q is an independent Gaussian distributed number [Meh90]. The squared modulus $|\alpha_q|^2$ has probability density

$$P(|\alpha_q|^2) = \frac{1}{2\pi|\alpha_q|^2}\left(\frac{2\pi^3|\alpha_q|^2}{w\Delta}\right)^{\beta/2}\exp\left(-\frac{\beta\pi^2}{2w\Delta}|\alpha_q|^2\right). \tag{6.20}$$

Eq. (6.20) is a χ^2-distribution with β degrees of freedom and mean $\Delta w/\pi^2$.

We first determine the distribution of the decay rate Γ of the lasing mode, following Ref. [Mis98]. Since the lasing mode is the mode closest to the real axis, its decay rate is much smaller than the typical decay rate of a mode, which is $\simeq T\Delta$. Then we calculate the conditional distribution and mean of the Petermann factor for given Γ. The unconditional distribution of the Petermann factor is found by folding the conditional distribution with the distribution of Γ, but will not be considered here.

6.3.1 Decay rate of the lasing mode

The amplification with rate $1/\tau_a$ is assumed to be effective over a window $\Omega_a = L\Delta$ containing many modes. The lasing mode is the mode within this window that has the smallest decay rate Γ. For such small decay rates we can use first-order perturbation theory to obtain the decay rate of mode q,

$$\Gamma_q = 2\pi|\alpha_q|^2 \,. \tag{6.21}$$

The χ^2-distribution (6.20) of the squared moduli $|\alpha_q|^2$ translates into a χ^2-distribution of the decay rates,

$$P(\Gamma) \propto \Gamma^{(2-\beta)/2} \exp\left(-\frac{\beta\pi\Gamma}{4w\Delta}\right) \,. \tag{6.22}$$

Ignoring correlations, we may obtain the decay rate of the lasing mode by considering the L decay rates as independent random variables drawn from the distribution $P(\Gamma)$. The distribution of the smallest among the L decay rates is then given by

$$P_L(\Gamma) = L\,P(\Gamma)\left[1 - \int_0^\Gamma P(\Gamma')\,\mathrm{d}\Gamma'\right]^{L-1} \,. \tag{6.23}$$

For small rates Γ we can insert the distribution (6.22) and obtain

$$P_L(\Gamma) \approx \frac{1}{\sqrt{\Gamma}} \exp\left(-\frac{L\pi\Gamma}{4w\Delta}\right)\left[\mathrm{erf}\left(\frac{\pi\Gamma}{4w\Delta}\right)\right]^{L-1} \,, \qquad \beta = 1 \,, \tag{6.24a}$$

$$P_L(\Gamma) \approx \exp\left(-\frac{L\pi\Gamma}{2w\Delta}\right) \,, \qquad \beta = 2 \,. \tag{6.24b}$$

Here $\mathrm{erf}(x) = 2\pi^{-1/2}\int_0^x \exp(-y^2)\,\mathrm{d}y$ is the error function. The decay rate of the lasing mode decreases with increasing width of the amplification window as $\Gamma \sim w\Delta(\Omega_a/\Delta)^{-2/\beta} \ll w\Delta$.

6.3.2 First-order perturbation theory

If the opening is much smaller than a wavelength, then a perturbation theory in $\vec{\alpha}$ seems a natural starting point. We assign the index l to the lasing mode, and write the perturbed right eigenfunction $|l\rangle' = \sum_q d_q|q\rangle$ and the perturbed left eigenfunction $\langle l|' = \sum_q e_q\langle q|$, in terms of the eigenfunctions of H_0. The coefficients are $d_q = U_{ql}/U_{ll}$ and $e_q = U_{lq}^{-1}/U_{ll}^{-1}$, i. e., we do not normalise the perturbed eigenfunctions but rather choose $d_l = e_l = 1$.

To leading order the lasing mode remains at $\Omega = \omega_l$ and has width

$$\Gamma = 2\pi|\alpha_l|^2 \,. \tag{6.25}$$

The coefficients of the wave function are

$$d_q = \mathrm{i}\frac{\pi\alpha_q\alpha_l^*}{\omega_q - \omega_l} \,, \qquad e_q = \mathrm{i}\frac{\pi\alpha_q^*\alpha_l}{\omega_q - \omega_l} \,. \tag{6.26}$$

The Petermann factor of the lasing mode follows from Eq. (6.19),

$$K = \frac{\left(1+\sum_{q\neq l}|d_q|^2\right)\left(1+\sum_{q\neq l}|e_q|^2\right)}{\left|1+\sum_{q\neq l} d_q e_q\right|^2} \approx 1+\sum_{q\neq l}\left|d_q - e_q^*\right|^2 \,, \tag{6.27}$$

where we linearised with respect to Γ because the lasing mode is close to the real axis. From Eq. (6.26) one finds

$$K = 1+\left(2\pi|\alpha_l|\right)^2 \sum_{q\neq l}\frac{|\alpha_q|^2}{(\omega_l-\omega_q)^2} \,. \tag{6.28}$$

We seek the distribution $P(K)$ and the average $\langle K\rangle_{\Omega,\Gamma}$ of K for a given value of Ω and Γ.

For $\beta = 1$, the probability to find an eigenvalue at ω_q given that there is an eigenvalue at ω_l vanishes *linearly* for small $|\omega_q - \omega_l|$, as a consequence of eigenvalue repulsion constrained by time-reversal symmetry. Since the expression (6.28) for K diverges *quadratically* for small $|\omega_q - \omega_l|$, we conclude that $\langle K\rangle_{\Omega,\Gamma}$ does not exist in perturbation theory.[2] This severely complicates the problem.

6.3.3 Summation of the perturbation series

To obtain a finite answer for the average Petermann factor we need to go beyond perturbation theory. By a complete summation of the perturbation series we will in this section obtain results that are valid for all values $T \leqslant 1$ of the transmission probability. Our starting point are the exact relations

$$d_q z_l = \omega_q d_q - \mathrm{i}\pi\alpha_q \sum_p \alpha_p^* d_p \,, \tag{6.29a}$$

$$e_q z_l = \omega_q e_q - \mathrm{i}\pi\alpha_q^* \sum_p \alpha_p e_p \,, \tag{6.29b}$$

[2]For broken time-reversal symmetry there is no divergence. We can use the known two-point correlation function $R(\omega_l,\omega_q)$ of the Gaussian unitary ensemble to obtain $\langle K\rangle_{\Omega,\Gamma} = 1+\frac{1}{3}\pi T\Gamma/\Delta$ for $T \ll 1$.

between the complex eigenvalues z_q of H and the real eigenvalues ω_q of H_0. Distinguishing between $q = l$ and $q \neq l$, we obtain three recursion relations,

$$z_l = \omega_l - \mathrm{i}\pi|\alpha_l|^2 - \mathrm{i}\pi\alpha_l \sum_{q\neq l} \alpha_q^* d_q \,, \tag{6.30a}$$

$$\mathrm{i}d_q = \frac{\pi\alpha_q}{z_l - \omega_q}\Big(\alpha_l^* + \sum_{p\neq l} \alpha_p^* d_p\Big) \,, \tag{6.30b}$$

$$\mathrm{i}e_q = \frac{\pi\alpha_q^*}{z_l - \omega_q}\Big(\alpha_l + \sum_{p\neq l} \alpha_p e_p\Big) \,. \tag{6.30c}$$

We now use the fact that z_l is the eigenvalue closest to the real axis. We may therefore assume that z_l is close to the unperturbed value ω_l and replace the denominator $z_l - \omega_q$ in Eq. (6.30c) by $\omega_l - \omega_q$. That decouples the recursion relations, which may then be solved in closed form,

$$z_l = \omega_l - \mathrm{i}\pi|\alpha_l|^2(1 + \mathrm{i}\pi A)^{-1} \,, \tag{6.31a}$$

$$\mathrm{i}d_q = \frac{\pi\alpha_q\alpha_l^*}{\omega_l - \omega_q}(1 + \mathrm{i}\pi A)^{-1} \,, \tag{6.31b}$$

$$\mathrm{i}e_q = \frac{\pi\alpha_q^*\alpha_l}{\omega_l - \omega_q}(1 + \mathrm{i}\pi A)^{-1} \,. \tag{6.31c}$$

We have defined

$$A = \sum_{q\neq l} |\alpha_q|^2(\omega_l - \omega_q)^{-1} \,. \tag{6.32}$$

The decay rate of the lasing mode is

$$\Gamma = -2\,\mathrm{Im}\, z_l = 2\pi|\alpha_l|^2(1 + \pi^2 A^2)^{-1} \,. \tag{6.33}$$

From Eq. (6.27) we find

$$K = 1 + \frac{2\pi\Gamma}{\Delta}\frac{B}{1 + \pi^2 A^2} \,, \tag{6.34}$$

with

$$B = \Delta \sum_{q\neq l} |\alpha_q|^2(\omega_l - \omega_q)^{-2} \,. \tag{6.35}$$

The problem is now reduced to a calculation of the joint probability distribution $P(A, B)$. This problem is closely related to the level curvature problem of

random-matrix theory [Opp94, Opp95, Fyo95]. The calculation is presented in Appendix 6.A. The result is

$$P(A,B) = \frac{\pi}{24}\left(\frac{8}{\pi w}\right)^{\beta/2} \frac{(\pi^2A^2+w^2)^\beta}{B^{2+3\beta/2}} \exp\left[-\frac{\beta w}{2B}\left(\frac{\pi^2A^2}{w^2}+1\right)\right]. \quad (6.36)$$

6.3.4 Probability distribution of the Petermann factor

From Eqs. (6.20), (6.33), (6.34), and (6.36) we can compute the probability distribution

$$P(K) = \langle Z\rangle^{-1}\left\langle \delta\left(K-1-\frac{2\pi\Gamma}{\Delta}\frac{B}{1+\pi^2A^2}\right) Z\right\rangle, \quad (6.37a)$$

$$Z = \delta(\Omega-\omega_l)\delta\left(\Gamma-\frac{2\pi|\alpha_l|^2}{1+\pi^2A^2}\right), \quad (6.37b)$$

of K at fixed Γ and Ω by averaging over $|\alpha_l|^2$, A, and B. In principle one should also require that the decay rates of modes $q \neq l$ are bigger than Γ, but this extra condition becomes irrelevant for $\Gamma \to 0$. The average of Z over $|\alpha_l|^2$ with Eq. (6.20) yields a factor $(1+\pi^2A^2)^{\beta/2}$. (Only the behaviour of $P(|\alpha_l|^2)$ for small $|\alpha_l|^2$ matters, because we concentrate on the lasing mode.) After integration over B the distribution can be expressed as a ratio of integrals over A,

$$P(K) = \frac{(2\pi)^{2\beta}}{3\beta}\frac{\Delta w}{\Gamma}\left(\frac{(K-1)\Delta}{w\Gamma}\right)^{-2-3\beta/2} \times \int_0^\infty \mathrm{d}A\, \frac{(1+\pi^2A^2/w^2)^\beta}{(1+\pi^2A^2)^{1+\beta}} \exp\left(-\frac{\beta\pi w\Gamma(1+\pi^2A^2/w^2)}{(K-1)\Delta(1+\pi^2A^2)}\right) \times \left(\int_0^\infty \mathrm{d}A\, \frac{(1+\pi^2A^2)^{\beta/2}}{(1+\pi^2A^2/w^2)^{1+\beta/2}}\right)^{-1}. \quad (6.38)$$

We introduce the rescaled Petermann factor $\kappa = (K-1)\Delta/\Gamma T$. A simple result for $P(\kappa)$ follows for $T = 1$,

$$P(\kappa) = \frac{4\beta\pi^{2\beta}}{3\kappa^{2+3\beta/2}} \exp\left(-\frac{\beta\pi}{\kappa}\right), \quad (6.39)$$

and for $T \ll 1$,

$$P(\kappa) = \frac{\pi}{12\kappa^2}\left(1+\frac{\pi}{2\kappa}\right)\exp\left(-\frac{\pi}{4\kappa}\right), \qquad \beta = 1, \quad (6.40a)$$

$$P(\kappa) = \frac{\pi}{8\sqrt{2\kappa^5}}\left(1+\frac{2\pi}{3\kappa}+\frac{\pi^2}{3\kappa^2}\right)\exp\left(-\frac{\pi}{2\kappa}\right), \qquad \beta = 2. \quad (6.40b)$$

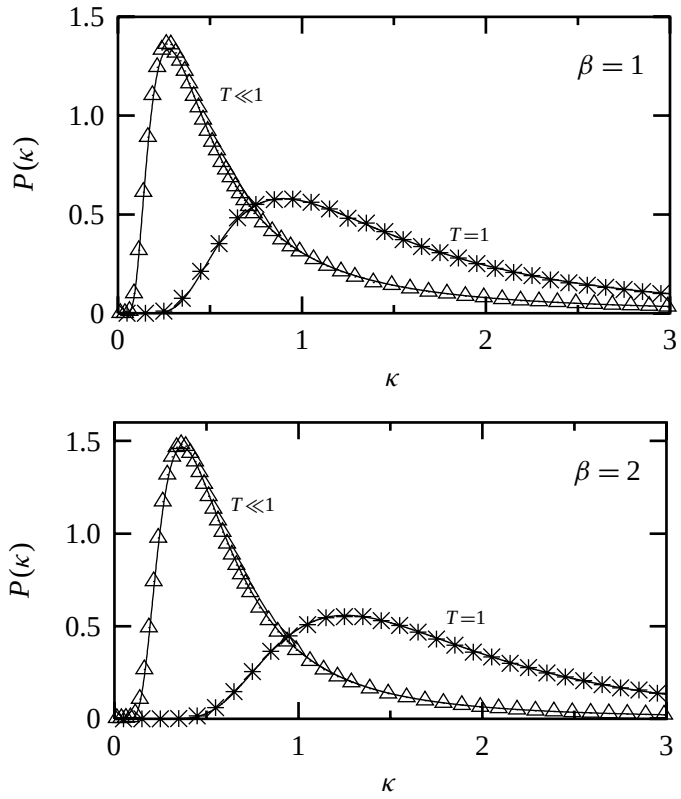

Figure 6.1: Probability distribution of the rescaled Petermann factor $\kappa = (K - 1)\Delta/\Gamma T$ for $T = 1$ and $T \ll 1$, in the presence of time-reversal symmetry (top) respectively absence of time-reversal symmetry (bottom). The solid curves follow from Eqs. (6.39) and (6.40), the data points follow from a numerical simulation of the random-matrix model.

As shown in Fig. 6.1, the distributions are very broad and asymmetric, with a long tail towards large κ.

To check our analytical results we have also done a numerical simulation of the random-matrix model, generating a large number of random matrices H and computing K from Eq. (6.19). As one can see from Fig. 6.1, the agreement with the theoretical predictions is flawless.

6.3.5 Mean Petermann factor

The distribution (6.38) gives for preserved time-reversal symmetry ($\beta = 1$) the mean Petermann factor

$$\langle K \rangle_{\Omega,\Gamma} = 1 - \frac{\Gamma}{\Delta}\frac{2\pi}{3}\frac{G^{22}_{22}\left(w^2 \left| \begin{matrix} 0 & 0 \\ -\frac{1}{2} & -\frac{1}{2} \end{matrix} \right.\right)}{G^{22}_{22}\left(w^2 \left| \begin{matrix} -\frac{1}{2} & \frac{1}{2} \\ -1 & 0 \end{matrix} \right.\right)}, \tag{6.41}$$

in terms of the ratio of two Meijer G functions. We have plotted the result in Fig. 6.2, as a function of $T = 4w(1+w)^{-2}$.

It is remarkable that the average K depends *non-analytically* on T, and hence on the area of the opening. (The transmission probability T is related to the area

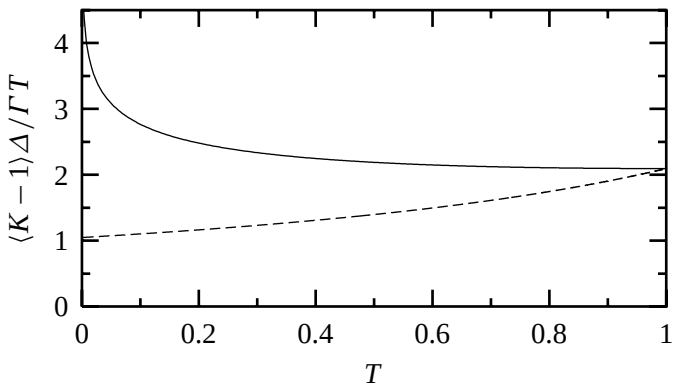

Figure 6.2: Average of the rescaled Petermann factor κ as a function of transmission probability T. The solid curve is the result (6.41) in the presence of time-reversal symmetry, the dashed curve is the result (6.43) for broken time-reversal symmetry. For small T, the solid curve diverges $\propto \ln T^{-1}$ while the dashed curve has the finite limit of $\pi/3$. For $T = 1$ both curves reach the value $2\pi/3$.

$\mathcal{A}$ of the opening by $T \simeq \mathcal{A}^3/\lambda^6$ for $T \ll 1$ [Bet44].) For $T \ll 1$, the average approaches the form

$$\langle K \rangle_{\Omega,\Gamma} = 1 + \frac{\pi}{6}\frac{T\Gamma}{\Delta}\ln\frac{16}{T} \,. \tag{6.42}$$

The most probable (or modal) value of $K - 1 \simeq T\Gamma/\Delta$ is parametrically smaller than the mean value (6.42) for $T \ll 1$. The non-analyticity results from the relatively weak eigenvalue repulsion in the presence of time-reversal symmetry. If time-reversal symmetry is broken, then the stronger quadratic repulsion is sufficient to overcome the ω^{-2} divergence of perturbation theory (6.28) and the average K becomes an analytic function of T. For this case, we find from Eq. (6.38) the mean Petermann factor

$$\langle K \rangle_{\Omega,\Gamma} = 1 + \frac{\Gamma}{\Delta}\frac{4\pi w}{3(1+w^2)} \,, \tag{6.43}$$

shown dashed in Fig. 6.2.

6.4 Many scattering channels

For arbitrary number of scattering channels N the coupling matrix W is an $M \times N$ rectangular matrix. The square matrix $\pi W^\dagger W$ has N eigenvalues $(M\Delta/\pi)w_n$. The transmission coefficients of the eigenchannels are

$$T_n = \frac{4w_n}{(1+w_n)^2} \,. \tag{6.44}$$

A single hole of area $\mathcal{A} \gg \lambda^2$ (at wavelength λ) corresponds to $N \simeq 2\pi\mathcal{A}/\lambda^2$ fully transmitted scattering channels, with all $T_n = w_n = 1$ the same. We will only discuss this case in the following. As in the single-channel case, we first determine the distribution of the decay rate Γ of the lasing mode. Then we discuss the mean Petermann factor $\langle K \rangle$ for given Γ.

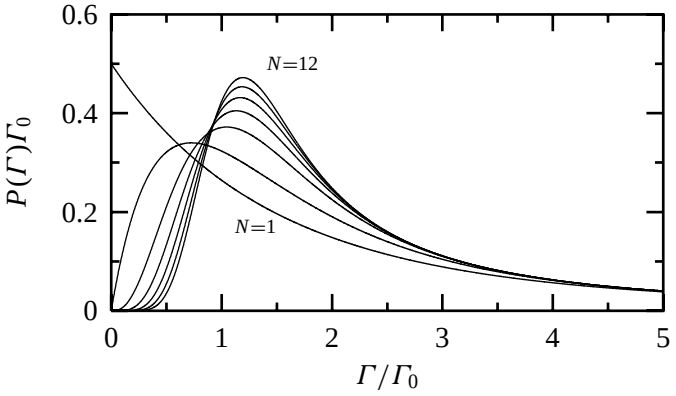

Figure 6.3: Decay-rate distribution $P(\Gamma)$ of a chaotic cavity with an opening that supports $N = 1, 2, 4, 6, 8, 10, 12$ fully transmitted scattering channels. Computed from Eq. (6.45), for the case of broken time-reversal symmetry.

6.4.1 Decay rate of the lasing mode

The distribution of decay rates $P(\Gamma)$ has been calculated by Fyodorov and Sommers. For broken time-reversal symmetry the result is [Fyo96, Fyo97]

$$P(\Gamma) = \frac{\pi}{\Delta}\mathcal{F}_1\left(\frac{\pi}{\Delta}\Gamma\right)\mathcal{F}_2\left(\frac{\pi}{\Delta}\Gamma\right), \tag{6.45a}$$

$$\mathcal{F}_1(y) = \frac{1}{(N-1)!}y^{N-1}\mathrm{e}^{-y}, \tag{6.45b}$$

$$\mathcal{F}_2(y) = \sum_{n=0}^{N}(-1)^n\binom{N}{n}\frac{\mathrm{d}^n}{\mathrm{d}y^n}\left(\frac{\sinh y}{y}\right). \tag{6.45c}$$

The behaviour of $P(\Gamma)$ for various numbers N of fully transmitted scattering channels is illustrated in Fig. 6.3.

The case $N = 1$ is special in that only for this case $P(\Gamma = 0)$ is non-zero. For the other extreme, $N \gg 1$, there even appears a gap and the distribution $P(\Gamma)$ becomes non-zero only for $\Gamma > \Gamma_0$ (with $\Gamma = N\Delta/2\pi$), where it is equal to [Haa92, Leh95]

$$P(\Gamma) = \frac{\Gamma_0}{\Gamma^2}, \qquad \Gamma > \Gamma_0. \tag{6.46}$$

The smallest decay rate Γ_0 corresponds to the inverse mean dwell time in the

cavity. For large but finite N, the tail $\Gamma \lesssim \Gamma_0$ of the distribution is given by

$$P(\Gamma) = \frac{\pi}{NT^2\Delta}\big[1+\mathrm{erf}(u)\big] + \mathcal{O}(N^{-3/2})\,, \tag{6.47}$$

where we have defined $u = \sqrt{N/2}(\Gamma/\Gamma_0 - 1)$.

The distribution $P_L(\Gamma)$ of the lasing mode follows from Eq. (6.23), and is sharply peaked around a value of Γ deviating from Γ_0 only by order $\Delta\sqrt{N} \ll \Gamma_0$ (as long as $L \ll \mathrm{e}^N$). This is in contrast to the results for $N = 1$, where Γ of the lasing mode is very small. This enabled us in Sec. 6.3 to only consider the limit $\Gamma \to 0$, which proved to be essential in the derivation presented there. In the calculation for $N > 1$ this limit is not applicable, making the calculation much more difficult and disallowing to simply follow the lines of Sec. 6.3. As result, only the average of the Petermann factor has been calculated, whereas its distribution is not known for $N > 1$.

The results for preserved time-reversal symmetry are more involved [Som99]. Fortunately, we can draw all important conclusions from the results for broken time-reversal symmetry, on which we will concentrate here. Especially, the large-N limit (6.46) remains valid.

6.4.2 Mean Petermann factor

The mean Petermann factor is [Fra00, Sch00]

$$\langle K\rangle_{\Omega,\Gamma} = 1 + \frac{2S(\pi\Gamma/\Delta)}{\mathcal{F}_1(\pi\Gamma/\Delta)\mathcal{F}_2(\pi\Gamma/\Delta)}\,, \tag{6.48a}$$

$$S(y) = \sum_{n=0}^{N-1} \frac{(-1)^n}{n!} y^n \frac{\mathrm{d}^n}{\mathrm{d}y^n}\left[\mathrm{e}^{-y}\frac{\mathrm{d}}{\mathrm{d}y}\left(\frac{\sinh y}{y}\right)\right], \tag{6.48b}$$

with $\mathcal{F}_1$ and $\mathcal{F}_2$ given in Eq. (6.45). For $N \gg 1$ and $\Gamma \lesssim \Gamma_0$, this can be simplified to give

$$\begin{aligned}\langle K\rangle_{\Omega,\Gamma} &= \sqrt{2N}[F(u)+u] \\ &\quad + F(u)\big[(3-g)u + \tfrac{4}{3}u^3 + \tfrac{4}{3}(1+u^2)F(u)\big] + \mathcal{O}(N^{-1/2})\,,\end{aligned} \tag{6.49a}$$

$$F(u) = \frac{\exp(-u^2)}{\sqrt{\pi}\big[1+\mathrm{erf}(u)\big]}\,. \tag{6.49b}$$

For $\Gamma = \Gamma_0$ ($u = 0$) this simplifies further to

$$\langle K\rangle_{\Omega,\Gamma=\Gamma_0} = \sqrt{\frac{2N}{\pi}} + \frac{4}{3\pi}\,. \tag{6.50}$$

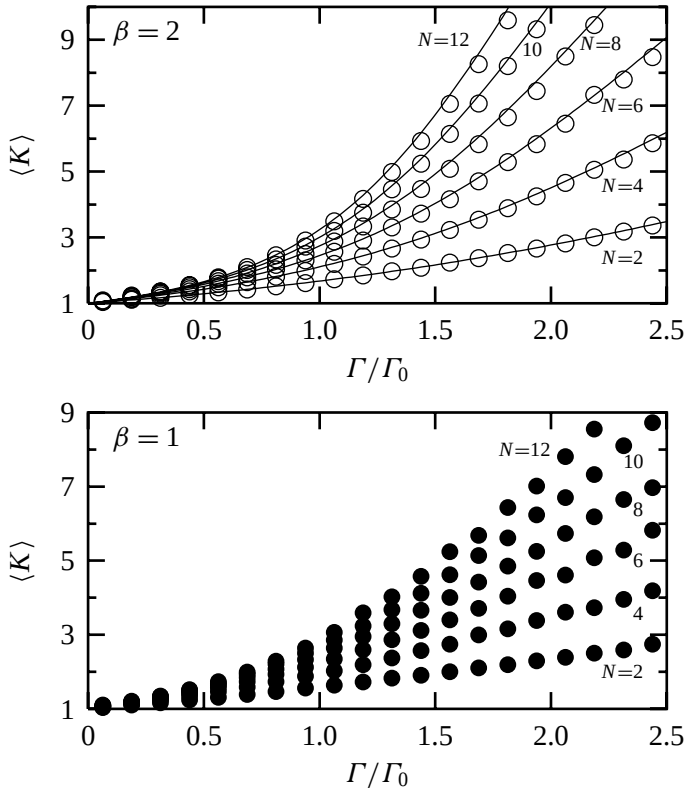

Figure 6.4: Average Petermann factor $\langle K \rangle$ as a function of the decay rate Γ for different numbers N of fully transmitted scattering channels, when time-reversal symmetry is broken (top) respectively preserved (middle). The solid curves are the analytical result (6.48), the data points are obtained by a numerical simulation.

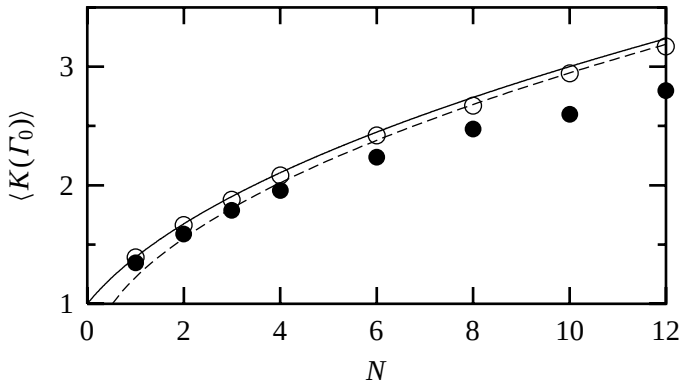

Figure 6.5: Average of the Petermann factor K at $\Gamma = \Gamma_0$ as function of the number N of fully transmitted scattering channels. The analytical result (6.48) for broken time-reversal symmetry (full curve) is compared with the result of a numerical simulation (open circles for broken time-reversal symmetry, filled circles for preserved time-reversal symmetry). The dashed line is the large-N result (6.50).

We now compare the analytical findings with the results of numerical simulations. We generated a large number of random matrices H with dimension $M = 120$ ($M = 200$) for $N = 2,4,6,8$ ($N = 10,12$) fully transmitted scattering channels. Fig. 6.4 shows the mean K at given Γ. We find excellent agreement with the analytical result (6.48). The behaviour $\langle K \rangle \sim \sqrt{N}$ at $\Gamma = \Gamma_0$ predicted by Eq. (6.50) is verified in Fig. 6.5.

In the absence of an analytical result, the numerical simulation can be used to compute the distribution of K at given Γ. The result depicted in Fig. 6.7 shows that, similar to the single-channel case, the distribution is wide and highly asymmetric with a long tail towards high K.

For preserved time-reversal symmetry ($\beta = 1$), no analytical result for the mean of K at given Γ is known for $N > 2$. For larger numbers of channels we can draw our conclusions from the numerical results that are presented in Fig. 6.4. Interestingly enough the data points for N channels are close to the results for broken time-reversal symmetry with $N/2$ channels, when the decay rate is given in units of Γ_0. This is illustrated for $N = 8$ in Fig. 6.6. Such a rule of thumb (motivated by the number of real degrees of freedom that enter the non-Hermitian part of H) was already known for the decay rate distribution (Fig. 6.6, bottom). Hence the Petermann factor for the lasing mode should also for $\beta = 1$ display a

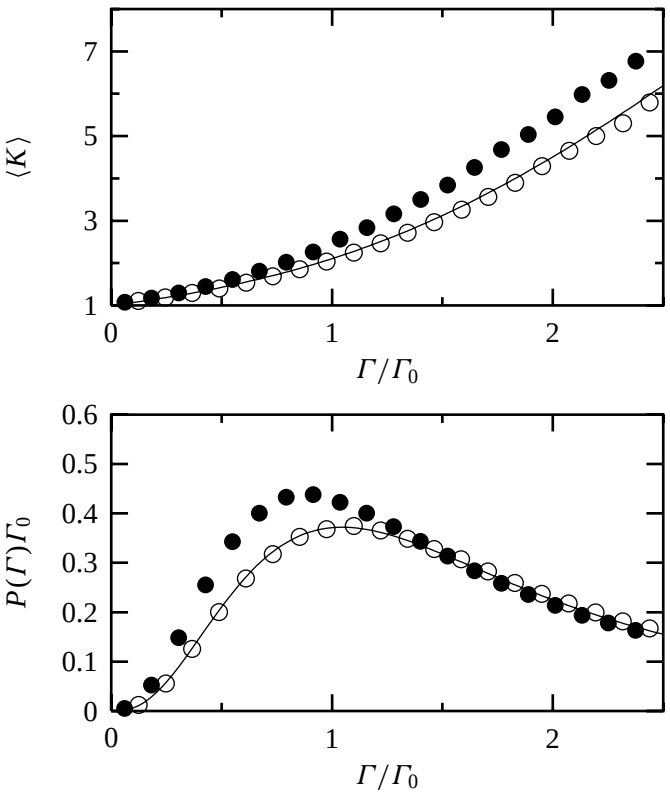

Figure 6.6: Top: Average Petermann factor $\langle K \rangle$ for $N = 4$, $\beta = 2$ [open circles: result of a numerical simulation, curve: Eq. (6.48)] and for $N = 8$, $\beta = 1$ (filled circles: numerical simulation). The parameter Γ_0 equals $N\Delta/2\pi$ in both cases, so it is twice as large for $\beta = 2$ as for $\beta = 1$. Bottom: Probability distribution of Γ for $N = 4$, $\beta = 2$ [open circles: numerical simulation, curve: Eq. (6.45)] and for $N = 8$, $\beta = 1$ (filled circles: numerical simulation).

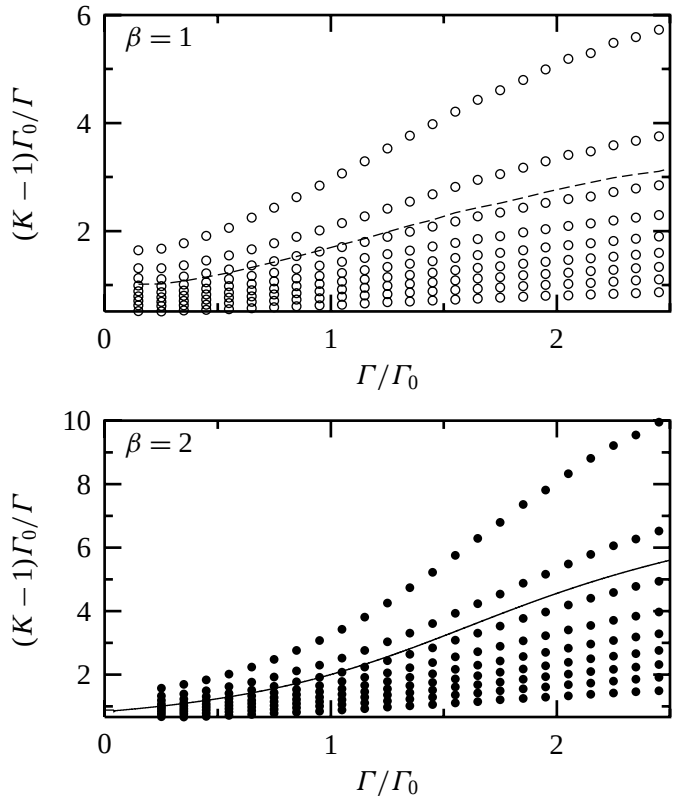

Figure 6.7: Numerically computed distribution of the scaled Petermann factor $(K-1)/\Gamma$ for $N = 10$ when time-reserval symmetry is preserved (top) respectively broken (bottom) as a function of Γ. The points mark the values below which $10\%, 20\%, \ldots, 90\%$ of all computed data points lie. The lines are the average [computed numerically for $\beta = 1$, computed analytically from Eq. (6.48) for $\beta = 2$].

sublinear growth with increasing channel number N. This expectation is indeed confirmed by the numerical simulations, see the filled circles in Fig. 6.5.

6.5 Discussion

The Petermann factor K enters the fundamental lower limit of the laser linewidth due to vacuum fluctuations and is a measure of the non-orthogonality of cavity modes. We related the Petermann factor to the residue of the scattering-matrix pole that pertains to the lasing mode and computed statistical properties of K in an ensemble of chaotic cavities. Lasing action selects a mode which has a small decay rate Γ, and hence belongs to a pole that lies anomalously close to the real axis. For a single scattering channel this simplifies the calculation, yielding a mean Petermann factor depending non-analytically on the transmission probability T. On the other hand, for large number N of scattering channels non-perturbative statistical methods have now to be employed [Fra00, Sch00], resulting in parametrically large Petermann factors $\propto \sqrt{N}$.

The quantity K is also of fundamental significance in the general theory of scattering resonances, where it enters the width-to-height relation of resonance peaks and determines the scattering strength of a quasi-bound state with given decay rate Γ. If we write the scattering matrix (6.7) in the form

$$S_{nm} = \delta_{nm} + \sigma_n \sigma'_m (\omega - \Omega + \mathrm{i}\Gamma/2)^{-1} , \tag{6.51}$$

then the scattering strengths σ_n, σ'_m are related to Γ by a sum rule. For resonances close to the real axis ($\Gamma \ll \Delta$) the relation is

$$\sum_{n,m} |\sigma_n \sigma'_m|^2 = \Gamma^2 . \tag{6.52}$$

For poles deeper in the complex plane, however, the sum rule has to be replaced by

$$\sum_{n,m} |\sigma_n \sigma'_m|^2 = K \Gamma^2 , \qquad K \geqslant 1 . \tag{6.53}$$

6.A Joint distribution of A and B

We calculate the joint distribution $P(A, B)$ [Eq. (6.36)] of the quantities A [Eq. (6.32)] and B [Eq. (6.35)] by generalising the theory of Ref. [Fyo95]. We give the lasing mode ω_l the new index M and assume that it lies at the centre

of the semicircle (6.3), $\omega_M = 0$. Other choices just renormalise the mean modal spacing Δ, which we can set to $\Delta = 1$. The quantities A and B are then of the form

$$A = \sum_{m=1}^{M-1} \frac{|\alpha_m|^2}{\omega_m}, \qquad B = \sum_{m=1}^{M-1} \frac{|\alpha_m|^2}{\omega_m^2}. \tag{6.54}$$

The joint probability distribution of A and B,

$$P(A,B) = \left\langle \delta\Big(A - \sum_{m=1}^{M-1} \frac{|\alpha_m|^2}{\omega_m}\Big)\delta\Big(B - \sum_{m=1}^{M-1} \frac{|\alpha_m|^2}{\omega_m^2}\Big)\right\rangle, \tag{6.55}$$

is obtained by averaging over the variables $\{|\alpha_m|^2, \omega_m\}$. The quantities $|\alpha_m|^2$ are independent numbers with probability distribution (6.20). The joint probability distribution of the eigenfrequencies $\{\omega_m\}$ of the closed cavity is the eigenvalue distribution of the Gaussian ensembles (6.2) of random-matrix theory,

$$P(\{\omega_m\}) \propto \prod_{i<j} |\omega_i - \omega_j|^\beta \exp\Big(-\frac{\beta M}{4\mu^2} \sum_k \omega_k^2\Big). \tag{6.56}$$

Our choice $\Delta = 1$ translates into $\mu = M/\pi$.

The joint probability distribution of the eigenvalues $\{\omega_m\}$ ($m = 1, \ldots, M-1$) is found by setting $\omega_M = 0$ in Eq. (6.56). It factorises into the eigenvalue distribution of $M-1$ dimensional Gaussian matrices $\boldsymbol{H}'$ [again distributed according to Eq. (6.2)], and the term $\prod_{j=1}^{M-1} |\omega_i|^\beta = |\det \boldsymbol{H}'|^\beta$.

In the first step of our calculation, we use the Fourier representation of the δ-functions in Eq. (6.55) and write

$$P(A,B) \propto \left\langle \int_{-\infty}^{\infty} \mathrm{d}x \int_{-\infty}^{\infty} \mathrm{d}y\, \mathrm{e}^{\mathrm{i}xA + \mathrm{i}yB} \prod_{m=1}^{M-1} \int_0^\infty \mathrm{d}|\alpha_m|^2\, P(|\alpha_m|^2) \right.$$
$$\left. \times \exp\Big(-\mathrm{i}x \sum_{m=1}^{M-1} \frac{|\alpha_m|^2}{\omega_m} - \mathrm{i}y \sum_{m=1}^{M-1} \frac{|\alpha_m|^2}{\omega_m^2}\Big)\right\rangle, \tag{6.57}$$

where the average refers to the variables $\{\omega_m\}$. The integrals over $|\alpha_m|^2$ can be performed, resulting in

$$P(A,B) \propto \int \mathrm{d}x \int \mathrm{d}y\, \mathrm{e}^{\mathrm{i}xA + \mathrm{i}yB} \left\langle \frac{\det \boldsymbol{H}'^{2\beta}}{\det\big[\boldsymbol{H}'^2 + 2\mathrm{i}w(x\boldsymbol{H}' + y)/\pi^2\beta\big]^{\beta/2}}\right\rangle, \tag{6.58}$$

where the average is now over the Gaussian ensemble of $\boldsymbol{H}'$-matrices. It is our goal to relate this average to autocorrelators of the secular polynomial of Gaussian distributed random matrices, given in Refs. [And95, Ket97].

The determinant in the denominator can be expressed as a Gaussian integral,

$$P(A,B) \propto \int \mathrm{d}x \int \mathrm{d}y\, \mathrm{e}^{\mathrm{i}xA+\mathrm{i}yB} \int \mathrm{d}\boldsymbol{z} \int \mathrm{d}\boldsymbol{H}'\, \det \boldsymbol{H}'^{2\beta} \times \exp\left[-\frac{\beta\pi^2}{4M} \operatorname{tr} \boldsymbol{H}'^2 - \boldsymbol{z}^\dagger \left(\boldsymbol{H}'^2 + \frac{2\mathrm{i}w}{\beta\pi^2}(x\boldsymbol{H}' + y) \right) \boldsymbol{z} \right], \quad (6.59)$$

where the $M-1$ dimensional vector $\boldsymbol{z}$ is real (complex) for $\beta = 1$ (2). Since our original expression did only depend on the eigenvalues of $\boldsymbol{H}'$, the formulation above is invariant under orthogonal (unitary) transformations of $\boldsymbol{H}'$, and we can choose a basis in which $\boldsymbol{z}$ points into the direction of the last basis vector (index $M-1$). Let us denote the Hamiltonian in the block form

$$\boldsymbol{H}' = \begin{pmatrix} \boldsymbol{V} & \boldsymbol{h} \\ \boldsymbol{h}^\dagger & g \end{pmatrix}. \quad (6.60)$$

Here $\boldsymbol{V}$ is a $(M-2)\times(M-2)$ matrix, g a number, and $\boldsymbol{h}$ a $(M-2)$ dimensional vector. In this notation,

$$P(A,B) \propto \int \mathrm{d}x \int \mathrm{d}y\, \mathrm{e}^{\mathrm{i}xA+\mathrm{i}yB} \int \mathrm{d}\boldsymbol{z} \int \mathrm{d}g \int \mathrm{d}\boldsymbol{V} \int \mathrm{d}\boldsymbol{h} \times \det\left[\boldsymbol{V}^{2\beta}(g - \boldsymbol{h}^\dagger \boldsymbol{V}^{-1}\boldsymbol{h})^{2\beta}\right] \exp\left[-\frac{\beta\pi^2}{4M}\left(g^2 + 2|\boldsymbol{h}|^2 + \operatorname{tr}\boldsymbol{V}^2\right)\right] \times \exp\left[-|\boldsymbol{z}|^2 \left(g^2 + |\boldsymbol{h}|^2 + \frac{2\mathrm{i}w}{\beta\pi^2}[xg + y] \right)\right]. \quad (6.61)$$

The integrals over x and y give δ-functions,

$$P(A,B) \propto \int \mathrm{d}\boldsymbol{z} \int \mathrm{d}g \int \mathrm{d}\boldsymbol{V} \int \mathrm{d}\boldsymbol{h}\, \det\left[\boldsymbol{V}^{2\beta}(g - \boldsymbol{h}^\dagger \boldsymbol{V}^{-1}\boldsymbol{h})^{2\beta}\right] \times \exp\left[-\frac{\beta\pi^2}{4M}\left(g^2 + 2|\boldsymbol{h}|^2 + \operatorname{tr}\boldsymbol{V}^2\right) - |\boldsymbol{z}|^2\left(g^2 + |\boldsymbol{h}|^2\right)\right] \times \delta(A - gB)\,\delta\left(B - 2w|\boldsymbol{z}|^2/\beta\pi^2\right). \quad (6.62)$$

We then integrate over g and $\boldsymbol{z}$,

$$P(A,B) \propto \int \mathrm{d}\boldsymbol{V}\, \mathrm{d}\boldsymbol{h}\, \det\left[\boldsymbol{V}^{2\beta}\left(\frac{A}{B}-\boldsymbol{h}^{\dagger}\boldsymbol{V}^{-1}\boldsymbol{h}\right)^{2\beta}\right] B^{\frac{\beta}{2}(M-1)-2} \times \exp\left[-\frac{\beta\pi^2}{4M}\left(2|\boldsymbol{h}|^2+\operatorname{tr}\boldsymbol{V}^2\right)-\frac{\beta\pi^2 B}{2w}\left(\frac{A^2}{B^2}+|\boldsymbol{h}|^2\right)\right]. \quad (6.63)$$

We already anticipated $B \gg 1/M$ and omitted in the exponent a term $-\beta\pi^2 A^2/4MB^2$.

The integral over $\boldsymbol{h}$ can be interpreted as an average over Gaussian random variables with variance

$$h^2 \equiv \langle |h_i|^2 \rangle = \frac{1}{\pi^2}\frac{1}{B/w+1/M} \approx \frac{w}{\pi^2 B}\left(1-\frac{w}{MB}\right). \quad (6.64)$$

For the stochastic interpretation one also has to supply the normalisation constants proportional to

$$h^{\beta(M-2)} = \left(\frac{w}{\pi^2 B}\right)^{\beta(M-2)/2} \exp\left(-\frac{\beta w}{2B}\right). \quad (6.65)$$

The integral over $\boldsymbol{V}$ is another Gaussian average, and thus

$$P(A,B) \propto Q_\beta B^{\frac{\beta}{2}-2} \exp\left[-\frac{\beta w}{2B}\left(1+\frac{\pi^2 A^2}{w^2}\right)\right], \quad (6.66a)$$

$$Q_\beta = \left\langle \det\left[\boldsymbol{V}^{2\beta}\left(\frac{A}{B}-\boldsymbol{h}^{\dagger}\boldsymbol{V}^{-1}\boldsymbol{h}\right)^{2\beta}\right]\right\rangle. \quad (6.66b)$$

After averaging over $\boldsymbol{h}$, one has now to consider for $\beta = 1$

$$Q_1 = \left\langle \det\left(\boldsymbol{V}^2\frac{A^2}{B^2}+h^4\boldsymbol{V}^2\left[(\operatorname{tr}\boldsymbol{V}^{-1})^2+2\operatorname{tr}\boldsymbol{V}^{-2}\right]\right)\right\rangle, \quad (6.67)$$

where only the even terms in $\boldsymbol{V}$ have been kept. The ratio of coefficients in this polynomial in A/B can be calculated from the autocorrelator [Ket97]

$$G_1(\omega,\omega') = \frac{\left\langle \det(\boldsymbol{V}+\omega)(\boldsymbol{V}+\omega')\right\rangle}{\langle \det \boldsymbol{V}^2\rangle} = -\frac{3}{\pi^2 x}\frac{\mathrm{d}}{\mathrm{d}x}\frac{\sin\pi x}{\pi x}\bigg|_{x=\omega-\omega'} \quad (6.68)$$

of the secular polynomial of Gaussian distributed real matrices $\boldsymbol{V}$. This is achieved by expressing the products of traces and determinants through secular coefficients,

and these then as derivatives of the secular determinant,

$$\frac{\langle \det \boldsymbol{V}^2 (\mathrm{tr}\, \boldsymbol{V}^{-1})^2 \rangle}{\langle \det \boldsymbol{V}^2 \rangle} = \frac{\partial^2}{\partial\omega \partial\omega'} G_1(\omega,\omega')\Big|_{\omega=\omega'=0} = -\frac{\partial^2}{\partial\omega^2} G_1(\omega,0)\Big|_{\omega=0} = \frac{\pi^2}{5}\,, \tag{6.69a}$$

$$\frac{2\langle \det \boldsymbol{V}^2 (\mathrm{tr}\, \boldsymbol{V}^{-2}) \rangle}{\langle \det \boldsymbol{V}^2 \rangle} = -4\frac{\partial^2}{\partial\omega^2} G_1(\omega,0)\Big|_{\omega=0}\,. \tag{6.69b}$$

[We used the translational invariance of $G(\omega,\omega')$.] Eqs. (6.64) and (6.68) yield

$$Q_1 \propto \frac{A^2}{B^2} + \frac{w^2}{\pi^2 B^2}\,. \tag{6.70}$$

For $\beta = 2$, the average over $\boldsymbol{h}$ yields the expression

$$Q_2 \propto \frac{A^4}{B^4} + q_1 h^4 \frac{A^2}{B^2} + q_2 h^8\,, \tag{6.71a}$$

$$q_1 = 6\langle \det \boldsymbol{V}^4 \big[(\mathrm{tr}\, \boldsymbol{V}^{-1})^2 + \mathrm{tr}\, \boldsymbol{V}^{-2} \big] \rangle\,, \tag{6.71b}$$

$$\begin{aligned} q_2 = \langle \det \boldsymbol{V}^4 \big[&(\mathrm{tr}\, \boldsymbol{V})^{-4} + 6\,\mathrm{tr}\, \boldsymbol{V}^{-2} (\mathrm{tr}\, \boldsymbol{V}^{-1})^2 \\ &+ 8\,\mathrm{tr}\, \boldsymbol{V}^{-1}\,\mathrm{tr}\, \boldsymbol{V}^{-3} + 6\,\mathrm{tr}\, \boldsymbol{V}^{-4} + 3(\mathrm{tr}\, \boldsymbol{V}^{-2})^2 \big] \rangle\,. \end{aligned} \tag{6.71c}$$

The coefficients can now be computed from the four-point correlator of the Gaussian unitary ensemble [And95],

$$\begin{aligned} G_2(\omega_1,\omega_2,\omega_3,\omega_4) &= \frac{\langle \det(\boldsymbol{V}+\omega_1)(\boldsymbol{V}+\omega_2)(\boldsymbol{V}+\omega_3)(\boldsymbol{V}+\omega_4) \rangle}{\langle \det \boldsymbol{V}^4 \rangle} \\ &= \frac{3}{2\pi^4} \Bigg[\frac{\cos\pi(\omega_1+\omega_2-\omega_3-\omega_4)}{(\omega_1-\omega_3)(\omega_1-\omega_4)(\omega_2-\omega_3)(\omega_2-\omega_4)} \\ &\quad + \frac{\cos\pi(\omega_1+\omega_3-\omega_2-\omega_4)}{(\omega_1-\omega_2)(\omega_1-\omega_4)(\omega_3-\omega_2)(\omega_3-\omega_4)} \\ &\quad + \frac{\cos\pi(\omega_1+\omega_4-\omega_3-\omega_2)}{(\omega_1-\omega_3)(\omega_1-\omega_2)(\omega_4-\omega_3)(\omega_4-\omega_2)} \Bigg]\,, \end{aligned} \tag{6.72a}$$

$$G_2(\omega,0,0,0) = \frac{3}{\pi^3\omega^3}(\sin\pi\omega - \pi\omega\cos\pi\omega)\,, \tag{6.72b}$$

$$G_2(\omega,\omega,0,0) = \frac{3}{2\pi^4\omega^4}(\cos 2\pi\omega - 1 + 2\pi^2\omega^2)\,. \tag{6.72c}$$

In this case

$$q_1 = \frac{\partial^2}{\partial\omega^2}\big[6G_2(\omega,\omega,0,0) - 18G_2(\omega,0,0,0)\big]\Big|_{\omega=0} = 2\pi^2\,, \tag{6.73a}$$

$$q_2 = \frac{\partial^4}{\partial\omega^4}\big[10G_2(\omega,\omega,0,0) - 15G_2(\omega,0,0,0)\big]\Big|_{\omega=0} = \pi^2\,, \tag{6.73b}$$

which gives

$$Q_2 \propto Q_1^2 \,. \tag{6.74}$$

Collecting results we obtain Eq. (6.36), where we also included the normalisation constant.

References

[Abd99] G. M. Abd Al-Kader, *Statistical properties of the output of linear amplifier with superpositions of squeezed displaced Fock states as an input state*, Eur. Phys. J. B **8** (1999), 429–438.

[Alt91] B. L. Altshuler, P. A. Lee, and R. A. Webb (eds.), *Mesoscopic phenomena in solids*, Amsterdam, North-Holland, 1991.

[Alt97] H. Alt, C. Dembowski, H.-D. Gräf, R. Hofferbert, H. Rehfeld, A. Richter, R. Schuhmann, and T. Weiland, *Wave dynamical chaos in a superconducting three-dimensional Sinai billiard*, Phys. Rev. Lett. **79** (1997), 1026–1029.

[And95] A. V. Andreev and B. D. Simons, *Correlators of spectral determinants in quantum chaos*, Phys. Rev. Lett. **75** (1995), 2304–2307.

[Art99] M. Artoni and R. Loudon, *Propagation of nonclassical light through an absorbing and dispersive slab*, Phys. Rev. A **59** (1999), 2279–2290.

[Bar91] H. U. Baranger, D. P. DiVincenzo, R. A. Jalabert, and A. D. Stone, *Classical and quantum ballistic-transport anomalies in microjunctions*, Phys. Rev. B **44** (1991), 10637–10675.

[Bar98] S. M. Barnett, J. Jeffers, A. Gatti, and R. Loudon, *Quantum optics of lossy beam splitters*, Phys. Rev. A **57** (1998), 2134–2145.

[Bee92] C. W. J. Beenakker and M. Büttiker, *Suppression of shot noise in metallic diffusive conductors*, Phys. Rev. B **46** (1992), 1889–1892.

[Bee96] C. W. J. Beenakker, J. C. J. Paasschens, and P. W. Brouwer, *Probability of reflection by a random laser*, Phys. Rev. Lett. **76** (1996), 1368–1371.

[Bee97] C. W. J. Beenakker, *Random-matrix theory of quantum transport*, Rev. Mod. Phys. **69** (1997), 731–808.

[Bee98] C. W. J. Beenakker, *Thermal radiation and amplified spontaneous emission from a random medium*, Phys. Rev. Lett. **81** (1998), 1829–1832.

[Bee99] C. W. J. Beenakker, *Photon statistics of a random laser*, In Fouque [Fou99], pp. 137–164.

[Bet44] H. A. Bethe, *Theory of diffraction by small holes*, Phys. Rev. **66** (1944), 163–182.

[Boa90] D. H. Boal, C.-K. Gelbke, and B. K. Jennings, *Intensity interferometry in subatomic physics*, Rev. Mod. Phys. **62** (1990), 553–602.

[Boh84] O. Bohigas, M. J. Giannoni, and C. Schmit, *Characterization of chaotic quantum spectra and universality of level fluctuation laws*, Phys. Rev. Lett. **52** (1984), 1–4.

[Bro95] P. W. Brouwer, *Generalized circular ensemble of scattering matrices for a chaotic cavity with nonideal leads*, Phys. Rev. B **51** (1995), 16878–16884.

[Bro98] P. W. Brouwer, *Transmission through a many-channel random waveguide with absorption*, Phys. Rev. B **57** (1998), 10526–10536. Equation (13c) contains a misprint: The second and third term between brackets should have, respectively, signs minus and plus instead of plus and minus.

[Bru97] M. Brunel, G. Ropars, A. Le Floch, and F. Bretenaker, *Transverse excess noise factor in geometrically stable laser resonators*, Phys. Rev. A **55** (1997), 4563–4567.

[Büt90] M. Büttiker, *Scattering theory of thermal and excess noise in open conductors*, Phys. Rev. Lett. **65** (1990), 2901–2904.

[Büt99] M. Büttiker, *Bunches of photons–antibunches of electrons*, Science **284** (1999), 275–276.

[Cao99] H. Cao, Y. G. Zhao, S. T. Ho, E. W. Seelig, Q. H. Wang, and R. P. H. Chang, *Random laser action in semiconductor powder*, Phys. Rev. Lett. **82** (1999), 2278–2281.

[Cav82] C. M. Caves, *Quantum limits on noise in linear amplifiers*, Phys. Rev. D **26** (1982), 1817–1839.

[Cha98] J. T. Chalker and B. Mehlig, *Eigenvector statistics in non-Hermitian random matrix ensembles*, Phys. Rev. Lett. **81** (1998), 3367–3370.

[Che96] Y. J. Cheng, C. G. Fanning, and A. E. Siegman, *Experimental observation of a large excess quantum noise factor in the linewidth of a laser oscillator having nonorthogonal modes*, Phys. Rev. Lett. **77** (1996), 627–630.

[Eij96] M. A. van Eijkelenborg, Å. M. Lindberg, M. S. Thijssen, and J. P. Woerdman, *Resonance of quantum noise in an unstable cavity laser*, Phys. Rev. Lett. **77** (1996), 4314–4317.

[Eij97] M. A. van Eijkelenborg, Å. M. Lindberg, M. S. Thijssen, and J. P. Woerdman, *Unstable-resonator diffraction losses and the excess-noise factor*, Phys. Rev. A **55** (1997), 4556–4562.

[Ein09] A. Einstein, *Zum gegenwärtigen Stand des Strahlungsproblems*, Phys. Z. **10** (1909), 185–193.

[Fan47] U. Fano, *Ionization yields of radiation. II. The fluctuations of the number of ions*, Phys. Rev. **72** (1947), 26–29.

[Fou99] J.-P. Fouque (ed.), *Diffuse waves in complex media*, NATO Science Series C, vol. 531, Dordrecht, Kluwer, 1999.

[Fra00] K. M. Frahm, H. Schomerus, M. Patra, and C. W. J. Beenakker, *Large Petermann factor in chaotic cavities with many scattering channels*, Europhys. Lett. **49** (2000), 48–54.

[Fyo95] Y. V. Fyodorov and H.-J. Sommers, *Universality of "level curvature" distribution for large random matrices: systematic analytical approach*, Z. Phys. B **99** (1995), 123–135.

[Fyo96] Y. V. Fyodorov and H.-J. Sommers, *Statistics of S-matrix poles in few-channel chaotic scattering: Crossover from isolated to overlapping resonances*, Pis'ma Zh. Eksp. Teor. Fiz. **63** (1996), 970–973 [JETP Lett. **63** (1996), 1026–1030].

[Fyo97] Y. V. Fyodorov and H.-J. Sommers, *Statistics of resonance poles, phase shifts and time delays in quantum chaotic scattering: Random matrix approach for systems with broken time-reversal invariance*, J. Math. Phys. **38** (1997), 1918–1981.

[Gla63] R. J. Glauber, *Photon correlations*, Phys. Rev. Lett. **10** (1963), 84–86.

[Gol91] P. Goldberg, P. W. Milonni, and B. Sundaram, *Theory of the fundamental laser linewidth*, Phys. Rev. A **44** (1991), 1969–1985.

[Gra98] P. Grangier and J.-P. Poizat, *A simple quantum picture for the Petermann excess noise factor*, Eur. Phys. J. D **1** (1998), 97–104.

[Gru96a] T. Gruner and D.-G. Welsch, *Green-function approach to the radiation-field quantization for homogeneous and inhomogeneous Kramers-Kronig dielectrics*, Phys. Rev. A **53** (1996), 1818–1829.

[Gru96b] T. Gruner and D.-G. Welsch, *Quantum-optical input-output relations for dispersive and lossy multilayer dielectric plates*, Phys. Rev. A **54** (1996), 1661–1677.

[Guh98] T. Guhr, A. Müller-Groeling, and H. A. Weidenmüller, *Random-matrix theories in quantum physics: common concepts*, Phys. Rep. **299** (1998), 189–425.

[Haa91] F. Haake, *Quantum signatures of chaos*, Springer series in synergetics, vol. 54, Springer, Berlin, 1991.

[Haa92] F. Haake, F. Izrailev, N. Lehmann, D. Saher, and H.-J. Sommers, *Statistics of complex levels of random matrices for decaying systems*, Z. Phys. B **88** (1992), 359–370.

[HB56] R. Hanbury-Brown and R. Q. Twiss, *A test of a new type of stellar interferometer on Sirus*, Nature (London) **178** (1956), 1046–1048.

[Hen96] C. H. Henry and R. F. Kazarinov, *Quantum noise in photonics*, Rev. Mod. Phys. **68** (1996), 801–853.

[Ish78] A. Ishimaru, *Wave propagation and scattering in random media*, Academic, New York, 1978.

[Jan99] R. A. Janik, W. Nörenberg, M. A. Nowak, G. Papp, and I. Zahed, *Correlations of eigenvectors for non-Hermitian random-matrix models*, Phys. Rev. E **60** (1999), 2699–2705.

[Jef93] J. Jeffers, N. Imoto, and R. Loudon, *Quantum optics of traveling-wave attenuators and amplifiers*, Phys. Rev. A **47** (1993), 3346–3358.

[Jef94] J. Jeffers and S. M. Barnett, *Propagation of squeezed-light in dielectrics*, J. Mod. Opt. **41** (1994), 1121–1133.

[Jon92] M. J. M. de Jong and C. W. J. Beenakker, *Mesoscopic fluctuations in the shot-noise power of metals*, Phys. Rev. B **46** (1992), 13400–13406.

[Jon95] M. J. M. de Jong and C. W. J. Beenakker, *Semiclassical theory of shot-noise suppression*, Phys. Rev. B **51** (1995), 16867–16870.

[Jon99] M. J. M. de Jong and C. W. J. Beenakker, *Shot noise in mesoscopic systems*, Mesoscopic Electron Transport (Dordrecht) (L. L. Sohn, L. P. Kouwenhoven, and G. Schön, eds.), NATO ASI Series E, vol. 345, Kluwer, 1999, pp. 225–258.

[Kel64] P. L. Kelley and W. H. Kleiner, *Theory of electromagnetic field measurement and photoelectron counting*, Phys. Rev. **136** (1964), A316–A334.

[Ket97] S. Kettemann, D. Klakow, and U. Smilansky, *Characterization of quantum chaos by the autocorrelation function of spectral determinants*, J. Phys. A: Math. Gen. **30** (1997), 3643–3662.

[Khl87] V. A. Khlus, *Current and voltage fluctuations in microjunctions between normal metals and superconductors*, Zh. Eksp. Teor. Fiz. **93** (1987), 2179–2190 [Sov. Phys. JETP **66** (1987), 1243–1249].

[Kir60] G. Kirchhoff, *Zusammenhang von Emission und Absorption von Licht und Wärme*, Ann. Phys. Chem. (Poggendorff) **109** (1860), 275.

[Knö99] L. Knöll, S. Scheel, E. Schmidt, D.-G. Welsch, and A. V. Chizhov, *Quantum-state transformation by dispersive and absorbing four-port devices*, Phys. Rev. A **59** (1999), 4716–4726.

[Kud95] A. Kudrolli, V. Kidambi, and S. Sridhar, *Experimental studies of chaos and localization in quantum wave functions*, Phys. Rev. Lett. **75** (1995), 822–825.

[Leh95] N. Lehmann, S. Saher, V. V. Sokolov, and H.-J. Sommers, *Chaotic scattering - the supersymmetry method for large number of channels*, Nucl. Phys. A **582** (1995), 223–256.

[Leo93] U. Leonhardt, *Influence of a dispersive and dissipative medium on spectral squeezing*, J. Mod. Opt. **40** (1993), 1123–1130.

[Les89] G. B. Lesovik, *Excess quantum noise in 2d ballistic point contacts*, Pis'ma Zh. Eksp. Teor. Fiz. **49** (1989), 513–515 [JETP Lett. **49** (1989), 592–594].

[Let67] V. S. Letokhov, *Generation of light by a scattering medium with negative resonance absorption*, Zh. Eksp. Teor. Fiz. **53** (1967), 1442–1452 [Sov. Phys. JETP **26** (1968), 835–840].

[Lou84] R. Loudon and T. J. Shepherd, *Properties of the optical quantum amplifier*, Opt. Acta **31** (1984), 1243–1269.

[Mah69] C. Mahaux and H. A. Weidenmüller, *Shell-model approach to nuclear reactions*, North-Holland, Amsterdam, 1969.

[Man95] L. Mandel and E. Wolf, *Optical coherence and quantum optics*, Cambridge University Press, New York, 1995.

[Man97] V. A. Mandelshtam and H. S. Taylor, *Spectral analysis of time correlation function for a dissipative dynamical system using filter diagonalization: Application to calculation of unimolecular decay rates*, Phys. Rev. Lett. **78** (1997), 3274–3277.

[Mat95] R. Matloob, R. Loudon, S. M. Barnett, and J. Jeffers, *Electromagnetic field quantization in absorbing dielectrics*, Phys. Rev. A **52** (1995), 4823–4838.

[Mat97] R. Matloob, R. Loudon, M. Artoni, S. M. Barnett, and J. Jeffers, *Electromagnetic field quantization in amplifying electrics*, Phys. Rev. A **55** (1997), 1623–1633.

[Meh90] M. Mehta, *Random matrices*, Academic, New York, 1990.

[Meh00] B. Mehlig and J. T. Chalker, *Statistical properties of eigenvectors in non-Hermitian Gaussian random matrix ensembles*, J. Math. Phys. **41** (2000), 3233–3256.

[Mel92] P. A. Mello and S. Tomsovic, *Scattering approach to quantum electronic transport*, Phys. Rev. B **46** (1992), 15963–15981.

[Mis98] T. Sh. Misirpashaev and C. W. J. Beenakker, *Lasing threshold and mode competition in chaotic cavities*, Phys. Rev. A **57** (1998), 2041–2045.

[Mis99] E. G. Mishchenko and C. W. J. Beenakker, *Radiative transfer theory for vacuum fluctuations*, Phys. Rev. Lett. **83** (1999), 5475–5478.

[Nag92] K. E. Nagaev, *On the shot noise in dirty metal contacts*, Phys. Lett. A **169** (1992), 103–107.

[Opp94] F. von Oppen, *Exact distribution of eigenvalue curvatures of chaotic quantum systems*, Phys. Rev. Lett. **73** (1994), 798–801.

[Opp95] F. von Oppen, *Exact distributions of eigenvalue curvatures for time-reversal-invariant chaotic systems*, Phys. Rev. E **51** (1995), 2647–2650.

[Per83] P. Pereyra and P. A. Mello, *Marginal distribution of the S-matrix elements for Dyson's measure and some applications*, J. Phys. A: Math. Gen. **16** (1983), 237–254.

[Pet79] K. Petermann, *Calculated spontaneous emission factor for double-heterostructure injection lasers with gain-induced waveguiding*, IEEE J. Quantum Electron. **15** (1979), 566–570.

[Por65] C. E. Porter, *Statistical theory of spectra: Fluctuations*, Academic, New York, 1965.

[Sch18] W. Schottky, *Über spontane Stromschwankungen in verschiedenen Elektrizitätsleitern*, Ann. Phys. (Leipzig) **57** (1918), 541–567.

[Sch58] A. L. Schawlow and C. H. Townes, *Infrared and optical masers*, Phys. Rev. **112** (1958), 1940–1949.

[Sch96] E. Schmidt, L. Knöll, and D.-G. Welsch, *Propagation of squeezed-light pulses in dispersive and absorbing linear dielectrics*, Phys. Rev. A **54** (1996), 843–855.

[Sch00] H. Schomerus, K. M. Frahm, M. Patra, and C. W. J. Beenakker, *Quantum limit of the laser linewidth in chaotic cavities and statistics of residues of scattering matrix poles*, Physica A **278** (2000), 469–496.

[She90] P. Sheng (ed.), *Scattering and localization of classical waves in random media*, World Scientific, Singapore, 1990.

[Sie89a] A. E. Siegman, *Excess spontaneous emission in non-Hermitian optical systems. I. Laser amplifiers*, Phys. Rev. A **39** (1989), 1253–1263.

[Sie89b] A. E. Siegman, *Excess spontaneous emission in non-Hermitian optical systems. II. Laser oscillators*, Phys. Rev. A **39** (1989), 1264–1268.

[Sie98] A. E. Siegman, *Excess noise in linear nonnormal systems: A general derivation*, 1998, preprint.

[Sok88] V. V. Sokolov and V. G. Zelevinsky, *On a statistical theory of overlapping resonances*, Phys. Lett. B **202** (1988), 10–14.

[Sok89] V. V. Sokolov and V. G. Zelevinsky, *Dynamics and statistics of unstable quantum states*, Nucl. Phys. A **504** (1989), 562–588.

[Som99] H.-J. Sommers, Y. V. Fyodorov, and M. Titov, *S-matrix poles for chaotic quantum systems as eigenvalues of complex symmetric random matrices: from isolated to overlapping resonances*, J. Phys. A: Math. Gen. **32** (1999), L77–L85.

[Ste86] S. Stenholm, *The theory of quantum amplifiers*, Phys. Scr. T **12** (1986), 56–66.

[Ver85] J. J. M. Verbaarschot, H. A. Weidenmüller, and M. R. Zirnbauer, *Grassmann integration in stochastic quantum physics: the case of compound-nucleus scattering*, Phys. Rep. **129** (1985), 367–438.

[Wal94] D. F. Walls and G. J. Milburn, *Quantum optics*, Springer, Berlin, 1994.

[Wie95] D. S. Wiersma, M. P. van Albada, and A. Lagendijk, *Random laser*, Nature **373** (1995), 203–204.

[Wie97] D. S. Wiersma and A. Lagendijk, *Laser action in very white paint*, Physics World **10** (1997), 33–37.

[Wig56] E. P. Wigner, *Results and theory of resonance absorption*, Conference on Neutron Physics by Time-of-Flight (Gatlinburg, Tennessee), 1956, pp. 59–70.

[Yue76] H. P. Yuen, *Two-photon coherent states of the radiation field*, Phys. Rev. A **13** (1976), 2226–2243.

Quantumoptica van wanordelijke systemen

Doel van dit proefschrift is de ontwikkeling van een theoretisch raamwerk om quantumoptica en wanorde te combineren. Beide onderwerpen apart zijn uitvoerig bestudeerd in het verleden, maar de combinatie is nieuw. Laten we deze twee onderwerpen apart onder de loep nemen.

Quantumoptica is op zichzelf een combinatie van twee vakgebieden, de optica en de quantummechanica. Volgens de quantumoptica bestaat het licht uit discrete "quanta" van energie, genaamd fotonen. De hoeveelheid energie van een foton is zo klein dat we meestal het bestaan van fotonen kunnen vergeten en doen alsof het licht een continue stroom van energie is. Echter, op atomaire schaal speelt de discreetheid (of quantisatie) van de energie een essentiële rol, omdat de atomaire energiën zelf ook heel klein zijn. Einsteins theorie van het foto-elektrische effect (waar hij de Nobelprijs voor ontving) was de eerste quantumoptische theorie. Na de ontdekking van de laser heeft de quantumoptica zich in de zestiger jaren snel ontwikkeld tot een rijp vakgebied.

Op macroscopische schaal kunnen we het bestaan van fotonen afleiden uit de fluctuaties van de energiestroom. Men spreekt van hagelruis, waarbij men de fotonen vergelijkt met hagelkorrels. Een wezenlijk verschil tussen hagel en licht is dat hagelkorrels voldoen aan de wetten van de klassieke mechanica, terwijl fotonen de wetten van de quantummechanica volgen. Volgens de quantummechanica hebben identieke deeltjes een mysterieuze kracht op elkaar, hoe ver ze ook van elkaar zijn verwijderd. Voor fotonen is die kracht aantrekkend. (Men noemt dit soort deeltjes bosonen.) Door die aantrekkende kracht is de ruis in een stroom licht groter dan je voor hagelruis zou verwachten. Deze toename in de ruis is ook voor het eerst voorspeld door Einstein.

Wanordelijke systemen zijn materialen waarin het licht op een onregelmatige, chaotische manier wordt verstrooid. Een vertrouwd voorbeeld is matglas. In matglas zijn opzettelijk verstoringen aangebracht, die het licht alle kanten op verstrooien. De preciese wijze van verstrooiing door deze strooicentra is onvoor-

spelbaar, tenzij je precies zou weten waar de verstoringen zijn aangebracht. Maar dit is meestal ondoenlijk. Het is zinvoller om een statische beschrijving te zoeken, die de gemiddelde eigenschappen van het matglas geeft in plaats van de specifieke eigenschappen van één bepaald stukje glas. Chaotische verstrooiing treedt ook op in trilholtes die een onregelmatige vorm hebben, zelfs al er zich in de trilholte geen strooicentra bevinden.

Er bestaat een gedetailleerde statistische theorie voor de chaotische verstrooiing van lichtgolven, gebaseerd op de wiskunde van toevalsmatrices. De matrix waar het om gaat is de zogenaamde verstrooiingsmatrix. De verstrooiingsmatrix van een stukje matglas is natuurlijk niet echt toevallig, maar in een statistische beschrijving is het toevallig aanwijzen van de matrixelementen een goede aanpak. Tot op heden speelden fotonen in deze theorie geen rol, men veronderstelde dat de energie in golven volledig continu kon variëren. Door de quantumoptica met de toevalsmatrixtheorie te combineren hebben we een theorie kunnen ontwikkelen voor de chaotische verstrooiing van *fotonen*, en zo een aantal interessante nieuwe problemen kunnen oplossen.

De inhoud van dit proefschrift bestaat dus enerzijds uit een algemeen theoretisch kader en anderzijds uit een aantal toepassingen. Het belangrijkste resultaat van de algemene theorie is een relatie tussen de correlatiefuncties van de fluctuaties in het licht en de verstrooiingsmatrix. Een hele eenvoudige toepassing is op de straling van een zwart lichaam. De verstrooiingsmatrix van een zwart lichaam is gelijk aan nul, omdat al het invallende licht door een zwart lichaam wordt geabsorbeerd en niets wordt teruggestrooid. Een realistisch voorwerp is grijs in plaats van zwart, dat wil zeggen, de verstrooiingsmatrix is niet precies nul. We geven een gedetailleerde beschrijving van hoe de fluctuaties voor een grijs lichaam afwijken van de ideale limiet van een zwart lichaam.

De afwijking is klein omdat de quantummechanische aantrekkingskracht tussen fotonen zo klein is. Veel grotere effecten treden op in een laser, of meer in het algemeen in een medium dat het invallende licht *versterkt* terugkaatst, in plaats van het te absorberen. Een laser met wanorde heet een “toevalslaser” en de toevalsmatrixtheorie is een krachtig hulpmiddel om de statistische eigenschappen van de versterkte straling te beschrijven.

De straling van een laser is in een zogenaamde “coherente” toestand, met gereduceerde fluctuaties. Nog lagere fluctuaties kunnen bereikt worden in een toestand die men “geperst” noemt (*squeezed* in het engels). De quantummechanische aantrekking die fotonen van nature op elkaar hebben is in een geperste toestand omgezet in een afstoting. Coherente en geperste toestanden zijn kwetsbare toestanden van het licht; een beetje absorptie zet ze al gauw om in de meer gewone “thermische” toestand van het licht. Hoe deze omzetting in zijn werk gaat wordt in dit proefschrift in detail beschreven.

List of publications

1. *Oscillatory instabilities and field domain formation in imperfect superlattices*, E. Schöll, G. Schwarz, M. Patra, F. Prengel, and A. Wacker, Proceedings of the 9th Int. Conf. on Hot Carriers in Semiconductors, Chicago, ed. by K. Hess, J. P. Leburton and U. Ravaioli, Plenum, New York (1996), pp. 177–181.

2. *Bifurcation analysis of electric field domains in semiconductor superlattices*, M. Patra, G. Schwarz, F. Prengel, and E. Schöll, Proceedings of the 157. WE-Heraeus Seminar "Selbstorganisation in Aktivator-Inhibitor Systemen" (Wissenschaft & Technik Verlag, Berlin 1996, pp. 56–61).

3. *Nonlinear dynamics of field domains in weakly disordered superlattices*, F. Prengel, M. Patra, G. Schwarz, and E. Schöll, Proc. 23rd Int. Conf. on the Physics of Semiconductors, Berlin 1996, ed. by M. Scheffler and R. Zimmermann (World Scientific, Singapore 1996) vol. 3, pp. 1667–1670.

4. *Bifurcation analysis of stationary and oscillating domains in semiconductor superlattices with doping fluctuations*, M. Patra, G. Schwarz, and E. Schöll, Phys. Rev. B **57**, 1824–1833 (1998).

5. *Multistable current-voltage characteristics as fingerprints of growth-related imperfections in semiconductor superlattices*, G. Schwarz, M. Patra, F. Prengel, and E. Schöll, Superlattices and Microstructures **23**, 1353–1357 (1998).

6. *Long-range correlation of thermal radiation*, M. Patra and C. W. J. Beenakker, Phys. Rev. A **59**, R43–R46 (1999).

7. *Excess noise for coherent radiation propagating through amplifying random media*, M. Patra and C. W. J. Beenakker, Phys. Rev. A **60**, 4059–4066 (1999).

8. *Photon shot noise*, C. W. J. Beenakker and M. Patra, Mod. Phys. Lett. B **13**, 337–347 (1999).

9. *Quantum-limited linewidth of a chaotic laser cavity*, M. Patra, H. Schomerus, and C. W. J. Beenakker, Phys. Rev. A **61**, 023810 (2000).

10. *Large Petermann factor in chaotic cavities with many scattering channels*, K. Frahm, H. Schomerus, M. Patra, and C. W. J. Beenakker, Europhys. Lett. **49**, 48–54 (2000).

11. *Propagation of squeezed radiation through amplifying or absorbing random media*, M. Patra and C. W. J. Beenakker, Phys. Rev. A **61**, 063805 (2000).

12. *Quantum limit of the laser linewidth in chaotic cavities and statistics of residues of scattering matrix poles*, H. Schomerus, K. M. Frahm, M. Patra, and C. W. J. Beenakker, Physica A **278**, 469–496 (2000).

13. *Photonic excess noise and wave localization*, C. W. J. Beenakker, M. Patra, and P. W. Brouwer, Phys. Rev. A **61**, 051801[R] (2000).

14. *Frequency dependence of the photonic noise spectrum in an absorbing or amplifying diffusive medium*, E. G. Mishchenko, M. Patra, and C. W. J. Beenakker, submitted to Phys. Rev. A (cond-mat/0003262).

Refs. 6, 7, and 11 are reproduced in Chapters 5, 2, and 3, respectively. Refs. 8 and 13 are combined in Chapter 4, Refs. 9, 10, and 12 are combined in Chapter 6.

Curriculum vitæ

Ik ben geboren op 27 april 1971 in West-Berlijn. Daar bezocht ik het Albert-Schweitzer-Gymnasium, waar ik in 1990 mijn eindexamen deed. In 1989 werd ik deelstaatskampioen van de Duitse wetenschapscompetitie “Jugend forscht” in het vakgebied wiskunde / informatica met een werkstuk over compilerontwikkeling.

In 1990 ben ik begonnen met mijn studie aan de Technische Universiteit Berlijn. In febuari 1997 studeerde ik cum laude af. Mijn afstudeerscriptie over velddomeinen in halfgeleidersuperroosters schreef ik in de groep “Nietlineaire dynamica in halfgeleiders” onder leiding van prof. dr. E. Schöll.

Sinds september 1997 ben ik assistent in opleiding op het Instituut-Lorentz voor theoretische natuurkunde aan de Universiteit Leiden, dat deel uitmaakt van het Leidse Instituut voor Onderzoek in de Natuurkunde (LION). Daar werkte ik onder leiding van prof. dr. C. W. J. Beenakker aan het onderzoek beschreven in dit proefschrift. Tevens vervulde ik werkzaamheden van systeembeheer op het Instituut-Lorentz.

Ik nam deel aan de volgende (zomer)scholen: “Self-Organization in Activator-Inhibitor Systems” in Bad Honnef (Duitsland, 1996), “Diffuse Waves in Complex Media” in Les Houches (Frankrijk, 1998), “Graßmann-Variablen” in Heidelberg (Duitsland, 1998), “Bose-Einstein Condensation” in Les Houches (Frankrijk, 1999), “Phase Coherent Dynamics in Hybrid Nanostructures” in Bad Herrenalb (Duitsland, 1999) en “Photonic Crystals and Light Localization” op Kreta (Griekenland, 2000). Voorts heb ik mijn resultaten op conferenties in Amsterdam, Münster (Duitsland) en Regensburg (Duitsland) gepresenteerd.

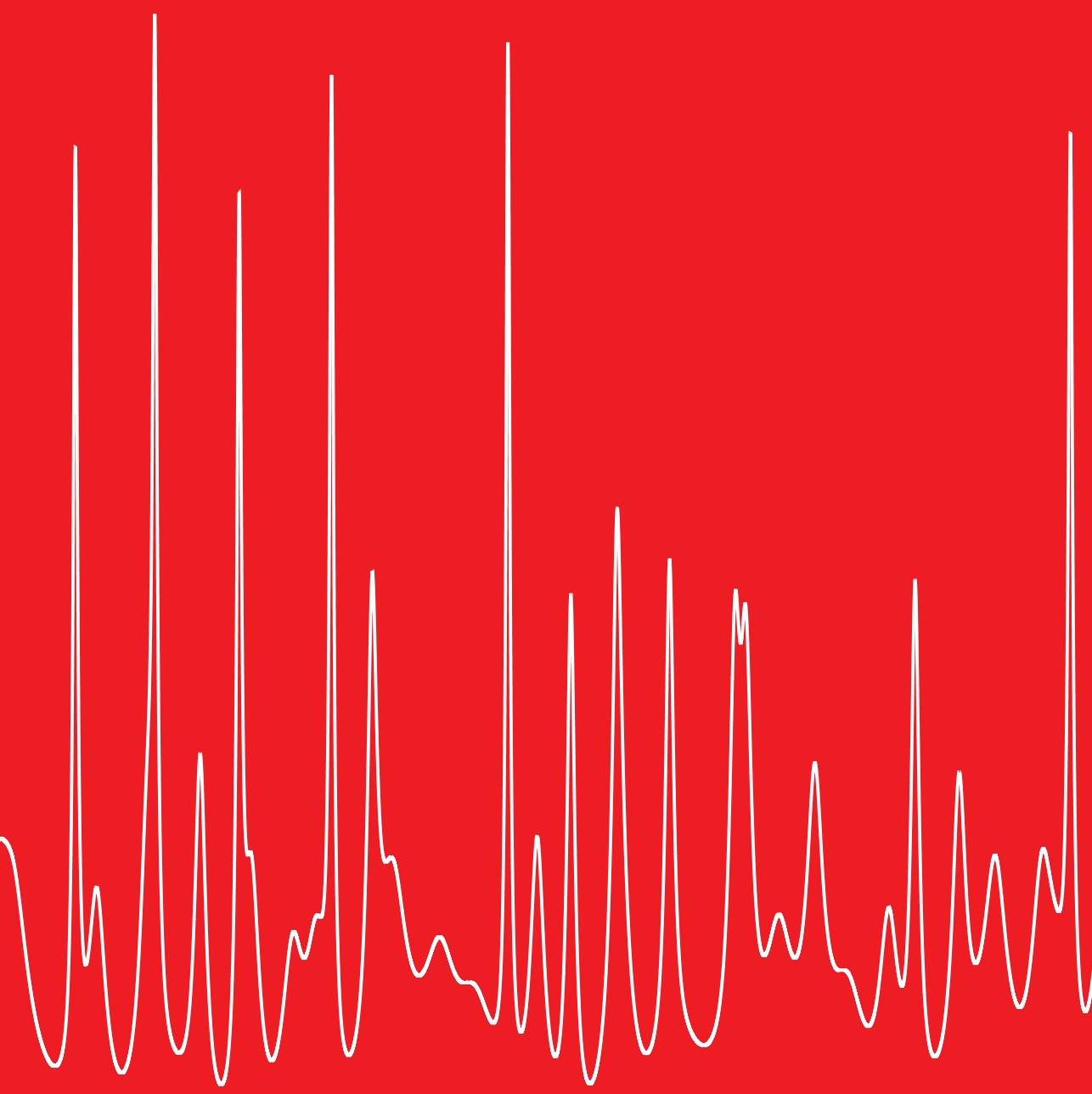

Stellingen

behorende bij het proefschrift
"On Quantum Optics of Random Media"

1. Elastische verstrooiing heeft geen invloed op de fluctuaties van coherente straling.

   Dit proefschrift, hoofdstuk 2.

2. De "squeezing" sterkte van "squeezed" straling in een wanordelijk medium neemt af op de schaal van de absorptielengte terwijl de "squeezing" hoek vervalt op de schaal van de vrije-weglengte.

   Dit proefschrift, hoofdstuk 3.

3. Voortplanting van coherente straling door een wanordelijke absorberende golfpijp leidt tot een toename van de Fanofactor met anderhalf keer de Bose-Einstein functie.

   Dit proefschrift, hoofdstuk 4.

4. De Petermannfactor in de quantumoptica van lasers komt overeen met het conditiegetal in de numerieke wiskunde van matrixinversie.

   Dit proefschrift, hoofdstuk 6.

5. De theorie van het effect van wanorde op optische fase-conjugatie van Paasschens, Brouwer en Beenakker schendt causaliteit.

   J. C. J. Paasschens, P. W. Brouwer en C. W. J. Beenakker,
   Europhysics Letters **38**, 651 (1997).

6. De Campbell-Baker-Hausdorff formule heeft het volgende analogon voor operatoren die bilineair zijn in de boson annihilatie- en creatie-operatoren a_i, $a_i^\dagger$ $(i = 1, 2, \ldots, N)$:

   $$\exp(\boldsymbol{a}^\dagger \boldsymbol{A} \boldsymbol{a}) \exp(\boldsymbol{a}^\dagger \boldsymbol{B} \boldsymbol{a}) = \exp\left(\boldsymbol{a}^\dagger \ln(\mathrm{e}^{\boldsymbol{A}} \mathrm{e}^{\boldsymbol{B}}) \boldsymbol{a}\right) ,$$

   waar $\boldsymbol{A}$ en $\boldsymbol{B}$ $N \times N$ complexe matrices zijn.

7. Het elektronische analogon van de Glauber-Kelley-Kleiner formule voor de telverdeling van fotonen, zoals gegeven door Muzykantskii en Khmelnitskii, is onjuist.

   B. A. Muzykantskii en D. E. Khmelnitskii,
   Physical Review B **50**, 3982 (1994).

8. Een puls die gereflecteerd wordt door een wanordelijk medium valt twee keer zo langzaam af in de tijd, indien zich achter het medium een fase-conjugerende spiegel bevindt.

Michael Patra
6 september 2000